Investigation into the regulatory mechanisms of resistance-nodulation-division efflux pumps in *Acinetobacter* spp.

BY

Tajinder Kainth

A thesis submitted to the Faculty of Graduate Studies of

The University of Manitoba

in partial fulfillment of the requirements of the degree of

MASTER OF SCIENCE

Department of Microbiology, Faculty of Science

University of Manitoba

Winnipeg, Canada

Abstract

Acinetobacter spp. play a significant role in colonizing and infecting immunocompromised patients in hospitals. They have been implicated in nosocomial infections in intensive care unit (ICU) patients. These infections are extremely hard to treat because of the broad resistance of these bacteria to numerous antimicrobials. A major contributor to *Acinetobacter*'s capability to cause these infections is its ability to sense and adapt to environmental and host stress signals, allowing it to persist in medical settings and human hosts. Intrinsic resistance can be generated by the interplay of decreased susceptibility due to active efflux systems and external stressors that bacteria experience. Catalase-peroxidases are enzymes responsible for detoxification of H_2O_2. The aim of this study is to study the regulatory mechanisms that control the expression of Resistance-Nodulation-Division (RND) efflux pumps in *Acinetobacter* spp. The first section of this thesis characterizes the involvement of catalase-peroxidases, *katG* and *katE*, in the oxidative stress - mediated antimicrobial susceptibility of *Acinetobacter baumannii* and second section characterizes a novel regulator of AdeDE RND efflux pump in *Acinetobacter pittii*. Mutants of *A. baumannii* ATCC17978 with deletions in *katG* and *katE* were tested for sensitivity to H_2O_2, RND efflux pump expression and susceptibility to antibiotics. *katG* and *katE* deletion resulted in reduced susceptibility to aminoglycoside antibiotics. Deletion of *katG* or *katE* results in *adeB,* gene that encodes the inner membrane component of AdeAB, an aminoglycoside pump and *adeR,* a response regulator that encodes the transcriptional activator of *adeAB* to be upregulated. RNA-Seq analysis was carried out to understand the global response of *A. baumannii* to oxidative stress revealed over 100 differentially expressed genes. Finally, a novel Tet-R type novel regulator upstream of AdeDE RND efflux pump in *A. pittii* was characterized. Deletion of the regulator results in overexpression of AdeDE efflux pump, reduced antibiotic susceptibility to multiple antibiotics, altered biofilm production and surface associated motility. These results indicate that efflux may be a part of *A.*

baumannii's response to oxidative stress, suggest that stress response are, thus, important determinants of antibiotic resistance in *A. baumannii* and AdeQ plays a role as a regulator of AdeDE RND efflux pump in *A. pittii*.

Table of Contents

List of Tables

List of Figures

Acknowledgments

I would like to thank my parents for putting their trust in me and always encouraging me to pursue my career in science.

Secondly, I would like to thank my supervisor, Dr. Ayush Kumar for accepting me into the laboratory and providing me with guidance and support. I would like to thank my committee, Dr. Ivan Oresnik and Dr. Miguel Uyaguari for their inputs and consultation.

Lastly, I would like to thank all the current and past members of Kumar lab that made these 2 years fly by quickly. I have learnt a lot from you all. Special mention to my friend and mentor Dr. Malaka De Silva for helping me in the initial steps in the Kumar lab and for being a great friend.

Contributions of authors

Chapter 2

katG and *katE* deletion mutants were previously made by Dr. Malaka De Silva. The rest of the constructs were created by Tajinder Kainth. All experimental work was carried out by Tajinder Kainth.

Chapter 3

All work presented was conducted by Tajinder Kainth.

Chapter 1 - Literature Review

1.1 Introduction

1.1.1 *Acinetobacter* spp.

Acinetobacter spp. are known as important opportunistic pathogens in immunocompromised patients, and are classified as catalase-positive, aerobic gram-negative coccobacilli [1]. The taxonomy of *Acinetobacter* genus has undergone many changes. It currently consists of 43 species defined by DNA-DNA hybridization (https://www.bacterio.net/genus/*Acinetobacter*). *Acinetobacter baumannii* and the closely related species *Acinetobacter calcoaceticus* (formerly genomic species 1), *Acinetobacter pittii* (formerly genomic species 3), and *Acinetobacter nosocomialis* (formerly 13 sensu Tjernberg and Ursing, 13TU) are the most relevant clinically [1]. Due to their close relatedness, they have been referred as the *A. calcoaceticus-A. baumannii* (Acb) complex [2].

The Acb complex has emerged to be highly troublesome opportunistic group of pathogens associated with hospital-acquired infections in immunocompromised patients worldwide, with high levels of multi-drug resistance [3]. Infections include bacteremia, catheter associated urinary tract infection, and secondary meningitis, but more commonly the Acb complex is associated with nosocomial pneumonia, particularly ventilator-associated pneumonia in patients confined to hospital intensive care units (ICUs) [3].

Within the Acb complex, *A. baumannii, A. nosocomalis,* and *A. pittii* are clinically relevant but differ in their susceptibility profiles, virulence and pathogenicity [4]. Their increasing resistance to carbapenems and polymyxins, the last resort antibiotics, poses an enormous threat to health care costs and patient outcomes [5]. These species exhibit broad intrinsic resistance, conferred by chromosomally encoded cephalosporinases, expression of efflux pumps, and a low membrane permeability [5].

1.1.2 *Acinetobacter baumannii*

A. baumannii, a Gram-negative, obligate aerobe, coccobacilli belonging to the class Gammaproteobacteria, is the most important member of the Acb complex. As a consequence of its immense ability to acquire resistance, it has demonstrated a significant insurgence in the prevalence of infections over recent decades [6]. A member of the ESKAPE (*Enterococcus faecium, Staphylococcus aureus, Klebsiella pneumoniae, A. baumannii, Pseudomonas aeruginosa*, and *Enterobacter* species) pathogen group, carbapenem-resistant *A. baumannii* is considered the World Health Organization's number one critical priority pathogen for which new antibiotics are urgently required [7].

A. baumannii is best known for causing ventilator-associated pneumonia, meningitis, urinary tract infection, central venous catheter-related infection, and bloodstream infection among immunocompromised and injured patients worldwide [3]. One of the main characteristics that helps it to be a successful pathogen is its ability to display multi-drug resistant (MDR) phenotypes [8]. It exhibits resistance to multiple clinically relevant antibiotics, including carbapenems and polymyxins, which are the last resort antibiotics for treatment [3]. As a result of this, CDC has classified carbapenem-resistant *Acinetobacter baumannii* as an "Urgent" threat level to human health [9].

1.1.3 *Acinetobacter nosocomialis* and *Acinetobacter pittii*

While *A. baumannii* is considered the most important and clinically relevant within the Acb complex, *A. nosocomialis* and *A. pittii* are other members of the Acb complex that are gaining importance as clinically-relevant pathogens as incidences of outbreaks in hospital settings are increasing [10,11]. Studies show that *A. pittii* and *A. nosocomialis* are associated with lower mortality rates and were less multidrug resistant than *A. baumannii* [11]. In a recent study, *A.*

nosocomialis bacteremia reported higher mortality rates than patients infected with *A. pittii*, however, patients with *A. pittii* had fewer comorbidities [11].

1.1.4 Mechanisms of Antibiotic Resistance

Members of the Acb complex exhibit resistance to many antibiotics effective against Gram-negative pathogens, including β-lactams, aminoglycosides, tetracyclines, erythromycin, trimethoprim [1]. The ability to develop rapid antibiotic resistance perhaps can be attributed to increased usage of antibiotics in hospital environments and consequence of increase exposure in soil environments where these bacteria are commonly found.

1.1.4.1 Acquired Resistance

Acinetobacter spp. is readily amenable to the transfer of genetic elements facilitating the acquisition of resistance genes [12]. For example, clinical isolates of *Acinetobacter* spp. have often been shown to contain integron-based antibiotic resistance genes such as those for β-lactams and carbapenems [13]. Genes conferring resistance to β-lactams, carbapenems, and sulfonamide have also been found on conjugative plasmids in *Acinetobacter* spp. [14]. In *Acinetobacter* spp., particularly *A. baumannii*, transposons have been shown to carry important resistance genes such as $bla_{\text{OXA-23}}$ which are carbapenem-hydrolyzing β-lactamases [14]. This ability to acquire foreign DNA carrying resistance genes from external sources contributes to decreased susceptibility of organisms in the Acb complex to a variety of antibiotics.

An abundance of β-lactamases have been described in *Acinetobacter* spp. [13]. These are enzymes produced by the bacterium that are responsible for degrading β-lactam antibiotics such as penicillin, ceftazidime and aztreonam [15]. More recently the emergence of oxacillinases (OXAs) and carbapenemases in *A. baumannii* has led to several outbreaks of infection with carbapenem

resistance *Acinetobacter* spp. [15]. Alternatively, *A. baumannii* possess ways in which the drug can be modified to decrease its efficacy. This commonly involves the utilization of aminoglycoside modifying enzymes, which can alter the drug by acetylation, phosphorylation and adenylation. These genes are acquired from mobile genetic elements and plasmids that are transferred among the *Acinetobacter* population [16].

Target modification of the antibiotic molecule so that it can no longer bind its target is mediated by several different methods, including mutating the target protein or post-translational modification of target site [17]. These mechanisms are commonly involved in the resistance to quinolones such as ciprofloxacin by targeting the essential bacterial enzymes DNA gyrase and topoisomerase IV [17]. Mutation that targets these enzymes decrease binding of fluoroquinolones to the enzyme-DNA complex.

1.1.4.2 Intrinsic Resistance

One of the most relevant mechanism of resistance in *Acinetobacter* spp. are the presence of efflux pumps resulting in increased efflux of antibiotics and decreased uptake. A decrease in expression of outer membrane proteins has been linked to carbapenem resistance [18]. The role of efflux is to actively pump out antibiotics that can disorganize the cytoplasmic membrane. Efflux pumps are able to expel the drug out of the cell at a high rate which prevents the intracellular drug concentrations reaching high enough to elicit an effect. *A. baumannii* has been shown to have different types of efflux pumps including the small multidrug resistance (SMR), multidrug and toxic compound extrusion (MATE), the major facilitator superfamily (MFS), proteobacterial antimicrobial compound efflux (PACE), and the resistance-nodulation-cell division (RND) family [19]. In the mentioned drug efflux families above, they all use either Na+ or H+ as an energy source [20]. The MFS, SMR, and PACE can efflux substrates into the periplasmic space whereas

RND efflux systems can transport substrates out of the bacterial cells [20,21]. RND family have been shown to be the most clinically relevant pumps which confer multidrug resistance in Gram-negative bacteria [21].

1.1.5 RND Efflux Systems

It has been well established that efflux mechanisms play an important role in multidrug resistance in Gram-negative bacteria. The major clinically relevant efflux systems are of the RND superfamily. These are tripartite complexes typically composed of an inner membrane protein (IMP), a membrane fusion protein (MFP), and an outer membrane channel factor (OMF) protein [22]. OMFs are embedded in the outer membrane with some part partially hanging in periplasmic space whereas IMP are embedded mostly in inner membrane but partially protrude in periplasmic space. They are brought together with the help of a linker MFP protein to form the tripartite complex with a tunnel opening outside the cell [20]. These tripartite pumps provide intrinsic resistance to a wide variety of antimicrobial compounds.

RND efflux pumps are prominent in both their efficiency of extruding antibiotics and broad substrate specificities. Overexpression of RND efflux pumps has been linked with clinically relevant levels of MDR phenotype in *A. baumannii*. [23]. RND pumps are capable of extruding not only antibiotics but other substrates including dyes, biocides, toxins, heavy metals and detergents [24]. In *A. baumannii*, there are three well characterized RND efflux pumps: AdeABC, AdeIJK, and AdeFGH.

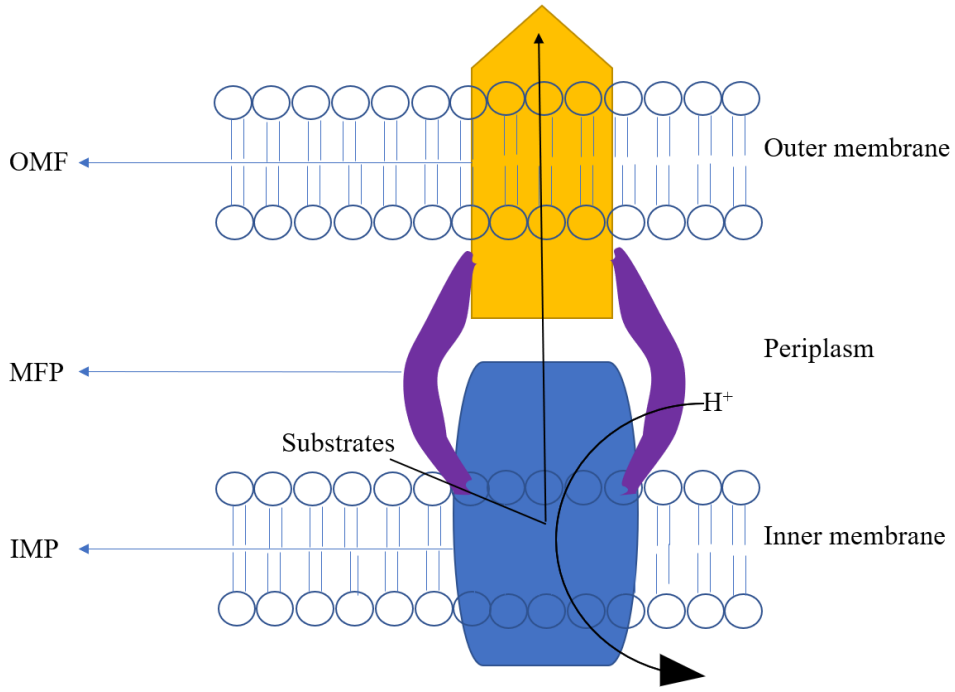

Figure 1.1. Schematic representation of a RND Efflux System in *Acinetobacter baumannii*
The complex structure consists of three proteins which span the inner membrane (IMP), outer membrane (OMF), and the periplasmic space. The IMP is responsible for substrates that are extruded from the cytoplasm through the periplasm out of the bacterial cell in an energy dependent manner using H+ ion gradient as the energy source. The MFP connects the IMP and OMF.

AdeABC was the first efflux pump identified in *A. baumannii* [25]. Its operon encodes the AdeA MFP, AdeB multidrug transporter and AdeC OMF [26]. The entire operon of AdeABC is not found in some isolates of *A. baumannii* and are shown to be lacking the outer membrane factor, AdeK suggesting that a different outer membrane factor is at play [26]. Overexpression of this RND pump confers resistance to mainly aminoglycosides but also fluoroquinolones, erythromycin, tetracyclines, chloramphenicol and trimethoprim [26]. Apart from AdeABC there are two other well characterized RND efflux pumps in *A. baumannii*, AdeIJK [27] and AdeFGH [25].

AdeFGH, encoded by the *adeFGH* operon [25] and similar to AdeABC, confers multidrug resistance phenotype when overexpressed. It confers resistance to fluoroquinolones, chloramphenicol, trimethoprim, and clindamycin [25]. AdeFGH is not constitutively expressed in wild-type strains and therefore does not contribute to intrinsic resistance in *A. baumannii*. It is regulated by a negative repressor, *adeL* [25]. Overexpression of the AdeFGH efflux pump in a strain lacking Δ*adeL* has been linked with decreased susceptibilities to tobramycin, gentamicin, tigecycline and ciprofloxacin [28].

AdeIJK, encoded by the a*deIJK* operon [27] is constitutively expressed in *A. baumannii* [29] and is present in all strains of *A. baumannii* [27]. Unlike other pump-encoding operons where the regulatory element is linked to the operon, *adeIJK* regulator, *adeN*, a TetR-type transcriptional repressor, lies 813 kb upstream of the operon. It contributes to intrinsic resistance to β-lactams, cephalosporins, aztreonam, chloramphenicol, novobiocin, fluroquinolones, and rifampin [27]. Interestingly, it has been shown that triclosan, a biocide commonly found in toothpastes and other antibacterial domestic products has been shown to select for AdeIJK overexpressing mutants and lead to reduced susceptibilities to various antibiotics [30].

AdeDE, encoded by the *adeDE* operon in *A. pittii* [29]. AdeDE RND efflux pump lacks an outer membrane factor which raises the question if it works with an outer membrane protein from a different efflux pump in *A. pittii*. Strains lacking AdeDE have been shown to contribute to resistance to ciprofloxacin, amikacin, erythromycin, rifampin and meropenem [29]. Very few studies have been conducted to finding out the role of the AdeDE efflux pump in antimicrobial resistance.

In addition, other RND pumps have also been characterized in *A. baumannii*. AbeD is an RND transporter that is not accompanied by MFP or OMP [31]. Deletion of this transporter resulted in increased susceptibility to aminoglycosides and rifampicin [31]. Another aminoglycoside RND pump identified in *A. baumannii* AB5075, ArpAB [32]. *arpA* codes for the PAP and *arpB* codes for the RND transporter and deletion of ArpB results in increase susceptibility to aminoglycosides [32]. However, it is currently not clear how relevant these additional RND pumps are in clinical isolates of *Acinetobacter* spp.

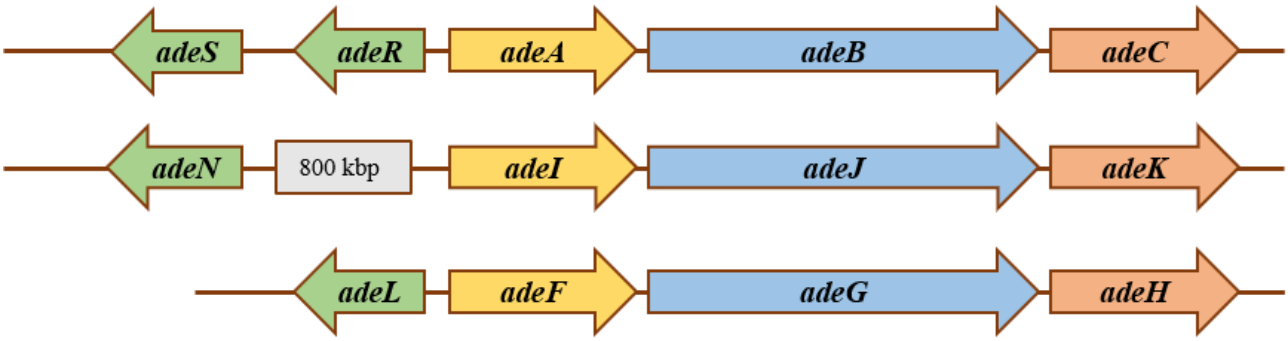

Figure 1.2 Schematic representation of operons of RND efflux systems in *A. baumannii*. Arrows represent coding sequences and indicate direction of transcription The *adeABC* operon encodes the AdeA MFP (yellow), AdeB IMP (blue), and the AdeC OMF (orange) and is regulated by AdeR-AdeS (green), encoded by *adeRS*. The *adeIJK* operon AdeI MFP, AdeJ IMP, and the AdeK OMF and is regulated by AdeN, present 800 kilobase pairs upstream of AdeI and is encoded by *adeN*. The *adeFGH* operson encodes the AdeF MFP, AdeF IMP, and the AdeH OMF and is regulated by AdeL, encoded by *adeL*.

1.1.6 Stress response in bacteria

Apart from antibiotics and dyes, bacteria experience additional stressors within the host. Bacteria need to sense and respond to diverse, complex, and harsh fluctuating environments during their lifecycle and infection process. This is crucial for their survival within a host to initiate and establish infection. Stressors include changes in pH, temperature, oxidative and nitrosative stress, heat, bile salts, osmotic changes, membrane damage and nutrient limitation/starvation [28,33,34]. Studies have shown that physiological conditions can have an effect on the gene expression patterns and cell physiology in ways that can influence antimicrobial susceptibilities [33,35]. For example, low pH and 8 mM of sodium salicylate has been shown to alter the expression of outer membrane proteins in *Serratia marcescens* and *Pseudomonas aeruginosa*, and associated with altered susceptibilities to fluroquinolones and carbapenem [33,34]. Additionally, acidic pH has been shown to enhance activity of a novel fluoroquinolone, finafloxacin, in *A. baumannii* [36]. Another study in *A. baumannii* showed that bacterial cells pretreated for 30 min at 45 °C were better able to survive streptomycin exposure than cells under physiological conditions [37]. Additionally, in response to high bile salts, *A. baumannii* shows increased motility, biofilm, and altered expression of genes involved in: (1) iron binding, (ii) Oxidoreductase, and (iii) DNA metabolism [28]. In *P. aeruginosa*, studies have found that under oxidative stress conditions, the MexAB-OprM efflux pump was shown to be overexpressed and conferring decreased susceptibility of aminoglycosides [38]. An increase in *mexXY* expression due to reactive oxygen species (ROS) suggests that a link between stress response and efflux pumps exists.

Antibiotic resistance is a natural biological phenomenon, but as shown in the examples above, it can be enhanced as a consequence of bacteria responding and adapting to environmental stressors. To understand that we need to examine the link between antimicrobial resistance and bacterial

stress response, with a particular focus on oxidative stress in the Gram-negative pathogen *A. baumannii*.

1.1.7 Oxidative Stress

Prior to oxygenation of the atmosphere, microbial life evolved in a world that was rich in iron and sulfur. About 2.4-2.8 billion years ago, with the rising amounts of oxygen in the environment, iron became scarce and organisms had to develop strategies to evolve to use oxygen and defend themselves since oxygen is a reactive chemical species [39]. Oxygen is a small, non-polar molecule which can adventitiously gain electrons from the environment and generates reduced reactive oxygen species (ROS), including superoxide anions (O_2^-), hydrogen peroxide (H_2O_2) and hydroxyl radicals (OH^-), which are harmful to the cell and can cause cell death [40]. Additionally, ROS can also cause damage to DNA, oxidation of fatty acids in lipids, and oxidation of amino acid in proteins. The shift in balance between oxidant/antioxidant in favor of oxidants is termed "oxidative stress". Aerobic organisms that live in oxygen rich environment are routinely exposed to these stressors. These reactive by products of oxygen are spontaneously generated by the unwanted electron transfer from the electron carriers to molecular oxygen as a consequence of aerobic respiration. Thus, all microorganisms have developed adaptive oxidative stress responses to allow survival in the presence of these stressors [40].

To protect themselves from oxidative stress, bacteria contain protective proteins that can detoxify ROS: (1) Superoxide dismutase, (2) Alkyl hydroperoxide reductase (AhpC), (3) catalase-peroxidases, (4) glutathione peroxidase (GPx). Superoxide dismutases catalyse the dismutation of superoxide into oxygen and hydrogen peroxide. Catalase reacts with the hydrogen peroxide to catalyse the formation of water and oxygen. Glutathione peroxidase reduces hydrogen peroxide [41]. Shortly after this discovery, *E. coli* mutants lacking cytoplasmic superoxide dismutases, sodA

and sodB, were found to grow poorly in aerobic media [42]. The slow growth of strains lacking sodA and sodB in rich medium suggests the serious damage that the cells incurred. Similar results were observed in strains lacking primary AhP and catalases [43].

1.1.8 Catalases

A focus of this study are catalases. Catalases are heme-containing enzymes that detoxify hydrogen peroxide by catalyzing its decomposition into oxygen and water. Most bacteria appear to express one or more catalases in response to peroxide stress. Catalases can also function as peroxidases, in which an organic compound is used as an electron donor.

Two types of structurally unrelated catalases are common in bacteria: a bifunctional catalase peroxidase (HPI) and a monofunctional catalase (HPII) encoded by separate, independently regulated genes [44]. Both of these types of catalases have heme as the prosthetic group. Several studies conducted in *E. coli* have given us insights into how these catalase genes are regulated. *katG*, encoding HPI, has been shown to be regulated by the OxyR regulon which responds to oxidative stress and involved in resistance to H_2O_2 [45]. HPI activity is observed in the periplasm and in cytoplasmic membrane fractions [46]. Alternatively, *katE*, encoding HPII, has been shown to be transcribed at stationary phase by the RNA polymerase containing the alternative sigma subunit σ^s, which is a product of the *rpoS* gene [44]. HPII is localized in the cytoplasm [46].

Studies conducted on *E. coli* and *Acinetobacter* spp. have shown the involvement of catalase-peroxidases in the susceptibility and degradation of H_2O_2 and antibiotic susceptibility [45,47]. Understanding how stress response and efflux mediated resistance mechanisms are regulated may help to overcome the increasing resistance in *Acinetobacter* spp.

1.1.9 Hypothesis and Research Objectives

We hypothesize that understanding the regulatory mechanisms underlying efflux will better allow us to elucidate conditions in which these pumps are expressed, providing deeper understanding of adaptive resistance mechanisms in *Acinetobacter* spp.

This hypothesis was tested through the following objectives:

1) Testing the effect of oxidative stress on antibiotic susceptibility
2) Characterize the role(s) of novel transcriptional regulator of AdeDE pump, AdeQ, with regards to antibiotic susceptibility phenotypes in *A. pittii*.

1.2 Bibliography

1. Bergogne-Bérézin E, Towner KJ (1996) *Acinetobacter* spp. as nosocomial pathogens: Microbiological, clinical, and epidemiological features. *Clinical Microbiology Reviews* 9: 148–165.
2. Gerner-Smidt P, Tjernberg I, Ursing J (1991) Reliability of phenotypic tests for identification of *Acinetobacter* species. *Journal of clinical microbiology* 29: 277–282.
3. Michalopoulos A, Falagas ME (2010) Treatment of *Acinetobacter* infections. *Expert Opinion on Pharmacotherapy* 11: 779–788.
4. Chen FJ, Huang WC, Liao YC, et al. (2019) Molecular epidemiology of emerging carbapenem resistance in *Acinetobacter nosocomialis* and *Acinetobacter pittii* in Taiwan, 2010 to 2014. *Antimicrobial Agents and Chemotherapy* 63.
5. Coyne S, Courvalin P, Périchon B (2011) Efflux-mediated antibiotic resistance in *Acinetobacter* spp. *Antimicrobial Agents and Chemotherapy* 55: 947–953.
6. Morris FC, Dexter C, Kostoulias X, et al. (2019) The Mechanisms of Disease Caused by *Acinetobacter baumannii*. *Frontiers in Microbiology* 10: 1601.
7. Shlaes DM, Bradford PA (2018) Antibiotics—From There to Where? *Pathogens and Immunity* 3: 19.
8. Calhoun JH, Murray CK, Manring MM (2008) Multidrug-resistant organisms in military wounds from Iraq and Afghanistan, *Clinical Orthopaedics and Related Research*, Springer New York, 1356–1362.
9. Biggest Threats and Data | Antibiotic/Antimicrobial Resistance | CDC Available from: https://www.cdc.gov/DrugResistance/Biggest-Threats.html.
10. Pailhoriès H, Tiry C, Eveillard M, et al. (2018) *Acinetobacter pittii* isolated more frequently than *Acinetobacter baumannii* in blood cultures: the experience of a French hospital. *Journal of Hospital Infection* 99: 360–363.
11. Lee Y-C, Huang Y-T, Tan C-K, et al. (2011) *Acinetobacter baumannii* and *Acinetobacter genospecies* 13TU and 3 bacteraemia: comparison of clinical features, prognostic factors and outcomes. *Journal of Antimicrobial Chemotherapy* 66: 1839–1846.
12. Peterson E, Kaur P (2018) Antibiotic resistance mechanisms in bacteria: Relationships between resistance determinants of antibiotic producers, environmental bacteria, and clinical pathogens. *Frontiers in Microbiology* 9: 1–21.
13. Pagano M, Martins AF, Barth AL (2016) Mobile genetic elements related to carbapenem resistance in *Acinetobacter baumannii*. *Brazilian Journal of Microbiology* 47: 785–792.
14. Leungtongkam U, Thummeepak R, Tasanapak K, et al. (2018) Acquisition and transfer of antibiotic resistance genes in association with conjugative plasmid or class 1 integrons of *Acinetobacter baumannii*. *PLoS ONE* 13.
15. Zhao Y, Hu K, Zhang J, et al. (2019) Outbreak of carbapenem-resistant *Acinetobacter*

baumannii carrying the carbapenemase OXA-23 in ICU of the eastern heilongjiang province, china. *BMC Infectious Diseases* 19: 452.

16. Lin MF, Liou ML, Tu CC, et al. (2013) Molecular epidemiology of integron-associated antimicrobial gene cassettes in the clinical isolates of *Acinetobacter baumannii* from northern taiwan. *Annals of Laboratory Medicine* 33: 242–247.

17. Seward RJ, Towner KJ (1998) Molecular epidemiology of quinolone resistance *Acinetobacter* spp. *Clinical Microbiology and Infection* 4: 248–254.

18. Houang ETS, Chu YW, Leung CM, et al. (2001) Epidemiology and infection control implications of *Acinetobacter* spp. in Hong Kong. *Journal of Clinical Microbiology* 39: 228–234.

19. Kröger C, Kary SC, Schauer K, et al. (2017) Genetic regulation of virulence and antibiotic resistance in *Acinetobacter baumannii*. *Genes* 8.

20. Kumar A, Schweizer HP (2005) Bacterial resistance to antibiotics: active efflux and reduced uptake. *Advanced Drug Delivery Reviews* 57: 1486–1513.

21. Sun J, Deng Z, Yan A (2014) Bacterial multidrug efflux pumps: mechanisms, physiology and pharmacological exploitations. *Biochemical and Biophysical Research Communications* 453: 254–267.

22. Lin L, Ling BD, Li XZ (2009) Distribution of the multidrug efflux pump genes, adeABC, adeDE and adeIJK, and class 1 integron genes in multiple-antimicrobial-resistant clinical isolates of *Acinetobacter baumannii-Acinetobacter calcoaceticus* complex. *International Journal of Antimicrobial Agents* 33: 27–32.

23. Yoon EJ, Balloy V, Fiette L, et al. (2016) Contribution of the ade resistance-nodulation-cell division-type efflux pumps to fitness and pathogenesis of *Acinetobacter baumannii*. *mBio* 7: 1–10.

24. Poole K, Krebes K, Neshat S (1993) Multiple antibiotic resistance in *Pseudomonas aeruginosa*: Evidence for Involvement of an Efflux Operon. 175: 7363–7372.

25. Coyne S, Rosenfeld N, Lambert T, et al. (2010) Overexpression of resistance-nodulation-cell division pump AdeFGH confers multidrug resistance in *Acinetobacter baumannii*. *Antimicrobial Agents and Chemotherapy* 54: 4389–4393.

26. Magnet S, Courvalin P, Lambert T (2001) Resistance-nodulation-cell division-type efflux pump involved in aminoglycoside resistance in *Acinetobacter baumannii* strain BM4454. *Antimicrobial Agents and Chemotherapy* 45: 3375–3380.

27. Damier-Piolle L, Magnet S, Brémont S, et al. (2008) AdeIJK, a resistance-nodulation-cell division pump effluxing multiple antibiotics in *Acinetobacter baumannii*. *Antimicrobial Agents and Chemotherapy* 52: 557–562.

28. López M, Blasco L, Gato E, et al. (2017) Response to bile salts in clinical strains of *Acinetobacter baumannii* lacking the AdeABC efflux pump: Virulence associated with quorum sensing. *Frontiers in Cellular and Infection Microbiology* 7.

29. Rosenfeld N, Bouchier C, Courvalin P, et al. (2012) Expression of the resistance-nodulation-cell division pump AdeIJK in *Acinetobacter baumannii* is regulated by AdeN, a TetR-type regulator. *Antimicrobial Agents and Chemotherapy* 56: 2504–2510.

30. Fernando DM, Xu W, Loewen PC, et al. (2014) Triclosan can select for an AdeIJK-overexpressing mutant of *Acinetobacter baumannii* ATCC 17978 that displays reduced susceptibility to multiple antibiotics. *Antimicrobial Agents and Chemotherapy* 58: 6424–6431.

31. Srinivasan VB, Venkataramaiah M, Mondal A, et al. (2015) Functional Characterization of AbeD, an RND-Type Membrane Transporter in Antimicrobial Resistance in *Acinetobacter baumannii*. *PLOS ONE* 10: e0141314.

32. Tipton KA, Farokhyfar M, Rather PN (2017) Multiple roles for a novel RND-type efflux system in *Acinetobacter baumannii* AB5075. *MicrobiologyOpen* 6.

33. Sumita Y, Fukasawa M (1993) Transient carbapenem resistance induced by salicylate in *Pseudomonas aeruginosa* associated with suppression of outer membrane protein D2 synthesis. *Antimicrobial Agents and Chemotherapy* 37: 2743–2746.

34. Begic S, Worobec EA (2006) Regulation of *Serratia marcescens* ompF and ompC porin genes in response to osmotic stress, salicylate, temperature and pH. *Microbiology* 152: 485–491.

35. Poole K, Krebes K, McNally C, et al. (1993) Multiple antibiotic resistance in *Pseudomonas aeruginosa*: evidence for involvement of an efflux operon. *Journal of Bacteriology* 175: 7363–7372.

36. Higgins PG, Stubbings W, Wisplinghoff H, et al. (2010) Activity of the investigational fluoroquinolone finafloxacin against ciprofloxacin-sensitive and -resistant *Acinetobacter baumannii* isolates. *Antimicrobial Agents and Chemotherapy* 54: 1613–1615.

37. Cardoso K, Gandra RF, Wisniewski ES, et al. (2010) DnaK and GroEL are induced in response to antibiotic and heat shock in *Acinetobacter baumannii*. *Journal of Medical Microbiology* 59: 1061–1068.

38. Fraud S, Poole K (2011) Oxidative stress induction of the MexXY multidrug efflux genes and promotion of aminoglycoside resistance development in *Pseudomonas aeruginosa*. *Antimicrobial Agents and Chemotherapy* 55: 1068–1074.

39. Anbar AD (2008) Oceans: Elements and evolution. *Science* 322: 1481–1483.

40. Imlay JA (2013) The molecular mechanisms and physiological consequences of oxidative stress: Lessons from a model bacterium. *Nature Reviews Microbiology* 11: 443–454.

41. Fridovich I (1978) The Biology of Oxygen Radicals. *Science* 201: 875–880.

42. Carlioz A, Touati D (1986) Isolation of superoxide dismutase mutants in *Escherichia coli*: is superoxide dismutase necessary for aerobic life? *The EMBO journal* 5: 623–630.

43. Seaver LC, Imlay JA (2001) Alkyl hydroperoxide reductase is the primary scavenger of endogenous hydrogen peroxide in *Escherichia coli*. *Journal of Bacteriology* 183: 7173–

7181.

44. Mulvey MR, Switala J, Borys A, et al. (1990) Regulation of transcription of *katE* and *katF* in *Escherichia coli*. *Journal of Bacteriology* 172: 6713–6720.

45. Sun D, Crowell SA, Harding CM, et al. (2016) KatG and KatE confer *Acinetobacter* resistance to hydrogen peroxide but sensitize bacteria to killing by phagocytic respiratory burst. *Life Sciences* 148: 31–40.

46. Heimberger A, Eisenstark A (1988) Compartmentalization of catalases in *Escherichia coli*.

47. Loewen PC, De Silva PM, Donald LJ, et al. (2018) KatG-mediated oxidation leading to reduced susceptibility of bacteria to kanamycin. *ACS Omega* 3: 4213–4219.

Chapter 2 Understanding the impact of oxidative stress on resistance-nodulation-division efflux pump-mediated antibiotic susceptibility in *Acinetobacter baumannii*

2.1 Introduction

Acinetobacter baumannii is an opportunistic pathogen known to cause nosocomial infections such as pneumonia, meningitis, and wound infections with high mortality in immunocompromised patients [1]. The increase in outbreaks of multi-drug resistant *A. baumannii* is of great concern. It is intrinsically resistant to a wide range of antimicrobials, long term desiccation, nutrient starvation, and reactive oxygen species (ROS) [1,2]. *A. baumannii* has the ability to form biofilm on both abiotic and biotic surfaces [3]. These factors combined with an increase in occurrences of outbreaks worldwide has led the World Health Organization to classify *A. baumannii* as a priority 1 (critical) pathogen [4].

Efflux pumps, membrane proteins that export substrates out of bacterial cell, have been largely implicated to play an important role in multidrug resistance in Gram-negative bacteria [5]. The major clinically relevant efflux systems are of the RND superfamily. These are tripartite complexes typically composed of an inner membrane protein (IMP), a periplasmic adapter protein (PAP; also called the membrane fusion protein, MFP), and an outer membrane factor (OMF) channel [6]. In recent studies, efflux pumps have been shown to have important functions in many other cellular processes, such as resistance to stress conditions [7]. It is important that we study the regulatory mechanisms involved in efflux-mediated resistance and stress tolerance.

Catalase-peroxidases are found in bacteria as well as fungi and have been the focus of study for quite some time. These enzymes decompose H_2O_2 into water and oxygen and protect the cell from the toxic effects of H_2O_2. Catalase positive pathogens such as *A. baumannii* and *Legionella pneumophila* make catalase to deactivate peroxide radicals to reduce the effect of reactive oxygen species.

In *Acinetobacter* species there are four catalase genes, *katA*, *katE*, *katG*, and *katX* [8]. Analogous to *E. coli*, results observed in *A. baumannii* also showed involvement of *katG* and *katE* in susceptibility and degradation of H_2O_2, respectively [8]. Further, in previously published findings from our group, it was shown that catalase plays a role in the susceptibility to *A. baumannii* to aminoglycoside antibiotics [9]. Aminoglycosides are the substrates of the AdeAB efflux pump of *A. baumannii* [10]. Therefore, the purpose of the study was to investigate the role of AdeAB pump in catalase-mediated aminoglycoside susceptibility of *A. baumannii*.

2.2 Materials and Methods

2.2.1 Bacterial Strains, Plasmids, and Oligonucleotides

All the bacterial strains and their characteristics are described in Table 1. All primers used in this study are described in table 2.

Table 2.1. List of bacterial strains and plasmids used in this study.

Strain or Plasmid	Characteristics	Reference or Source
A. baumannii ATCC17978	Type-strain	ATCC
A. baumannii AB155	ATCC17978:Δ*katG*	This Study
A. baumannii AB188	ATCC17978:Δ*katE*	This Study
A. baumannii AB189	ATCC17978:Δ*katG* Δ*katE*	This Study
A. baumannii AB363	ATCC17978:Δ*katG* Δ*katE*::*lacI*^{q} *katG*	This Study
A. baumannii AB364	ATCC17978:Δ*katG* Δ*katE*::*lacI*^{q} *katE*	This Study
A. baumannii AB370	ATCC17978:Δ*katG*::*lacI*^{q} *katG*	This Study
A. baumannii AB376	ATCC17978:Δ*katE*::*lacI*^{q} *katE*	This Study
E. coli DH5*α*	F– Φ80lacZΔM15 Δ(lacZYA-argF) U169 *recA1 endA1 hsdR17* (rK–, mK+) *phoA supE44* λ– thi-1 *gyrA96* relA1	Laboratory collection
E. coli SM10	*thi thr leu tonA lacY supE recA*::RP4-2-Tc::Mu Km λpir	Laboratory collection
pMO130	Suicide vector, Km^{r}	[11]
pUC18T-miniTn*7*-Gm-LAC	Single copy insertion vector, Gm^{r}, Amp^{r}	[12]
pFLP2	Plasmid expressing Flp-recombinase, Amp^{r}	[12]
pTNS2	Plasmid expressing transposon insertion machinery	Laboratory collection
pRK2013	Helper plasmid for conjugation, Kan^{r}	Laboratory collection
A. baumannii AB246	ATCC17978:Δ*adeN*::*lacI*^{q}*-adeN*	Laboratory collection

Table 2.2. List of primers used in this study.

Primer name	Sequence	Target gene/purpose	Reference
adeB qRT F	GGATTATGGCGACTGAAGGA	*adeB*, Gene expression	Kumar Lab collection
adeB qRT R	AATACTGCCGCCAATACCAG		
adeG qRT F	CGTAACTATGCGGTGCTCAA	*adeG*, Gene expression	Kumar Lab collection
adeG qRT R	ATCGCGTAGTCACCAGAACC		
adeJ qRT F	CATCGGCTGAAACAGTTGAA	*adeJ*, Gene expression	Kumar Lab collection
adeJ qRT R	GCCTGACCATTACCAGCACT		
16S qRT F	CTTCGGACCTTGCGCTAATA	16S, Reference gene expression	Kumar Lab collection
16S qRT R	ATCCTCTCAGACCCGCTACA		
adeR qRT F	GAGTGTTATTCGGGCCATGA	*adeR*, Gene expression	Kumar Lab collection
adeR qRT R	CCAACCGTTTAATTCGGGTA		
ABglmS_F_N	TATGGAAGAAGTTCAGGCTC	Screening primers for insertion from mini-Tn*7* vectors into *att*Tn*7* site	This study
Tn7R	CACAGCATAACTGGACTGATTTC		
KatG-FL-Fwd-PstI	CAGAATATAATCATGTCAA	Amplification of full length *katG* with *Pst*I and *Hind*III restriction sites for cloning into pUC18T-miniTn*7*-Gm-LAC	This study
KatG-FL-Rev-HindIII	TCGAGAAGGGCATAAA		
KatE-FL-Fwd-SacI	GCTCTTTCAAAAACATAGGTAATG	Amplification of full length *katE* with *Sac*I and *Hind*III restriction sites for cloning into pUC18T-miniTn*7*-Gm-LAC	This study
KatE-FL-Rev-HindIII	TACTGCAGTTTAGAAAAAGCCCTG		
katG qRT F	AGAGCTCAAGGCATCAACCC	*katG*, Gene expression	This study
katG qRT R	GTCAGCAAGACCGAGCAGTA		
katE qRT F	GCGGCATCAAATGGTGGTTT	*katE*, Gene expression	This study
katE qRT R	GCGGTGCAAGGCTTTTGTAA		

2.2.2 Media and Growth Conditions

Lysogeny broth (LB) Lennox and LB agar (Difco Laboratories, Mississauga, ON, Canada) was used for culturing bacterial strains unless stated differently. The culture conditions for liquid medium were at 37°C shaking at 250 rpm unless stated otherwise.

2.2.3 DNA extraction

Genomic DNA extraction was carried out using 3 mL of liquid overnight culture using a commercially available bacterial DNA isolation kit (Norgen Biotek Corp, ON, Canada) and following the manufacturer's instructions. Plasmid DNA extraction were performed using BioBasic Plasmid Miniprep Kit (BioBasic Inc. Markham, ON, Canada) following manufacturer's instructions. gDNA and plasmid DNA were eluted in 50 µL of the supplied buffers from each kit.

2.2.4 DNA Manipulations

2.2.4.1 PCR

Genomic DNA and plasmids extracted using the above-mentioned protocols were used as templates for general PCR reactions. Taq DNA polymerase (Froggabio, ON, Canada) or Q5 DNA polymerase (NEB, Pickering, Canada) were used in all reactions following the manufacturer's instructions. dNTPs (FroggaBio) were used at a concentration of 100µM. Primers were all purchased from IDT (Integrated DNA Technologies, Toronto, ON, Canada) and diluted to 9µM for all PCRs.

2.2.4.2 Splice Overlap Extension PCR (SOEing PCR)

Splice Overlap Extension (SOEing) PCR was the choice of PCR technique used to construct the knockout cassettes for the gene deletions in *A. baumannii* [13]. SOEing PCR was carried out following a previously described method [13] with modifications using the primers listed in Table 2.2. Briefly, the forward set of primers amplifying a ~1kb upstream region of the desired gene and

the reverse set of primers amplifying a ~1kb downstream region of the desired gene were used in two separate PCR reactions with Taq DNA polymerase. The *aacC1* (Gm^R) gene conferred resistance to gentamicin along with the FRT sites were also amplified using Taq DNA polymerase and each fragment was gel extracted. These fragments were used as templates for the SOEing PCR reaction using Taq DNA polymerase. The reaction mixture consisted of 50 ng of each fragment as template and contents of a Taq DNA polymerase PCR reaction mixture with the exception of primers. This PCR was cycled for 3 times with an annealing temperature of 55°C after which the PCR reaction was paused, and the upstream forward and the downstream reverse primers were added and cycled for 30 times with an annealing temperature specific to the primers used to facilitate the amplification of the ~3kb knockout cassette. The knockout cassette was then gel extracted and used to ligate into the suicide vector used.

2.2.4.3 Restriction Digestion and Ligation

All restriction digestion reactions were performed using enzymes from NEB (New England Biolabs, ON, Canada). Restriction digestion conditions were as follows, 2.5 μL of buffer, 1 unit of enzyme and, up to 1 μg of DNA in a total reaction volume of, 25 μL made up with water. Incubation times ranged from 60-120 minutes at 37^{o}C unless otherwise indicated.

DNA ligations were performed using T4 DNA ligase (Thermo Fisher Scientific, MA, USA) using the manufacturers conditions in a reaction volume of 10 μL. Sticky end ligations were done using a 3:1 insert to vector molar ratio while blunt end was done using a 6:1 insert to vector molar ratio. DNA concentrations were determined using the nanodrop (Thermo Fisher). In all ligations 50 ng of digested vector was used and incubated at 16°C overnight.

2.2.5 Preparation of Competent Cells

2.2.5.1 Chemically Competent Cells

Overnight cultures of *E. coli* cells were subcultured 1:100 (v/v) in 125 mL of fresh LB and grown to A600 nm of 0.4-0.6. Cultures were pelleted by centrifugation at 5000xg for 5 minutes at 4°C. While maintaining cells on ice supernatant was decanted before resuspending in 40% of the original culture volume of ice-cold TFB1 buffer (100 mM rubidium chloride, 50 mM manganese chloride, 30 mM potassium acetate, 10 mM calcium chloride, and 15% w/v glycerol; pH 5.8) and incubated for 5 minutes on ice. The cell suspension was centrifuged again at 5000 xg for 5 minutes at 4°C and the supernatant was discarded. The cell pellet was resuspended in 5 mL of sterile ice-cold TFB2 buffer (10mM MOPS, 10 mM rubidium chloride, 75 mM calcium chloride, and 15% w/v glycerol; pH 6.5) and incubated on ice for 30 – 60 minutes. 100 µL aliquots of the cells were then placed onto pre-chilled 1.5 mL microfuge tubes and frozen immediately in a dry ice/ethanol bath for 30 – 40 seconds. The frozen cells were immediately transferred to the -70°C freezer and stored there until used [14].

2.2.6 Transformation of Competent Cells

2.2.6.1 Chemical Transformations

Chemical transformation of *E. coli* were done using the heat shock method [15]. 5 µL of ligation mixture was incubated on ice with 50 µL chemically competent cells for 20 minutes. Transformation mixtures were then heat shocked at 42°C for 45 seconds and then allowed to rest for 2 minutes on ice before recovery in Super Optimal Broth (SOC) (Oxoid Inc., Nepean, ON, Canada) for 90 minutes at 37°C. Post recovery cells were pelleted at 10000 xg for 2 minutes and resuspended in 100 µL of SOC broth before plating the transformed cells on appropriate plates.

2.2.6.2 Electrocompetent cells

Electrocompetent cells were prepared for *A. baumannii* strains when prepared prior to the experiments. *A. baumannii* cells were grown overnight and 4 mL of the overnight culture was transferred to a 1.5 mL microfuge tube and centrifuged at 10000 xg for 2 minutes. The supernatant was discarded, and the cells were resuspended in 1 mL of sterile ice-cold distilled water and centrifuged again at 10000 xg for 2 minutes. This was repeated for another two more times and the cell pellet was resuspended in 100 µL of sterile ice-cold distilled water and placed on ice until use [16].

2.2.6.3 Electroporation

Freshly made electrocompetent *A. baumannii* cells were transferred into 2 mm electroporation cuvettes (Thermo Fisher Scientific) and then mixed with 200 ng of the DNA to be transformed [16]. The mixture was incubated on ice for 20 minutes and then electroporated at 2.0 kV in an Eppendorf Electroporator 2510 (Eppendorf, Mississauga, ON, Canada) and 1mL of prewarmed SOC was immediately added following charge. The entire content of the cuvette was transferred into a 1.5 mL microfuge tube. The time constant was observed for each electroporation and any reaction with less than 5 ms time constant was discarded. The microfuge tubes were then incubated for 1 hour at 37°C with shaking to facilitate the outgrowth of transformed cells. The culture was then centrifuged at 10000 xg for 2 minutes and the supernatant was discarded. The cell pellet was resuspended in 150 µL of sterile LB and spread plated onto LB agar plates with the appropriate antibiotics.

2.2.7 Gene Deletions in *Acinetobacter baumannii*

For gene deletions, the suicide plasmid created by SOE PCR (section 1.2.4.2) was introduced in cells using conjugation (section 1.2.8) or electroporation (section 1.2.6.3). Cells that contained the successful integration of the suicide plasmid via the first recombination event were selected on LB

agar supplemented with 50 μg/mL gentamicin and 50 μg/mL kanamycin. To select for the second recombination event required for the curing of the suicide plasmid, the *sacB* gene present on the pMO130 backbone was utilized. *sacB* encodes an enzyme from *B. subtilis* called levansucrase which converts sucrose into levans, a lethal compound for Gram positive bacteria [17]. Merodiploid colonies were streaked onto Vogel-Bonner minimal medium (VBMM) agar [18] supplemented with 10% sucrose (BioBasic) and 30μg/mL gentamicin and incubated at 30°C for 48 hours. Colonies from these plates were patched on 50μg/mL gentamicin LB agar and 50μg/mL kanamycin LB agar. Colonies that retained resistance to gentamicin and but displayed susceptibility to kanamycin had undergone the second recombination event resulting in a marked deletion of the target gene. Gene disruptions were further confirmed by PCR using the primers flanking the target gene with a PCR product of ~3kb as compared to the size of the wild type gene.

To achieve the markerless deletion of the target gene, conjugations were set up with *E. coli* SM10 harbouring pFLP2 plasmid and the *A. baumannii* strains with the genes disrupted with the knockout cassette containing the Gm^R marker [13]. Conjugations were carried out as described above with overnight cultures of both strains and conjugation mixtures were incubated for 16 hours at 30°C. After the incubation period, the conjugation mixtures were plated onto Simmons citrate agar supplemented with 200μg/mL carbenicillin to select for the *A. baumannii* colonies with the pFLP2 plasmid present. These colonies were cross patched onto LB agar supplemented with 50μg/mL gentamicin and LB agar supplemented with 200μg/mL carbenicillin to screen for the loss of Gm^R marker. Colonies that were only able to grow on carbenicillin were streaked onto LB+10% sucrose to facilitate the curing of the pFLP2 plasmid. The colonies from the LB+10% sucrose was then cross patched onto 50μg/mL gentamicin, 200μg/mL carbenicillin, and LB agar

to phenotypically reconfirm the loss of Gm^R marker as well as pFLP2 plasmid. The gene deletion strategy is shown in Appendix 7.

2.2.8 Conjugation

Conjugations were performed using a previously described method [19]. Briefly 200 μL of overnight cultures were mixed together in 1.1 mL of LB broth. The mixture was then centrifuged at 10000 xg for 2 minutes to pellet the cells and the supernatant was discarded. The cell pellet was washed three times using sterile LB to remove residual antibiotics from the overnight growth medium. After washing, the cell pellet was resuspended in 10 μL of sterile LB and spotted onto a sterile 3cm x 3cm nitrocellulose filter paper placed on a pre-warmed LB agar plate. The spot was allowed to dry and then incubated at 30°C for 16 hours to facilitate conjugation. After the incubation period, the nitrocellulose filter paper was carefully removed from the LB agar plate and placed into a 1.5 mL centrifuge tube containing 400 μL of sterile 0.85% saline. The bacterial cells were carefully mixed with the saline to remove it from the nitrocellulose paper into the saline. The nitrocellulose paper was then removed and the saline containing the bacterial cells was then plated onto Simmons citrate agar (Sigma-Aldrich, St. Louise, MO, USA) plates supplemented with 50μg/mL kanamycin. These plates were then incubated at 37°C for 48 hours or until colonies appeared. After incubation, colonies were patched on LB agar plates supplemented with 50 μg/mL kanamycin and 50μg/mL gentamicin (BioBasic), respectively. Patches resistant to both kanamycin and gentamicin, representing merodiploid cells with successful insertion of the suicide plasmid, were selected for the next step of curing of the suicide plasmid.

2.2.9 Genetic Complementation

2.2.9.1 Creating chromosomal insertions for gene complementations

katG and *katE* gene deletions in *A. baumannii* ATCC 17978 were made by Dr. Malaka De Silva (unpublished) using the homologous recombination method previously described. *katG* was deleted leaving 3 bp in the 5′-end and 9 bp in the 3′-end of the gene, resulting in a deletion of 2139 bp from 2154 bp long gene. In the case of *katE,* a total of 1869 bp were deleted from the full gene 2139 bp leaving 247 bp in the 5′-end and 25 bp in the 3′-end. Both gene deletions were confirmed initially with PCR. *katG* and *katE* were inserted in a single copy insertion system using miniTn*7* system [20]. *katG* and *katE* were cloned into the pUC18-miniTn*7*-Gm-LAC plasmid which utilizes the *lacI*^{q} repressor system and a P*tac* promoter allowing for induction with Isopropyl ß-D-1-thiogalactopyranoside (IPTG). Plasmids with the full-length gene of *katG* and *katE* were introduced into ATCC17978; Δ*katG*, ATCC17978; Δ*katE*, ATCC17978; Δ*katG* Δ*katE* with the pTNS2 plasmid which contains genes encoding enzymes necessary to insert the transposon into the target chromosome [20]. After electroporation cells were plated on 50µg/mL gentamicin LB agar and screened for insertion of the *katG*, *katE* gene downstream of *glmS2* via PCR primers listed in Table 2.2.

2.2.10 Quantitative Reverse Transcriptase PCR (RT-qPCR)

2.2.10.1 RNA extraction, DNase Treatment, and cDNA synthesis

Overnight cultures were sub-cultured in a 1:100 (v/v) ratio into fresh LB broth and grown to an OD_{600} of 0.6-0.8. Once reaching the desired OD_{600}, 1.5 mL of each culture was pelleted using centrifugation and the supernatant was removed. Pelleted cells were stored in -70°C overnight before total RNA extraction using a RNeasy Mini Kit (Qiagen Sciences Inc, Maryland, USA) according to the manufacturer's protocol. Sterile Milli-Q water was used to make 1 µg/µL solutions of RNA before carrying out DNase treatments using a RNase Free DNase Set (Qiagen) according to the manufacturer's protocol. DNase-treated RNA was converted to complimentary DNA

(cDNA) using a SuperScript VILO cDNA Synthesis Kit (Invitrogen, Burlington, Canada) according to the manufacturer's protocol. For RT-qPCR, SYBR Select Master Mix (Applied Biosystems Inc, Foster City, USA) was used for catalysis and fluorescent detection of product DNA on a StepOnePlus Real-Time PCR System (Applied Biosystems Inc). To ensure there was no genomic contamination of cDNA samples DNase treated RNA was used as a negative control for all primer sets in addition to a No-Template-Control which substituted water for cDNA. Relative expression was calculated using 16S rRNA as the reference gene by Pfaffl method [21]. DNA primers used to target each gene of interest are listed in Table 2.2.

2.2.11 Phenotypic Testing

2.2.11.1 Fitness in rich medium

Overnight cultures of bacterial cells were standardized to an OD 0.1 and 150µL of each standardized culture was then distributed into 3 wells of a round bottom 96 well polystyrene microtitre plate (Sarstedt, Montreal, QC, Canada). Plates were then incubated at 37°C in a SpectraMax M2 plate reader (Molecular Devices, CA, USA) with shaking at 200 rpm before each reading which occurred every thirty minutes unless stated differently. Three biological replicates were used for all strains.

2.2.11.2 ROS Generation Assay

Dichloro-dihydro-fluorescein diacetate (DCFH-DA) (BioBasic) is used for the ROS detection assay [22]. The overnight grown culture is sub-cultured and incubated at 37°C and 180 rpm, till an OD600 of 0.3 is reached. These cells are then washed and resuspended in 1X PBS and then incubated with DCFH-DA at 100µM for 30 minutes at 37ºC, 180 rpm. Cells are washed and resuspended in 1X PBS following which they are added to the compounds/antibiotics at varying concentrations in the Corning half area black plate and a kinetic fluorescence spectrum is run at

an excitation wavelength of 485 nm and emission wavelength of 528 nm for 20 mins with readings taken every 5 minutes using a plate reader. Methyl viologen (Thermo Fisher) is used as positive control and untreated cells as negative control. Fluorescence measured is normalized by OD600 to give Relative fluorescence units (RFU).

2.2.11.3 Antibiotic Susceptibility Testing

Antibiotic susceptibility testing was performed by the broth microdilution method described by the Clinical and Laboratory Standards Institute using at least three biological replicates [23]. Antibiotics were chosen to represent a broad variety of substrates of efflux pumps in *A. baumannii*. Results are shown as the Minimum Inhibitory Concentration (MIC) of the antibiotic that inhibited visible growth of the culture.

2.2.11.4 Hydrogen Peroxide (H_2O_2) Sensitivity Assay

Cultures were grown overnight with shaking at 37 °C. Following day, cultures are standardized to a 0.5 McFarland and 50 µL of standardized cells were diluted (1:10 v/v) of 0.85% NaCl (Saline). 10 µL of the dilutions were plated on LB agar supplemented with 1 mM H_2O_2 (+/- 1mM IPTG). After spotting plates were dried in the Bio Safety Cabinet (BSC) for 20 mins and incubated overnight at 37°C.

2.2.12 RNA – Sequencing (RNA-Seq) And Data Analysis

RNA extraction of the bacterial cultures for RNA-Seq was performed as described in the section 1.2.10.1 for RT-qPCR from two biological replicates and sent for sequencing on dry ice to Centre d'expertise et de services (Génome Québec Montréal, Québec, Canada) for sequencing using the Illumina MiSeq platform. Raw reads from sequencing were received and analysed for quality of the reads using Fast QC: a quality control tool for high throughput sequence data (Andrews S. 2010). It is available online at: (http://www.bioinformatics.babraham.ac.uk/projects/fastqc). The

reads were imported to Geneious Prime software for further analysis using the built-in plugins. The reads obtained from the sequencing data were aligned to the publicly available complete genome sequence of *A. baumannii* ATCC17978 (NCBI Reference Sequence: NZ_CP018664.1). Differential expression of the genes along with the statistical significance was calculated using the default modules in Geneious Prime (San Diego, California USA). Annotation table with the output of the differentially expressed genes was exported into Microsoft excel spreadsheet for further analysis. A log2 1.5-fold change with a $P<0.05$ was used as a cut-off to select the significant genes that were either up or downregulated for further analysis.

2.3 Results

2.3.1 Confirmation of unmarked complementation strains in ATCC 17978 via RT-qPCR

Complementation of *katG* and *katE* into ATCC17978: Δ*katG*, ATCC17978: Δ*katE* and ATCC17978: Δ*katG* Δ*katE* downstream of *glmS2* was confirmed by end point PCR (Fig 2.1). The insertion was confirmed by the use of GlmS_Fwd and Tn7_Rev primers listed in Table 2.2.2. The expected band-size for an unmarked complementation was 368bp (Fig 2.1).

Additionally, RT-qPCR was used to assess the expression of *katG* and *katE* in the deletion and complemented strains. ATCC17978:Δ*katG* and ATCC17978:Δ*katE* showed no expression of *katG* and *katE*, respectively confirming that the deletion mutants were constructed properly. ATCC17978:Δ*katG*::*lacI*^{q}-*katG*, ATCC17978:Δ*katE*::*lacI*^{q}-*katE*, ATCC17978:Δ*katG* Δ*katE*::*lacI*^{q}-*katG*, and ATCC17978:Δ*katG* Δ*katE*:: *lacI*^{q}-*katE* showed restoration of phenotype to wild-type ATCC 17978 upon induction with IPTG, thereby confirming the unmarked complementation.

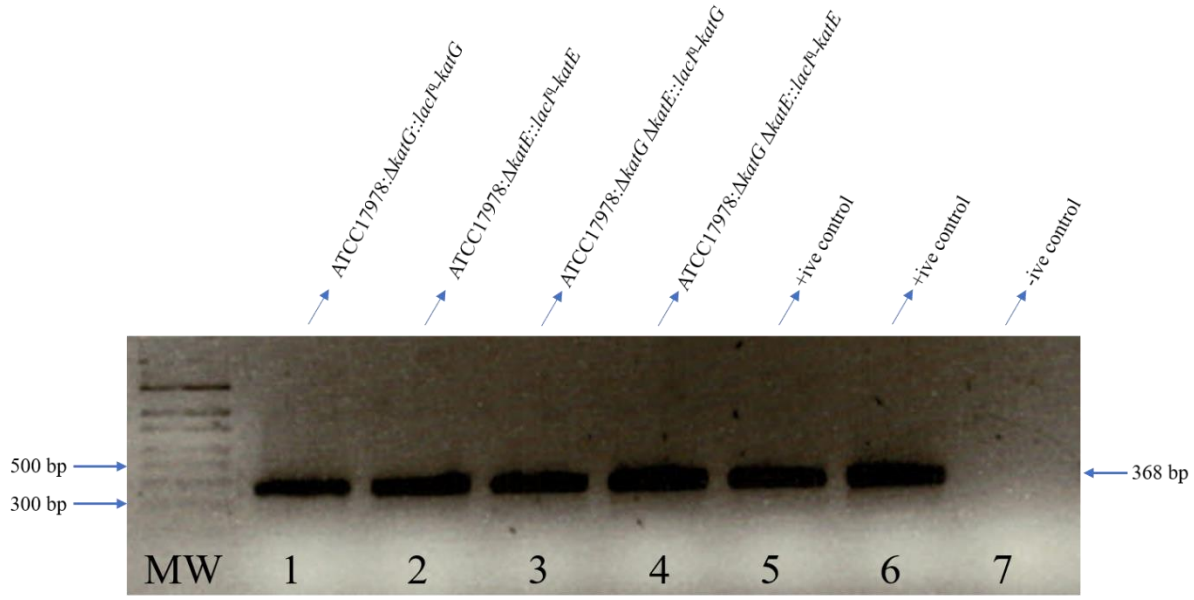

Figure 2.1. Creation of *katG* and *katE* complementation in ATCC17978.

Agarose gel electrophoresis of the PCR product produced using GlmS_Fwd and Tn*7*_Rev primers (Table 2.2.2) to confirm inserttion of miniTn*7* constructs. Expected product size for miniTn*7* insertion downstream of *glmS2* = 368bp. MW = 100 bp molecular weight marker (New England Biolabs). Lane 1 = ATCC17978:Δ*katG*::*lacI*^{q}-*katG*, Lane 2 = ATCC17978:Δ*katE*::*lacI*^{q}-*katE*, Lane 3 = ATCC17978:Δ*katG* Δ*katE*::*lacI*^{q}-*katG*, Lane 4 = ATCC17978:Δ*katG* Δ*katE*::*lacI*^{q}-*katE*, Lane 5 = ATCC17978:Δ*adeN*::*lacI*^{q}-*adeN*, Lane 6 = ATCC17978:Δ*adeN*::*lacI*^{q}-*adeN*, Lane 7 = No template control (NTC).

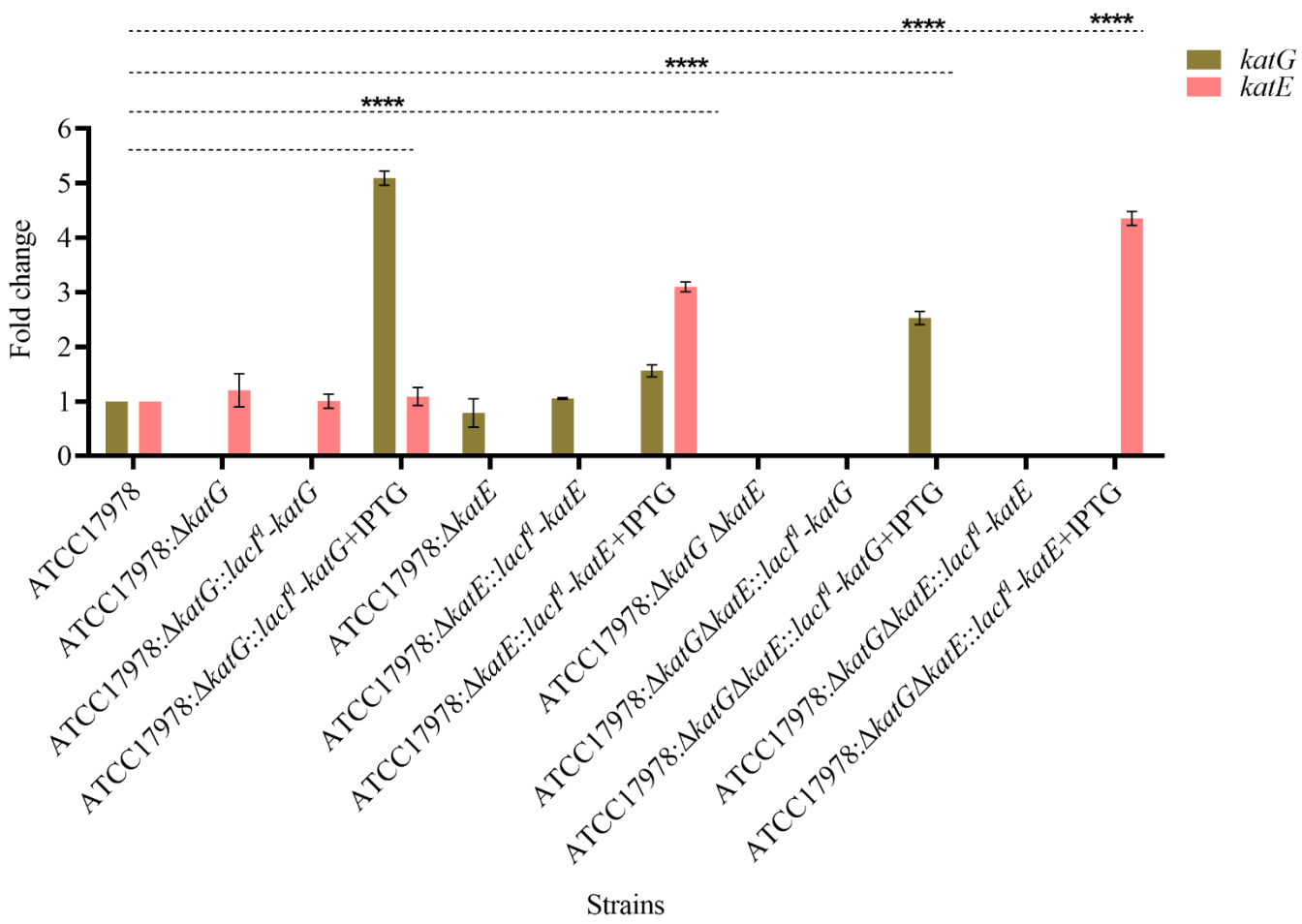

Figure 2.2. Expression of *katG* and *katE* in *A. baumannii* ATCC 17978.
The deletion and complementation of *katG* (brown) and *katE* (pink) was confirmed using RT-qPCR. 16S rRNA gene was used as the housekeeping control. The expression is normalized relative to the expression of *katG* and *katE* in the wildtype strain ATCC17978. IPTG inducible strains were induced with 1mM IPTG between OD 0.45-0.55. Error bars represent standard deviation. **** indicates $P<0.0001$determined via 2-way ANOVA statistical test. Graph generated in GraphPad Prism 6.0 (San Diego, California USA).

2.3.2 Fitness of bacterial strains in rich media (LB) with H_2O_2

Strains grown in LB are fit and do not have any apparent growth defects apart from the *katG* deletion and the double deletion mutant exhibiting significantly slower growth until 7 hours, however, growth is recovered to wild-type levels after 12 hrs. Complemented strains restored their phenotype to wild-type levels (Figure 2.3). When supplemented with 1mM H_2O_2, AB155 (ATCC17978; Δ*katG*), AB189 (ATCC17978:Δ*katG* Δ*katE*) and the uninduced complements suffered a major growth defect which is not surprising to see as AB189 is lacking both catalase genes and is therefore not able to grow well under exposure of H_2O_2. These results indicate that oxidative stress has a significant effect on the fitness of these strains.

2.3.3 Increased sensitivity of strains to H_2O_2

Exposure to H_2O_2 has a negative impact on fitness of these strains. Therefore, we sought to assess the sensitivity of these strains to H_2O_2. AB155 (ATCC17978; Δ*katG*) and AB188 (ATCC17978; Δ*katE*) show a moderate increase in sensitivity to H_2O_2 whereas AB189 (ATCC17978:Δ*katG* Δ*katE*) showed a drastic increase in sensitivity to H_2O_2 (Fig 2.5). Complemented strains show restoration of phenotype to wild type level.

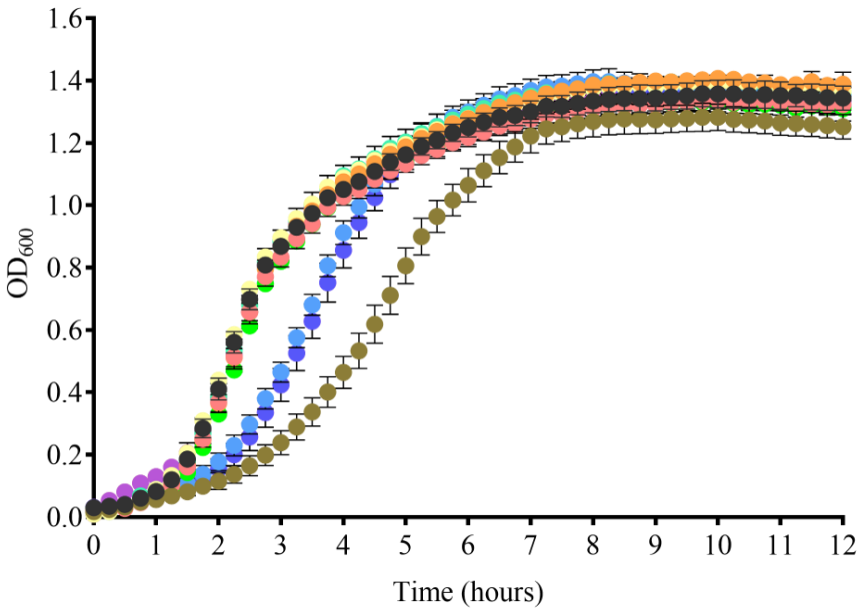

	4 hrs	6 hrs	12 hrs
ATCC17978			
ATCC17978:Δ*katG*	****	****	
ATCC17978:Δ*katG::lacI*^{q}-*katG*			
ATCC17978:Δ*katG::lacI*^{q}-*katG*+IPTG			
ATCC17978:Δ*katE*			
ATCC17978:Δ*katE::lacI*^{q}-*katE*			
ATCC17978:Δ*katE::lacI*^{q}-*katE*+IPTG			
ATCC17978:Δ*katG* Δ*katE*	***		
ATCC17978:Δ*katG* Δ*katE::lacI*^{q}-*katG*			
ATCC17978:Δ*katG* Δ*katE::lacI*^{q}-*katG*+IPTG			
ATCC17978:Δ*katG* Δ*katE::lacI*^{q}-*katE*			
ATCC17978:Δ*katG* Δ*katE::lacI*^{q}-*katE*+IPTG			

Figure 2.3. Fitness of bacterial strains in rich media (LB).
Growth curve of *A. baumannii* catalase-peroxidases strain derivatives. Growth was done in rich media (LB) and monitored for 12 hrs with continuous shaking at 37°C. IPTG induction was done overnight. Data shown is of 3 biological replicates. Statistical significance observed between the strains was determined by one-way ANOVA *indicates $P<0.05$. Graph generated in GraphPad Prism 6.0 (San Diego, California USA).

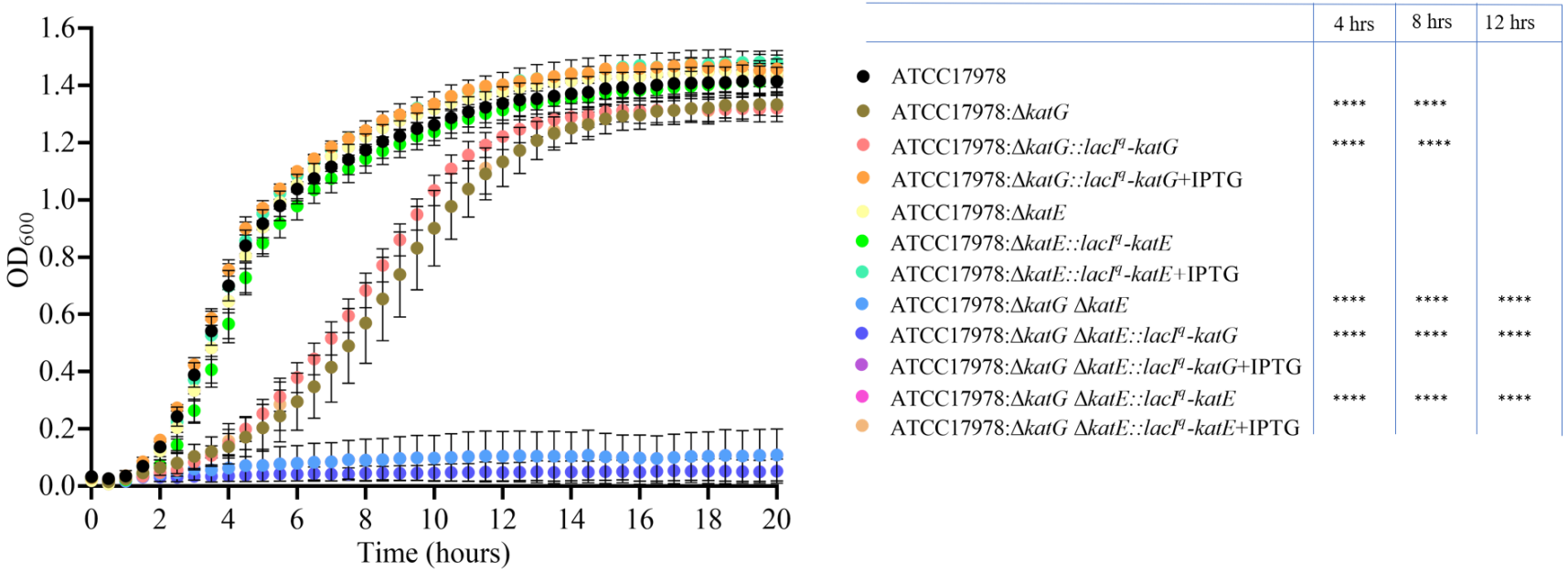

Figure 2.4. Fitness of strains in rich media (LB) with 1mM H_2O_2.
Growth curve of *A. baumannii* catalase-peroxidases strain derivatives. IPTG induction was done overnight. Strains were standardized with 1mM of H_2O_2 and monitored for 20 hours with continuous shaking at 37°C. Data shown is of 3 biological replicates. Statistical significance observed between the strains was determined by one-way ANOVA *indicates $P<0.05$. Graph generated in GraphPad Prism 6.0 (San Diego, California USA).

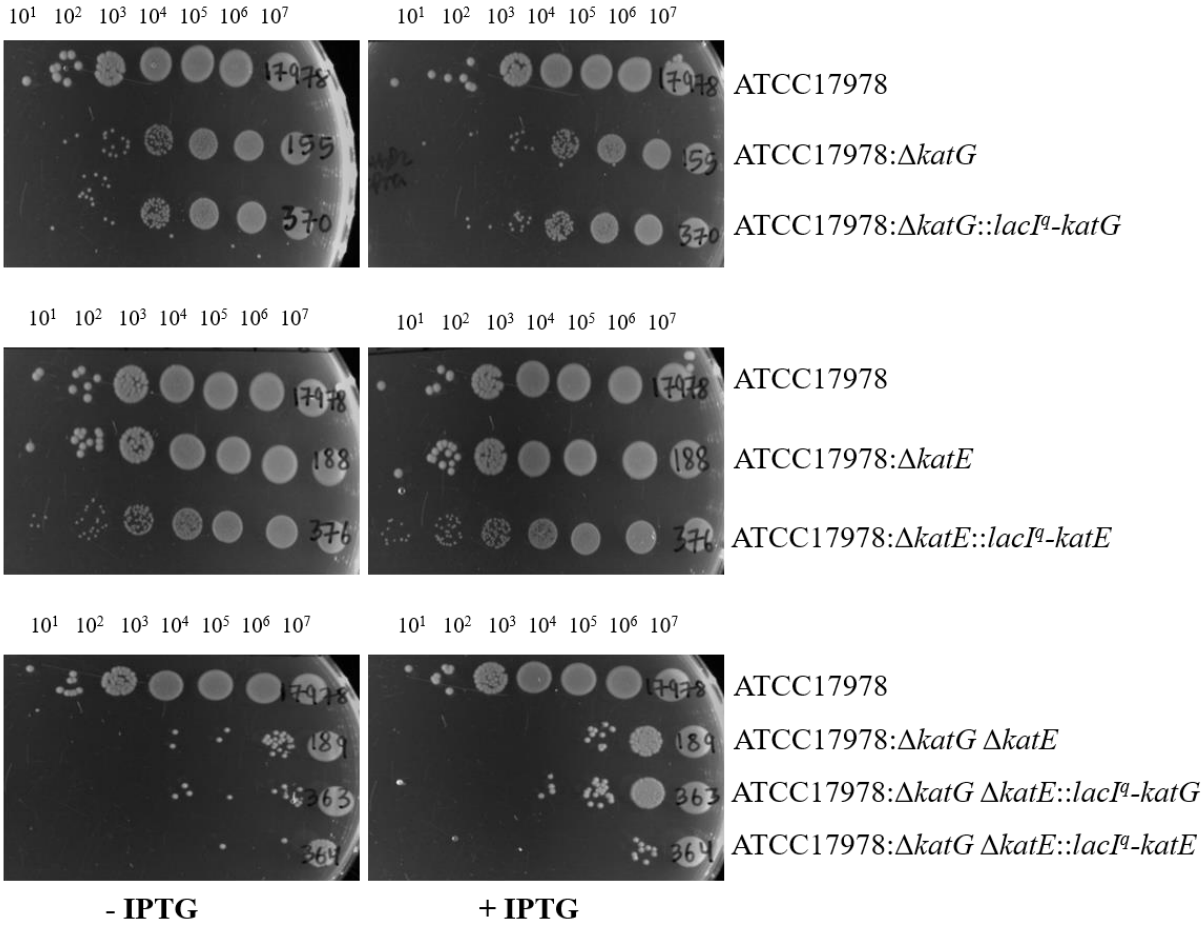

Figure 2.5. Sensitivity of bacterial strains to H_2O_2.
Cultures were grown overnight in LB +/- IPTG. Next day, cultures were standardized to 0.5 McFarland followed by dilutions 10^{7}, 10^{6}, 10^{5}, 10^{4}, 10^{3},10^{2}, 10^{1} and spotted on LB plates containing 1mM H_2O_2 +/- IPTG.

2.3.4 Increased reactive oxygen species (ROS) production in *katG/katE* deletion mutants

Strains exposed to DCF-DA resulted in increased ROS generation in *katG* and *katE* deletion mutants over the period of 20 minutes compared to ATCC 17978 (Figure 2.6). The untreated controls show similar level of fluorescence in all catalase gene derivative strains. Interestingly, AB189 (ATCC17978:Δ*katG* Δ*katE*) does not show a drastic increase in ROS production compared to AB155 (ATCC17978; Δ*katG*) or AB188 (ATCC17978; Δ*katE*) which is surprising as AB189 lacks both catalase genes. Complemented strains showed restoration of phenotype to wildtype ATCC 17978 levels after treatment with DCF-DA. The positive control here was methyl viologen which also shows comparable levels of ROS production in all deletion mutants and restoration to wildtype is observed in the complemented strains.

2.3.5 Antibiotic susceptibilities of catalase-peroxidase gene derivatives in ATCC17978

Decrease in susceptibility to aminoglycosides such as kanamycin, gentamicin, amikacin, tobramycin, and streptomycin was observed in the deletion strains (Table 2.3). These antibiotics are known substrates of the AdeAB efflux pump [5]. There was no change in susceptibility of ciprofloxacin and tetracycline which are known substrates of AdeIJK efflux pump [24]. Trimethoprim, which is a substrate of AdeFGH efflux pump [5] did not result in changes to MIC in the catalase deletion mutants [25]. Complemented strains showed restoration of MIC to wildtype levels upon induction with IPTG.

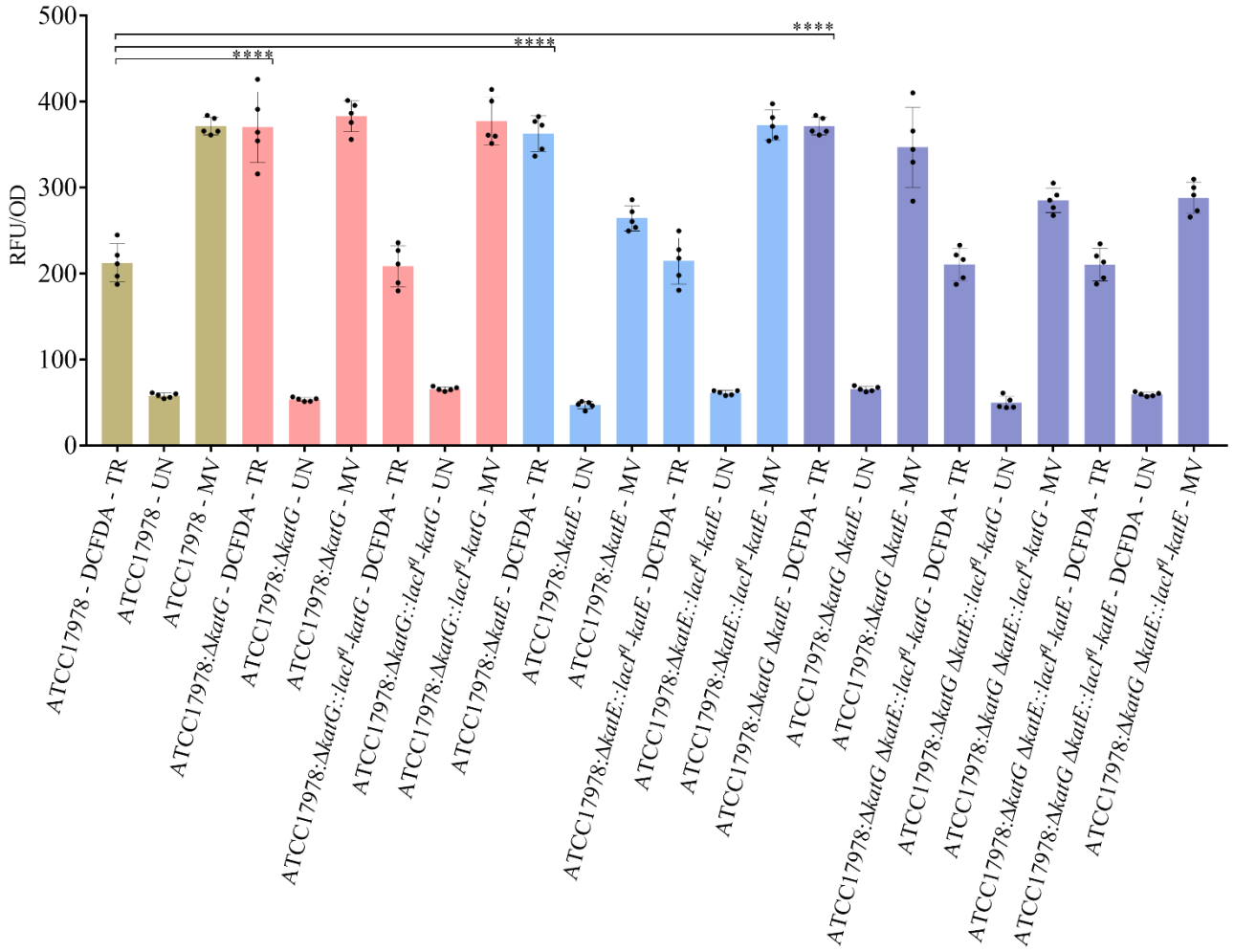

Figure 2.6. ROS production in *A. baumannii* strains.
ROS generation assay in *A. baumannii* catalase deletion and complementation strains. The fluorescence signal was measured using a microplate reader and was normalized to OD600 measuring relative fluorescence unit (RFU) over 20 minutes in response to treatment with DCF-DA. 64µg/mL of Methyl Viologen was used as the positive control. Data shown is representative of 5 biological replicates. TR, treated, UN, untreated, MV, methyl viologen. Error bars represent standard deviation. **** indicates P<0.0001 determined via 1-way ANOVA statistical test. Graph generated in GraphPad Prism 6.0 (San Diego, California USA).

Table 2.3. Antibiotic susceptibilities of catalase-peroxidase gene derivatives in ATCC17978.

Data expressed in μg/mL as determined by Broth dilution method and representative of three independent biological replicates. Changes greater than 4-fold are highlighted

Strains	**Kanamycin**		**Gentamycin**		**Amikacin**		**Tobramycin**		**Streptomycin**		**Tetracycline**		**Ciprofloxacin**		**Trimethoprim**		**Erythromycin**	
IPTG Induction	-	+	-	+	-	+	-	+	-	+	-	+	-	+	-	+	-	+
ATCC17978	4	-	1	-	1	-	1/2	-	16/32	-	0.5	-	0.125	-	8/16	-	32	-
ATCC17978:Δ*katG*	**16**	-	**4**	-	**4**	-	**4/8**	-	**128**	-	0.125	-	0.125	-	16	-	16	-
ATCC17978:Δ*katG*::*lacI*^{q}-*katG*	16	4	4	1	**4**	1	**4**	2	**128**	32	0.125	0.5	0.125	0.125	16	8	16	16
ATCC17978:Δ*katE*	**32**	-	**8**	-	**4**	-	**4**	-	**128**	-	0.5	-	0.125	-	32	-	16	-
ATCC17978:Δ*katE*::*lacI*^{q}-*katE*	**32**	4	**8**	1	**4**	1	**4**	2	**128**	32	0.5	0.5	0.125	0.125	32	8	16	16
ATCC17978:Δ*katG* Δ*katE*	**32**	-	**64**	-	**>8**	-	**8**	-	**256**	-	0.0625	-	0.125	-	32	-	16	-
ATCC17978:Δ*katG* Δ*katE*::*lacI*^{q} -*katG*	**32**	32	**32/32**	8	**4**	4	**8**	4	**128**	128	0.0625	0.5	0.125	0.125	32	16	16	16
ATCC17978:Δ*katG* Δ*katE*::*lacI*^{q} -*katE*	**32**	16	**32/32**	4	**4**	4	**8**	8	**128**	128	0.0625	0.5	0.125	0.125	32	16	16	16

2.3.6 Expression of *katG* and *katE* increases under exposure of 1mM H_2O_2

Upon treatment with 1mM H_2O_2, expression of *katG* and *katE* was measured via RT-qPCR. In AB155 (ATCC17978:Δ*katG*) we see a significant increase in expression of *katE* after 30 and 60 minutes indicating that oxidative stress results in increased expression of the catalase enzymes (Figure 2.7). Similar trend was observed in AB188 (ATCC17978:Δ*katE*), where *katG* was overexpressed, perhaps, compensating for the lack of *katE*. The changes are significant at the 30-minute time point; however, no trend was observed at 60 minutes compared to exposure after 30 minutes.

2.3.7 Expression of *adeJ* and *adeG* in *katG* and *katE* knockout

Upon examining the antibiotic susceptibility profile of the catalase deletion strains, we wanted to look at the involvement of RND efflux pumps that are responsible for extruding out these antibiotics. We discovered that expression of *adeJ* and *adeG* remains statistically unchanged (Figure 2.8) and that correlates with the antibiotic susceptibility assays as antibiotics that are substrates of AdeIJK and AdeFGH did not show any changes in MIC.

2.3.8 *katG* and *katE* knockout results in overexpression of the AdeAB efflux pump and regulator AdeRS

We observed increased expression of *adeB* and *adeR* in AB155 (ATCC17978:Δ*katG*), AB188 (ATCC17978:*Δ*katE*), and AB189 (ATCC17978:Δ*katG* Δ*katE*) (Figure 2.9). Expression of *adeG* and *adeJ* was not significantly affected by the deletion on *katG* or *katE* (Figure 2.8). This may be the reason we observed changes in MIC for aminoglycosides, particularly.

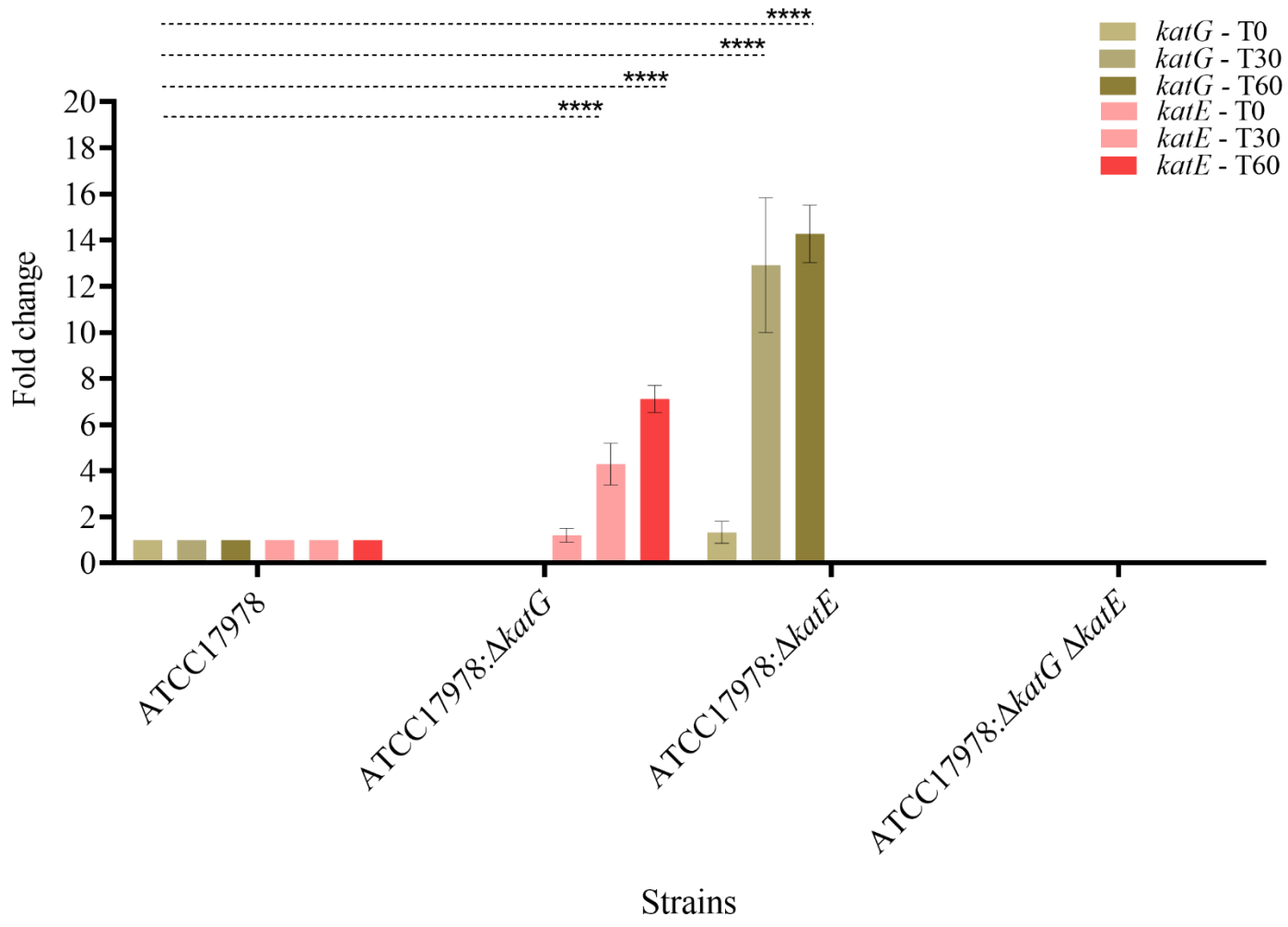

Figure 2.7. Expression of *katG* and *katE* increases under oxidative stress.
Expression of *katG* (brown) and *katE* (pink) with exposure to 1mM H_2O_2 in *A. baumannii* catalase mutants relative to that in *A. baumannii* ATCC 17978. 16S rRNA gene was used as the housekeeping control. Error bars represent standard deviation. **** indicates $P<0.0001$ determined via 2-way ANOVA statistical test. Graph generated in GraphPad Prism 6.0 (San Diego, California USA).

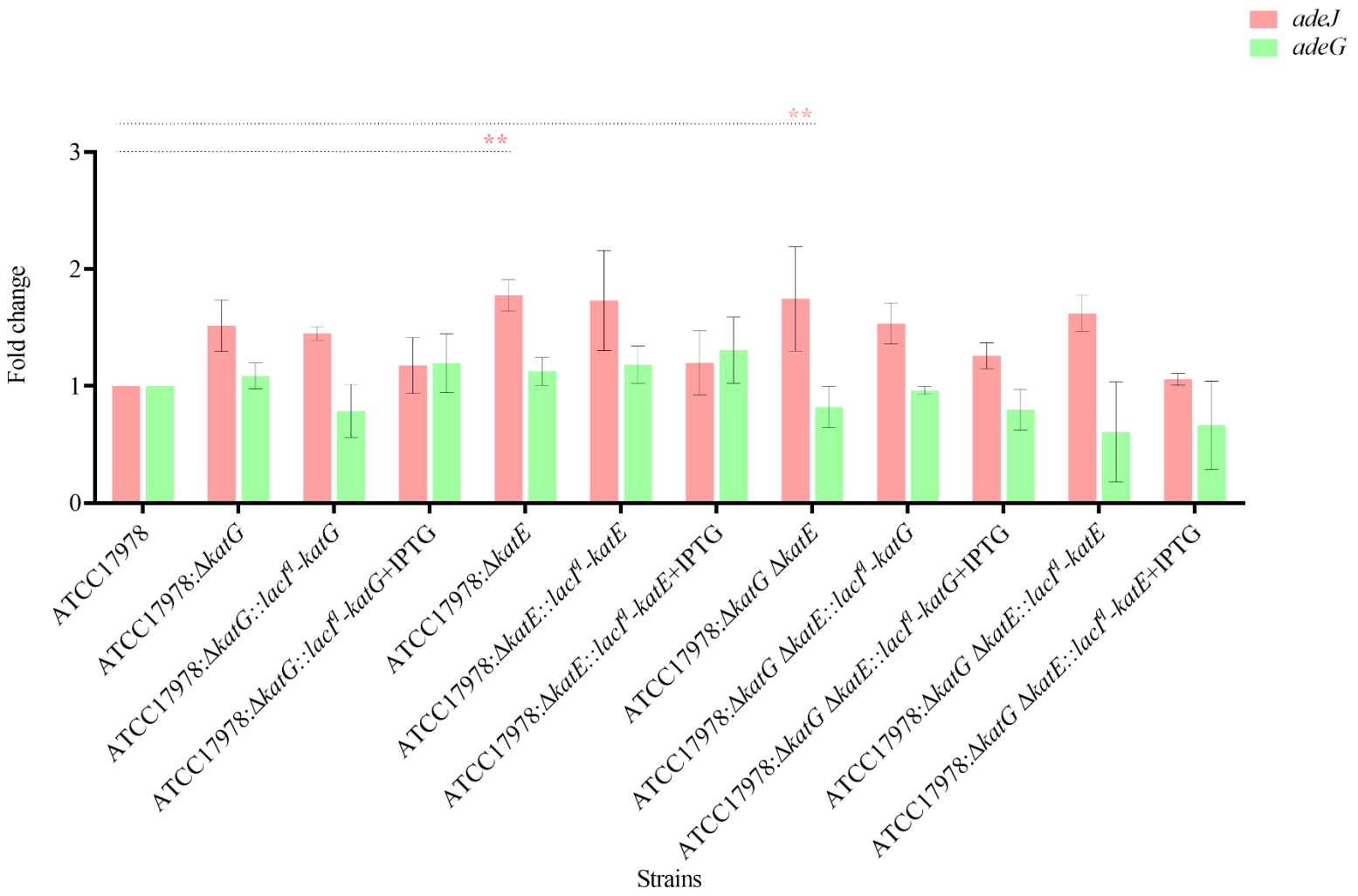

Figure 2.8 Expression of AdeIJK and AdeFGH RND efflux pump in *A. baumannii* catalase gene derivatives.
Expression of RND efflux pump genes *adeJ* (pink) and *adeG* (green) in *A. baumannii* catalase gene derivatives relative to that in *A. baumannii* ATCC 17978. 16S rRNA gene was used as the housekeeping control. Error bars represent standard deviation. ** indicates $P<0.05$ determined via 2-way ANOVA statistical test. Graph generated in GraphPad Prism 6.0 (San Diego, California USA).

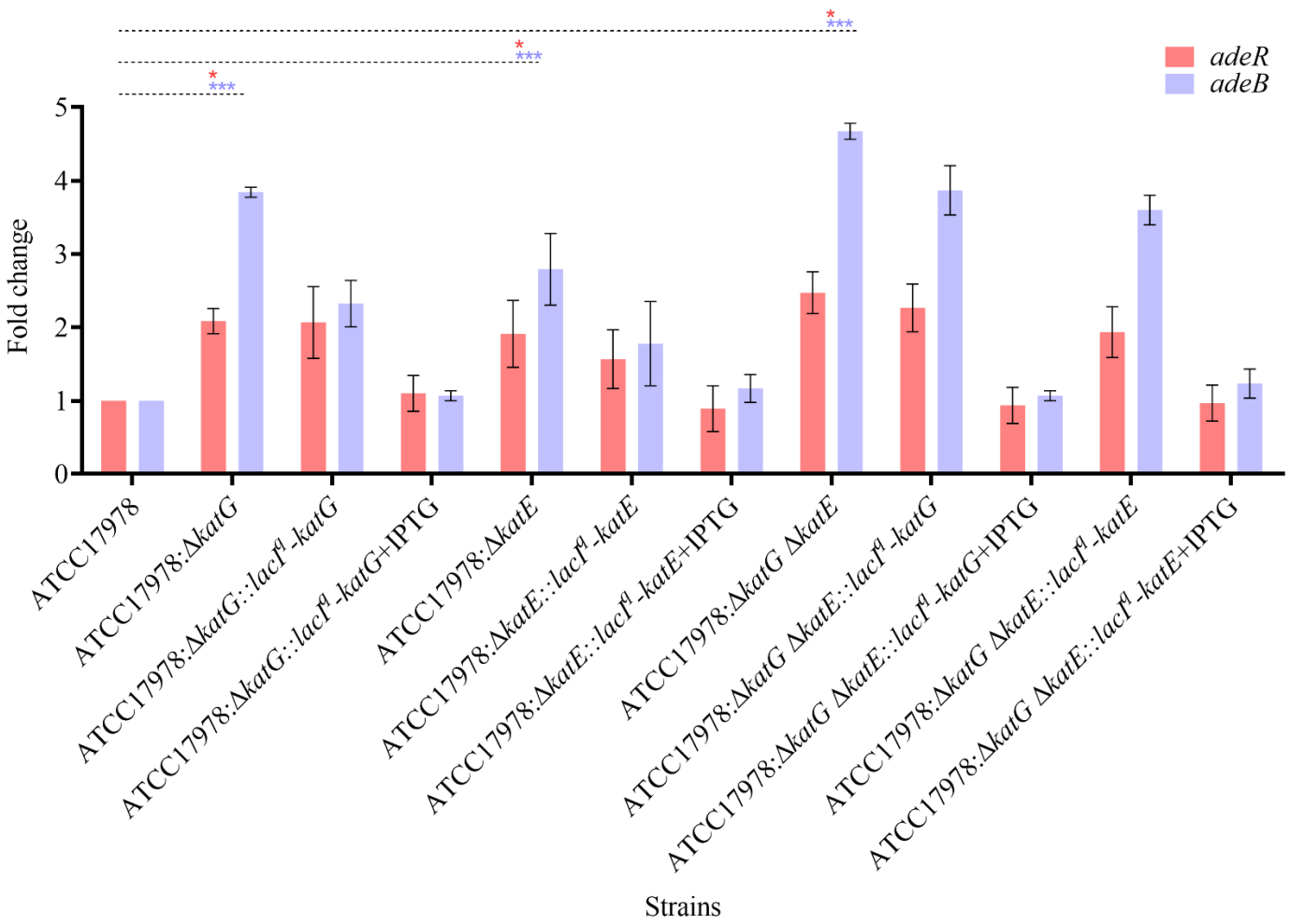

Figure 2.9. Expression of AdeABC RND efflux pump and regulator AdeRS in *A. baumannii* catalase gene derivatives.
Expression of RND efflux pump genes *adeB*, (purple) and *adeR* (red) in *A. baumannii* catalase gene derivatives relative to that in *A. baumannii* ATCC 17978. 16S rRNA gene was used as the housekeeping control. Error bars represent standard deviation. **** indicates $P<0.0001$ and *** indicates $P = 0.0003$ determined via 2-way ANOVA statistical test. Graph generated in GraphPad Prism 6.0 (San Diego, California USA).

2.3.9 Expression of *adeB* under exposure of 1mM H_2O_2 and 5mM Ascorbate

Upon treatment of catalase deletion mutants with 1mM H_2O_2, *adeB* is overexpressed at thirty minutes with no significant change at sixty minutes compared to thirty minutes post exposure. Interestingly, ascorbate, an antioxidant had the opposite effect upon treatment causing downregulation of *adeB* below wild type levels at all time points (Fig 2.10). Treatment with 1mM H_2O_2 does not result in significant changes in expression of *adeR* when compared to ATCC 17978 eluding to the fact that the increase in expression of *adeB* is AdeRS independent (Fig 2.11).

2.3.10 Expression of *adeG* and *adeJ* under exposure of 1mM H_2O_2

Treatment with 1mM H_2O_2 does not result in significant changes in expression of *adeG* and *adeJ* with less than 2-fold difference compared than ATCC 17978 (Fig 2.12, 2.13). We can correlate the data with the antibiotic susceptibility assays, where we did not see any changes in antibiotics that are known substrates of AdeFGH and AdeIJK (Table 2.3).

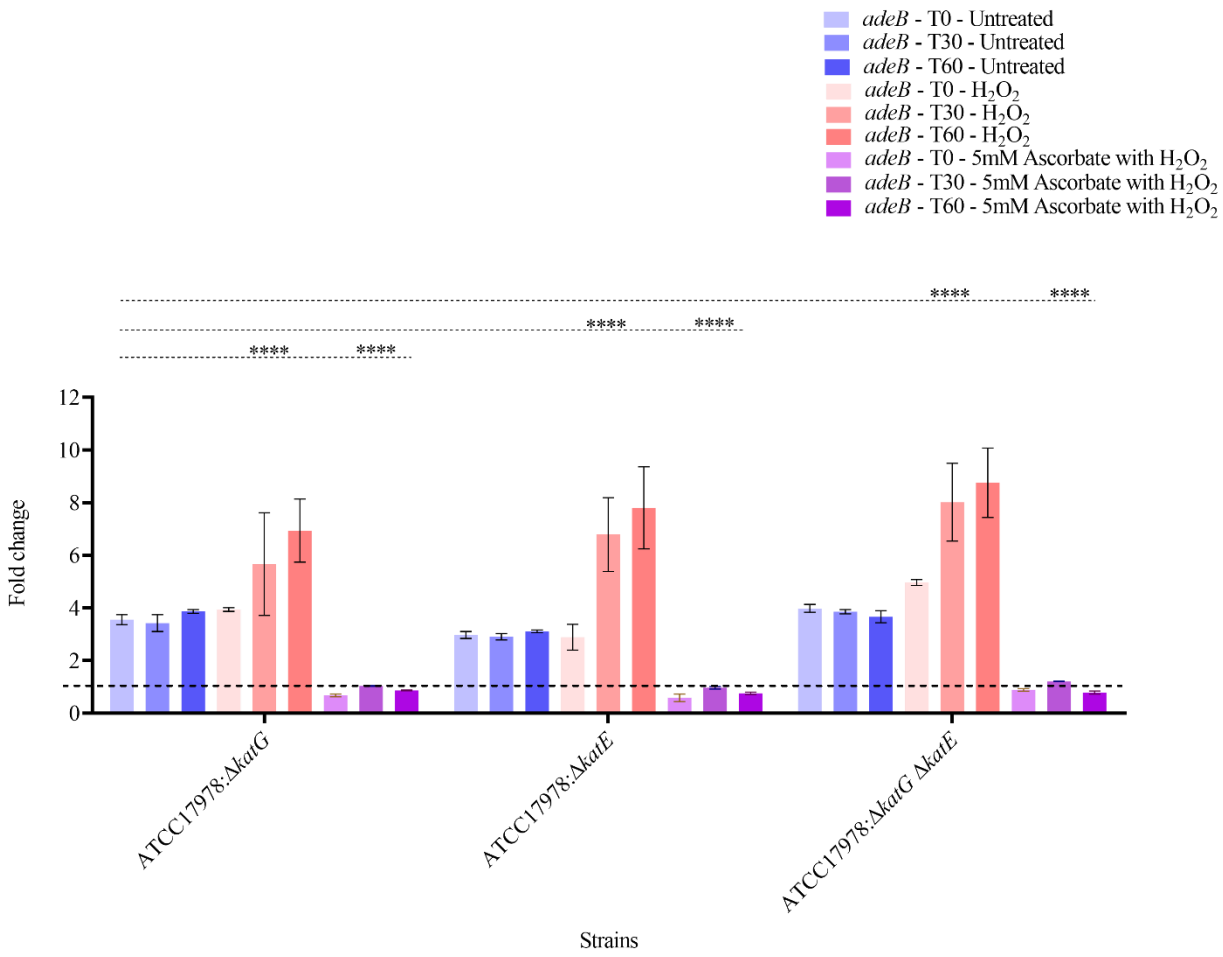

Figure 2.10. Expression of *adeB* under oxidative stress.
Expression of *adeB* with exposure to 1mM H_2O_2 and 5mM ascorbate in *A. baumannii* catalase deletion mutants relative to that in *A. baumannii* ATCC 17978 (indicated by the dashed line). Expression was measured at different time points (0, 30, 60 minutes). 16S rRNA gene was used as the housekeeping control. Error bars represent standard deviation. **** indicates $P<0.0001$ determined via 2-way ANOVA statistical test. Graph generated in GraphPad Prism 6.0 (San Diego, California USA).

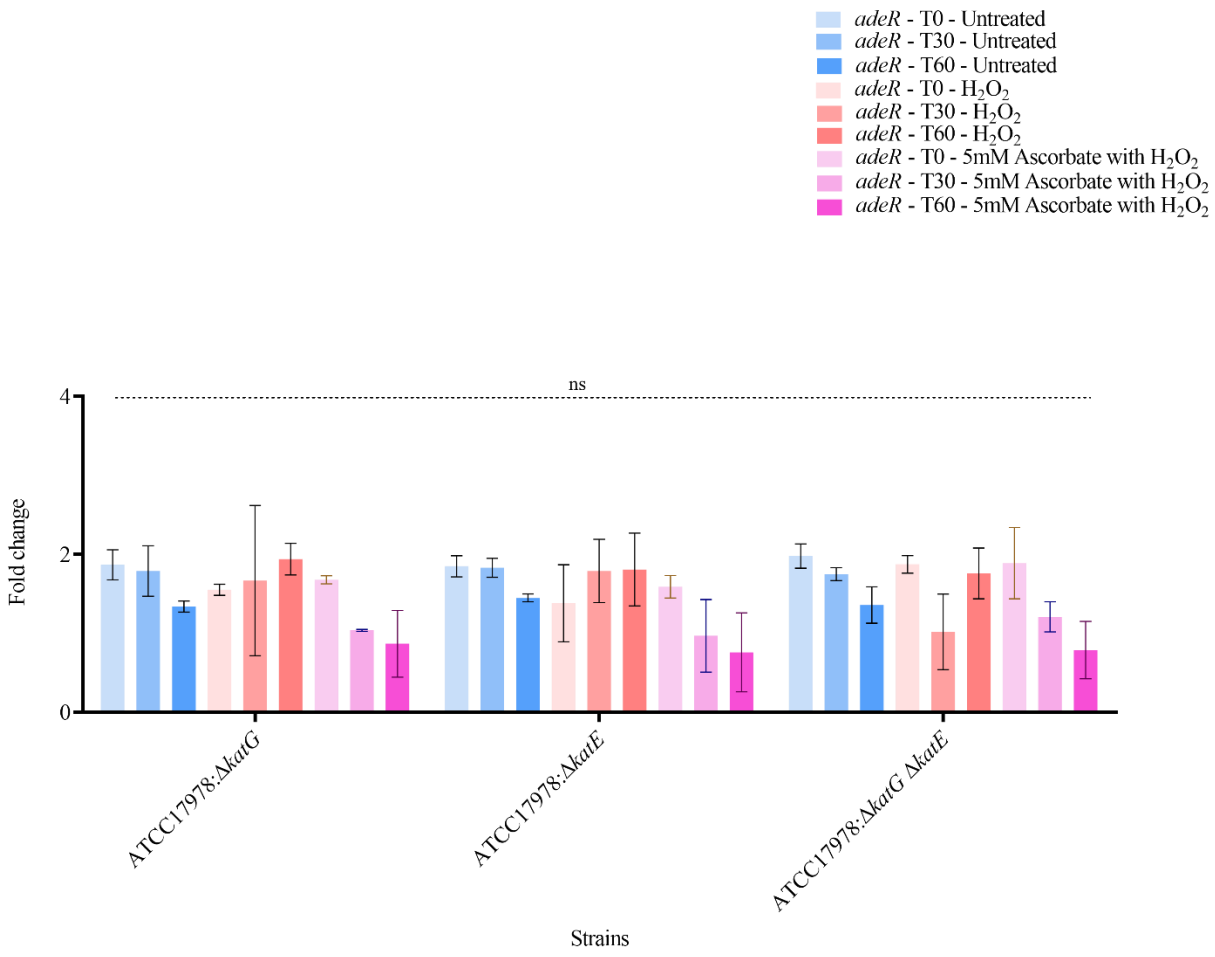

Figure 2.11. Expression of *adeR* under oxidative stress.
Expression of *adeR* with exposure to 1mM H_2O_2 and 5mM ascorbate in *A. baumannii* catalase deletion mutants relative to that in *A. baumannii* ATCC 17978. Expression was measured at different time points (0, 30, 60 minutes). 16S rRNA gene was used as the housekeeping control. Error bars represent standard deviation. *P* values were non-significant (ns) determined via 2-way ANOVA statistical test represented by the dotted line. Graph generated in GraphPad Prism 6.0 (San Diego, California USA).

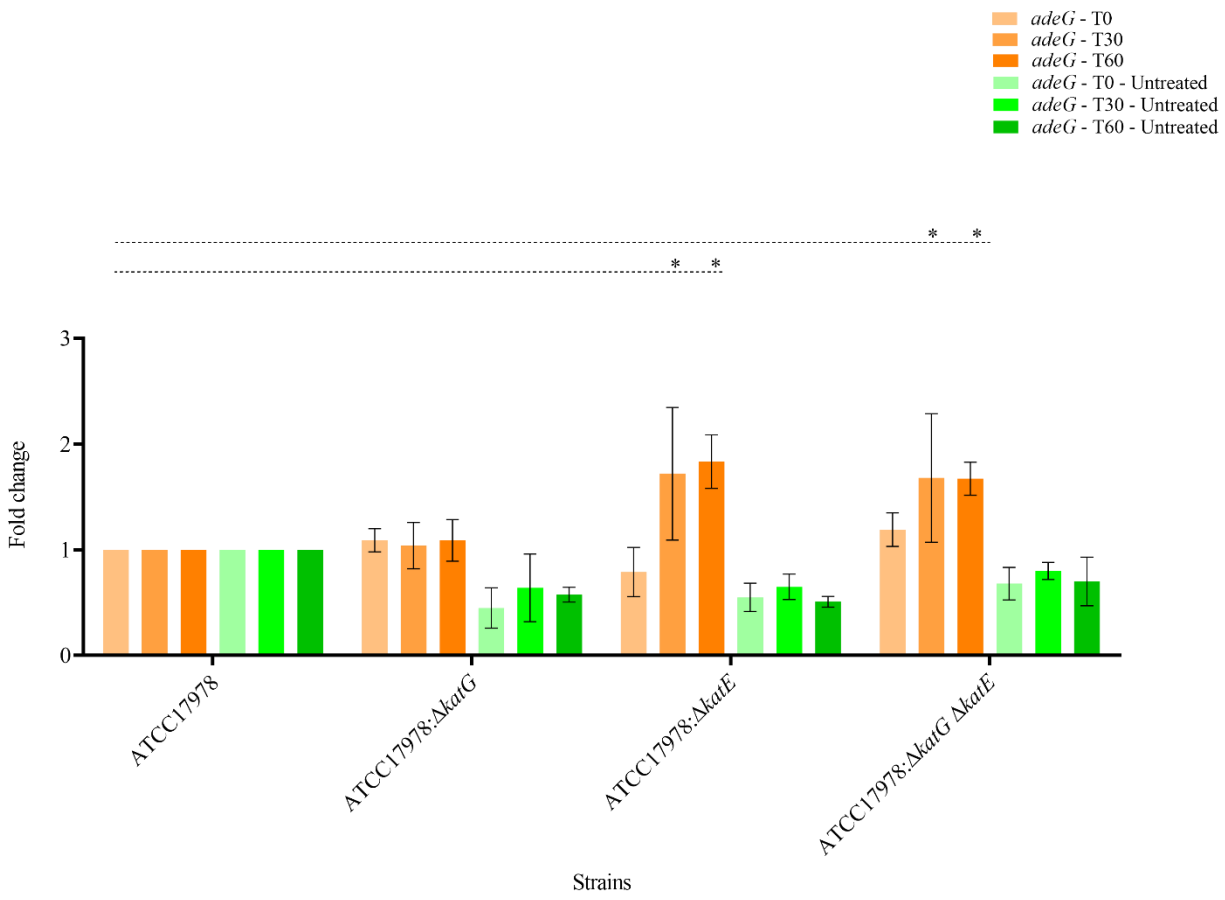

Figure 2.12. Expression of *adeG* under oxidative stress.
Expression of *adeG* with exposure to 1mM H_2O_2 in *A. baumannii* catalase deletion mutants relative to that in *A. baumannii* ATCC 17978. Expression was measured at different time points (0, 30, 60 minutes). 16S rRNA gene was used as the housekeeping control. Error bars represent standard deviation. *P* value determined via 2-way ANOVA statistical test. Graph generated in GraphPad Prism 6.0 (San Diego, California USA).

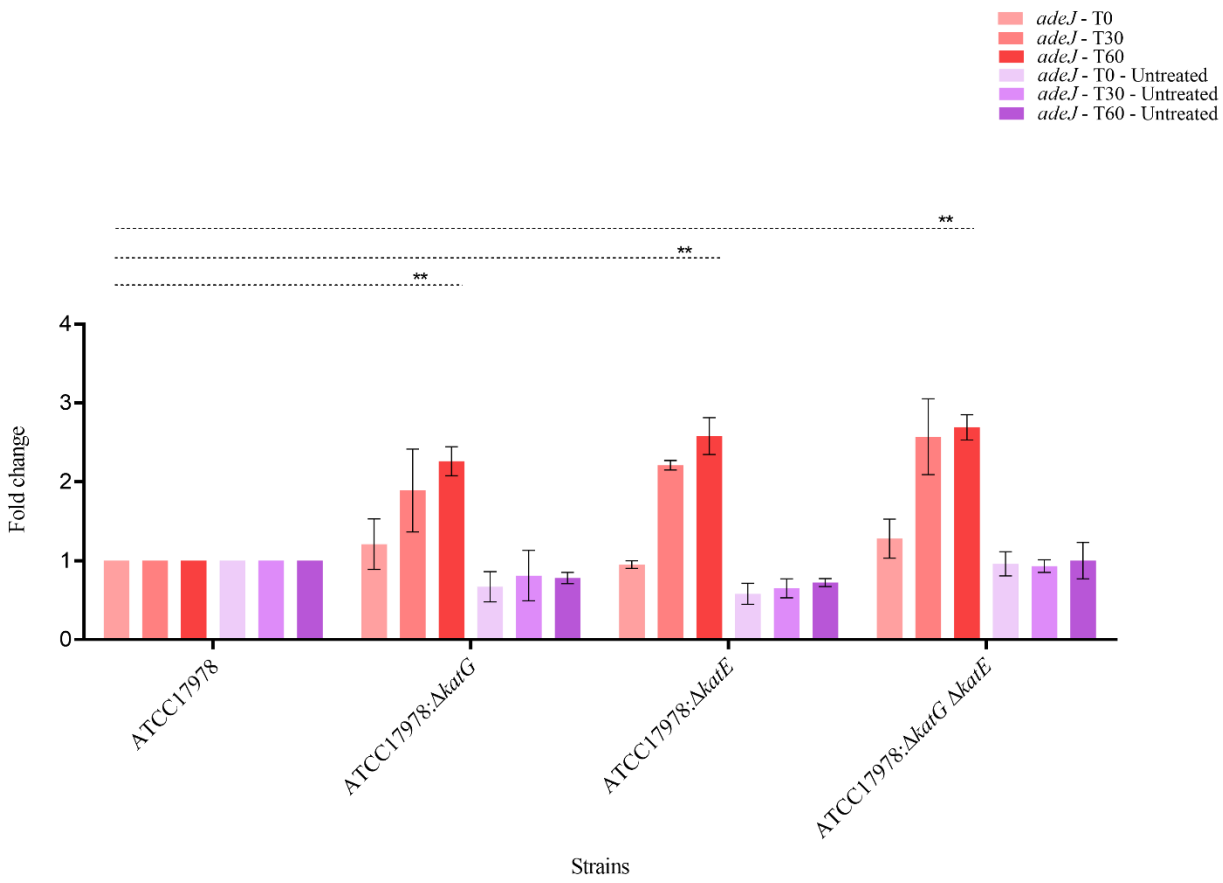

Figure 2.13. Expression of *adeJ* under oxidative stress.
Expression of *adeJ* with exposure to 1mM H_2O_2 in *A. baumannii* catalase deletion mutants relative to that in *A. baumannii* ATCC 17978. Expression was measured at different time points (0, 30, 60 minutes). 16S rRNA gene was used as the housekeeping control. Error bars represent standard deviation. **** indicates $P<0.0001$ determined via 2-way ANOVA statistical test. Graph generated in GraphPad Prism 6.0 (San Diego, California USA).

2.3.11 Deletion of *katG*/*katE* causes differential expression of more than hundred genes in *A. baumannii*

RNA-Seq was performed on AB189 (ATCC17978:Δ*katG* Δ*katE*), AB370+IPTG (ATCC17978:Δ*katG*::*lacI*^{q}-*katG*) and AB376+IPTG (ATCC17978:Δ*katE*::*lacI*^{q}-*katE*) to understand the changes in expression in genes resulting from the deletion and complementation of *katG* and *katE* and also to find the underlying molecular mechanism that causes changes in expression of AdeAB. This also gave us insights into the global transcriptomic landscape that resulted from deleting catalase. We found that expression of 71 genes were downregulated and 43 genes were upregulated in AB189 compared to ATCC17978 (Appendix 1 and 2, cut-off of log1.5 fold with a statistical significance of $P<0.05$). In AB370, we found that expression of 222 were upregulated and 153 were downregulated. Similarly, in AB376, we found that expression of 205 genes were upregulated and 142 were downregulated. Almost all genes with some notable exceptions listed in Section 2.4 were restored back to wildtype levels in the complemented strains. These genes were further classified into clusters of orthologous groups (COGs) using the web-based interface of EggNOG version 5.0.0 database [26] to find correlations with the phenotypes observed [27]. A large number of the genes were annotated as hypothetical proteins and were put into unknown category or with no COG orthologs reflecting on the large number of unknown genes in *A. baumannii* (Fig 2.14).

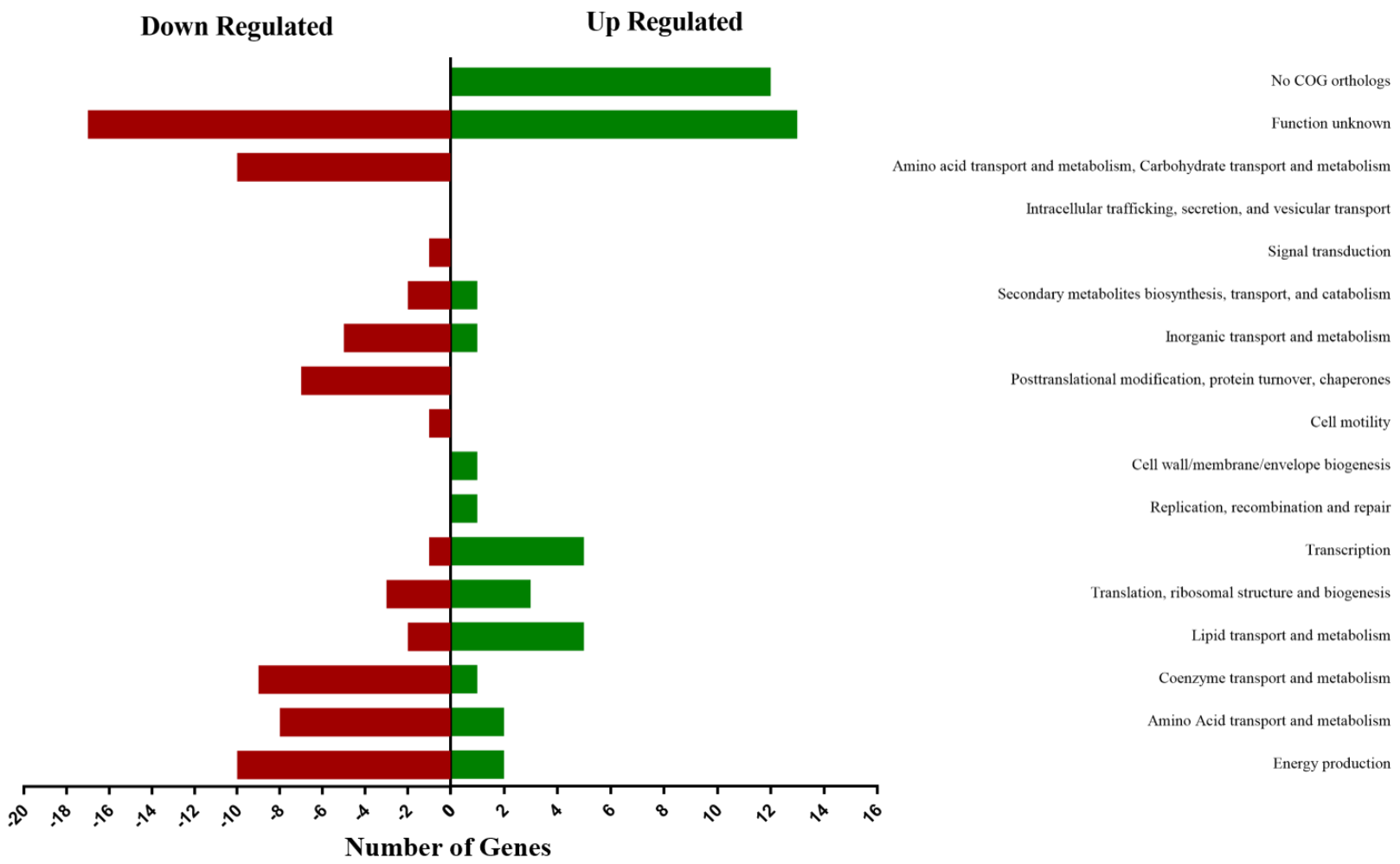

Figure 2.14. Differential expression of genes in AB189 catalase deletion mutant of *A. baumannii*
Graph generated in GraphPad Prism 6.0 (San Diego, California USA).

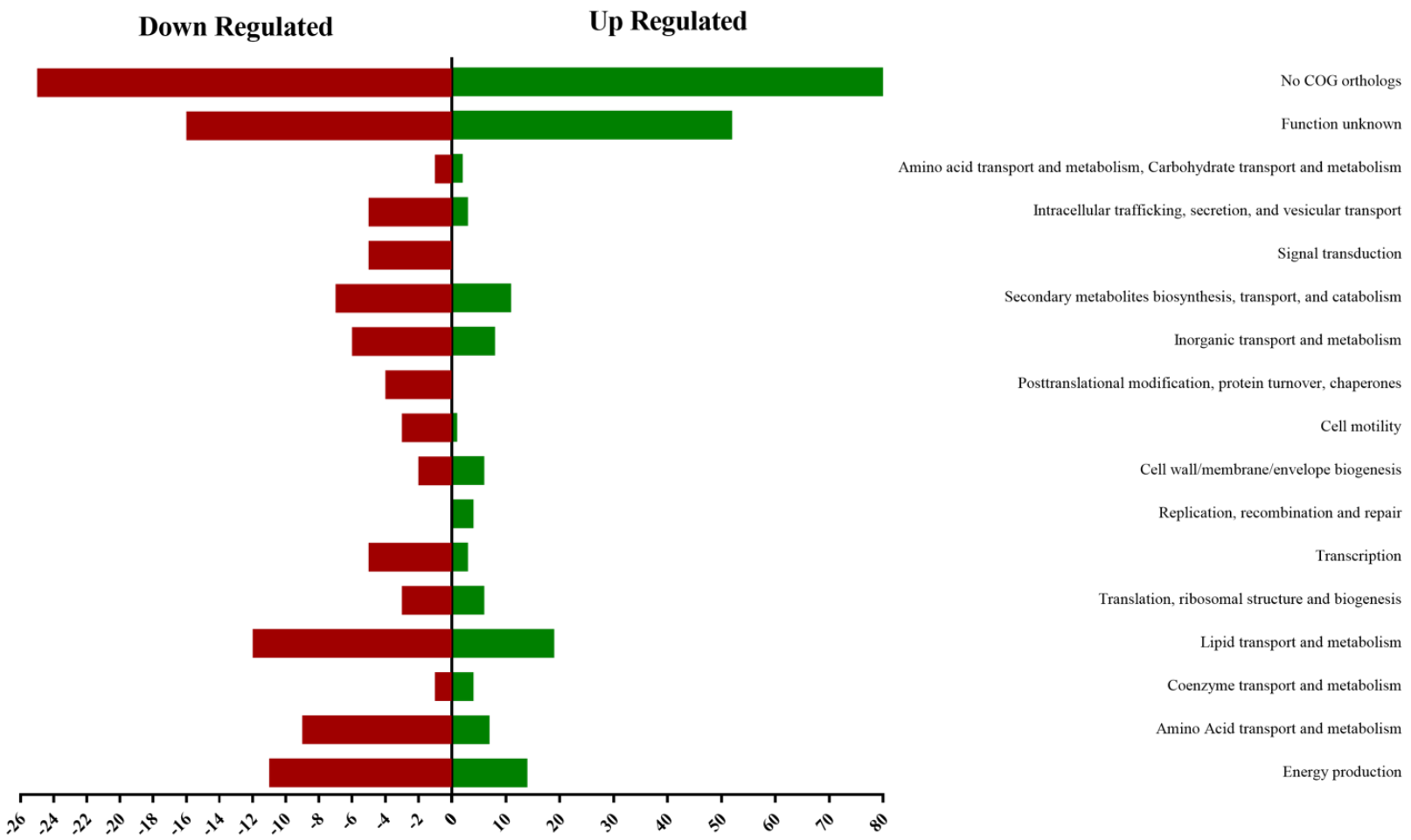

Figure 2.15 Differential expression of genes in AB370+IPTG (ATCC17978:Δ*katG*::*lacI*^{q}-*katG*) in *A. baumannii*
Graph generated in GraphPad Prism 6.0 (San Diego, California USA).

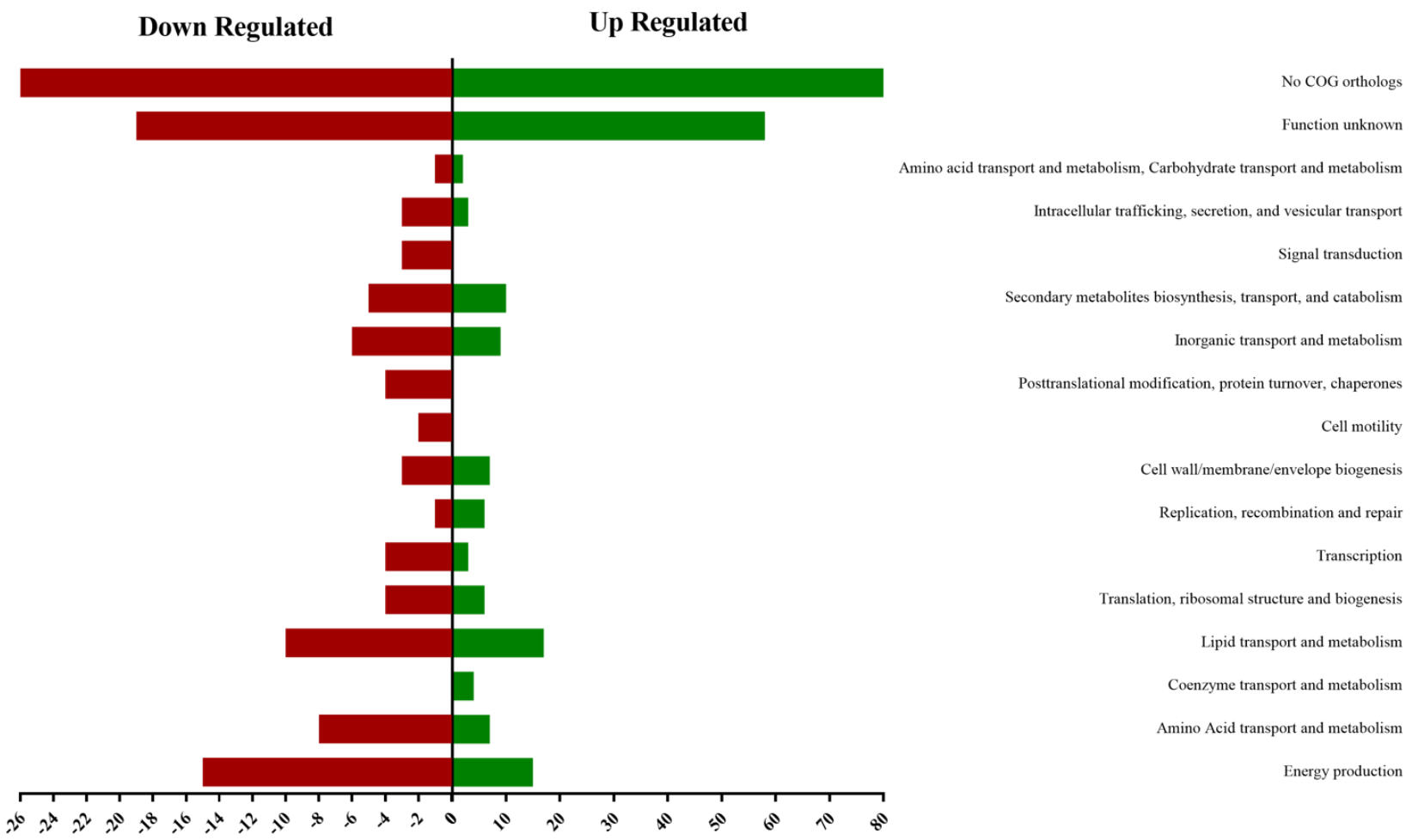

Figure 2.16. Differential expression of genes in AB376+IPTG (ATCC17978:Δ*katE*::*lacI*^{q}-*katE*) in *A. baumannii*
Graph generated in GraphPad Prism 6.0 (San Diego, California USA).

2.4 Discussion

With increasing reports of *Acinetobacter baumannii* strains being isolated from hospitals and human hosts, there is an interest in determining the mechanisms by which *A. baumannii* is able to survive such harsh and complex environments and be a successful pathogen. It is particularly adept at infecting patients with open wounds and weak immune system or with devices like urinary catheters. It can survive on biotic and abiotic surfaces for a prolonged time. These factors together contribute to the resistance in *A. baumannii*.

In this study, we examined the involvement of catalase-peroxidases and oxidative stress in *Acinetobacter baumannii*. We created strains with deletions in *katG* (AB155), *katE* (AB188), and a double deletion mutant lacking both *katG* and *katE* (AB189). The deletion mutants were complemented via a single-copy chromosomal insertion using a mini-Tn*7* system under IPTG inducible synthetic P_{tac} promoter. Next, these set of strains were subjected to a variety of phenotypic assays which are responsible for resistance and survival of *A. baumannii*.

Firstly, all strains were tested for expression of *katG* and *katE* via RT-qPCR to confirm the identity and if the strains are functioning as intended. We observed that deletion of *katG* results in only *katE* being expressed and in deletion of *katE* only *katG* is expressed, therefore, confirming the identity of the strains (Figure 2.2). Complementation resulted in restoration of phenotype back to wild-type levels.

The role of *katG* and *katE* in hydrogen peroxide resistance and degradation has previously been described [8]. With respect to that, we assessed the sensitivity of our strains to hydrogen peroxide. Results indicated that there was an increase in sensitivity to H_2O_2 upon deletion of catalase in the cell. The effect was more drastic in the double deletion mutant which exhibited the highest

sensitivity to H_2O_2 (Figure 2.5). Complemented strains show restoration of phenotype to wild type levels after IPTG induction.

Next, we decided to conduct antibiotic susceptibility assays and observed at least 4-fold reduced susceptibilities to aminoglycosides: Kanamycin, Gentamycin, Amikacin, Tobramycin, and Streptomycin (Table 2.3). MICs were restored to wild-type levels by IPTG induction of the complemented strains. What we observed here is that at-least one of the genes is required for the phenotype to be restored back to wild-type levels. We observed changes in aminoglycosides, antibiotics that are substrates of AdeAB efflux pump. Antibiotics which are substrates of AdeIJK and AdeFGH were also tested for susceptibility and there were no changes in MICs of Tetracycline (AdeIJK) and Ciprofloxacin (AdeIJK) and only 2-fold reductions in MIC for Trimethoprim (AdeFGH) and Erythromycin (AdeIJK) [10,25].

We conducted RT-qPCR expression analysis of *adeB*, *adeJ*, *adeG*, genes that code for the inner membrane component of AdeAB, AdeIJK, and AdeFGH, respectively to determine whether deletions in catalase have any effect on expression of RND efflux pumps. Also, to determine if the changes in the antibiotic susceptibility profile had a correlation with efflux pumps.

Interestingly, deletion of *katG* and *katE* displayed overexpression of AdeAB, an aminoglycoside efflux pump. Similar observation has been shown in *P. aeruginosa*, which under oxidative stress overexpresses MexXY-OprM efflux pump leading to decreased susceptibility of aminoglycosides [28]. We also observed the *katG/katE* deletion causes upregulation of *adeR*, that encodes the transcriptional activator of *adeAB.* Chromosomal complementation of the deletion mutants with the respective gene, resulted in downregulation of *adeR* and *adeB* to the wild-type levels (Figure 2.9). This was unexpected and promoted us to examine the link between oxidative stress and efflux pumps. The deletions, however, had no impact on the expression of AdeIJK and AdeFGH efflux

pumps. This is evident on our results observed from the RNA-Seq where we did not see any upregulation of AdeIJK and AdeFGH.

Efflux pumps are also known to act at defense against oxidative stress. In *Salmonella enterica* serovar Typhimurium, the ABC family pump MacAB is needed for survival inside macrophages where they are exposed to ROS [29]. To find out what may be causing the overexpression of *adeB*, we sought to determine if it is due to the excess amount of ROS generated in the cell due to the lack of catalase genes. ROS generation experiment was performed to see if we can make a correlation with upregulation of AdeAB and increase ROS production. We observed that after treating the deletion mutants with DCFDA for 30 minutes, the RFU was much higher for catalase deletion mutants confirming that deletion results in increased production of ROS in the cell and that correlates with our RT-qPCR expression data for AdeAB upregulation.

In most bacterial species, the expression of catalase is tightly regulated, their activity is kept at low levels until an oxidative challenge is presented or until the cells enter stationary phase [30]. To study this, we sought to examine the effect of external stressor in the form of H_2O_2 on the catalase deletion mutants. Strains were exposed to 1mM H_2O_2 and grown to late-exponential phase (OD 0.70-0.80), following which RT-qPCR expression analysis was conducted. After 30 minutes of exposure with H_2O_2, we observed significant upregulation of *katG* and *katE* in AB188 and AB155, respectively (Figure 2.7). This is expected because the addition of stressor is causing the catalase genes to compensate for the lack of the other and protecting the cell from ROS. However, at the 60-minute timepoint, we do not see any significant changes compared to 30 minutes. Interestingly, we also observed that *adeB* expression also goes up in response to treatment with 1mM H_2O_2 30 minutes post exposure, analogous to the results observed in ROS generation experiment. This suggests that increased ROS production results in increase in expression of catalase and AdeAB.

No significant changes in expression were seen for AdeIJK and AdeFGH in response to 1mM H_2O_2.

Concurrently, we wanted to test whether usage of an antioxidant can revert the expression levels of *adeB* back to wild-type levels in catalase deletion mutants. Studies done with ascorbic acid in *E. coli* have shown that addition of ascorbic acid results in increase in catalase activity [30]. We wanted to examine the effects of ascorbic acid in catalase deletion mutants to see whether it results in changes in expression of AdeAB. We observed significant changes in expression upon treatment with 5mM ascorbate, *adeB* was downregulated suggesting that ascorbic acid was successful at lowering the amount of ROS in the cell in the absence of catalase and in response to that we see downregulation of *adeB* (Figure 2.10). Additionally, measuring catalase activity under ascorbic acid exposure may be of interest in the future to see if it results in increased activity of catalase genes.

To find out the underlying molecular mechanism(s) that are involved in the interplay of stress response and efflux pump expression, we performed RNA-Seq studies on AB189, AB370+IPTG, and AB376+IPTG. RNA seq approaches serve as powerful tools to study the global impact of changes in bacterial systems. RNA-Sequencing of AB189 identified 114 genes that exhibited a statistically significant difference in expression or at least a 1.5log (2)-fold change compared to the wild-type ATCC 17978. A list of these genes is provided in Appendix 2.7.1. Of the 114 genes identified in the RNA-Seq analysis only 52 genes were annotated by Cluster of Orthologous genes (COG) analysis performed using the EggNOG database. This could be due to the large number of uncharacterized genes in the *A. baumannii* genome, and more research is needed to determine their roles. Genes involved in lipid transport were upregulated and one possible explanation for this could be that deletion of catalase perturbs the membrane and high ROS response due to the lack

of catalase results in oxidation of lipids, therefore bacteria need to compensate, hence we observe upregulation on lipid transport. Additionally, genes involved in replication, repair and transcription are upregulated whereas we see downregulation of carbohydrate and amino acid metabolism and energy production are downregulated. AUO97_RS00825, gene involved in transport of ferric chelates using PMF and AUO97_RS03410, gene needed for beta oxidation that requires energy are both downregulated. AUO97_RS06705, gene involved in amino acid metabolism is also downregulated. This is expected as the cells may not be prioritizing carbohydrate and amino acid metabolism and energy production under stress conditions. In the complemented strains, AB370 and AB376, expression of these genes is restored to wild-type level.

We also observed a cluster of genes (AUO97_RS18925, AUO97_RS18930, AUO97_RS18935, and AUO97_RS18940) annotated as PGA polysaccharide adhesin, which is a critical determinant of biofilm formation [31] to be highly upregulated in *katG* and *katE* deletion mutant. These were the most prominent genes that were restored back to wild-type levels in response to complementation of *katG* in AB370 and *katE* in AB376. In future, it may be of interest to look at biofilm production in catalase deletion mutants.

In Gram negative bacteria, lactate dehydrogenase enzyme is responsible for maintaining a redox balance and responding to oxidative stress [32]. A group of genes (AUO97_RS06855, AUO97_RS06860, AUO97_RS06865) encoding lactate dehydrogenase, lactate permease and a transcriptional regulator, respectively were found to be downregulated in AB370 and AB376. Interestingly, complementation had no effect on restoring the expression of these genes back to the wildtype levels.

The phenylacetic acid catabolic pathway (PAA) is an important route in the catabolism of several aromatic compounds related to the Krebs cycle [33]. In *A. baumannii*, genes required for this

pathway are encoded by the *paa* operon and alignment studies done with *E. coli* has shown that the structure of the operon is similar to what's been described in *E. coli* [34]. In pathogenic bacteria, the intermediates of this pathway play a role in virulence [34]. In AB189, there was upregulation of *paaJ*, encoding for a thiolase which is involved in catalyzing the last step of this pathway yielding acetyl-CoA and succinyl-CoA. To what extent upregulation of this gene has an impact on the virulence of *A. baumannii* needs to be explored.

In *E. coli*, multiple antibiotic resistance regulator (MarR) family of transcriptional regulators serve as sensors of stress responses, regulators of efflux pump operons, virulence, oxidative stress and degradation of antibiotics [35]. They are also implicated in mediating responses to oxidative stress. In *P. aeruginosa*, *ospR* (oxidative stress response and pigment production Regulator) gene senses oxidative stress and induces both antioxidant production and resistance to multiple antibiotics [36]. Interestingly, in AB189 we saw upregulation of a MarR transcriptional regulator (AUO97_RS17170) which could be of particular interest. Complementation had no effect on the gene expression of this particular gene, and it was not restored to the wild-type level. A possible explanation may be that deletion of catalase had a negative effect on this gene and this could be the link that finding out the regulatory overlap between efflux and oxidative stress response. These results will allow us to continue our efforts to understand the multifaceted oxidative stress response and the contribution to physiology and resistance in *Acinetobacter baumannii*.

2.5 Conclusions

With increasing reports of *A. baumannii* strains beings isolated from hospitals and human hosts, there is an interest in wanting to determine the mechanisms by which *A. baumannii* is able to survive such harsh and complex environments. We used strains with deletions in *katG* and *katE* and the chromosomally complemented strains to access the involvement of these peroxidases in the oxidative stress response and efflux-mediated antibiotic susceptibility to unravel the underlying molecular mechanism(s).

We observed that mutants derived from *A. baumannii* ATCC17978 with deletions in *katG*/*katE* and their complements exhibited increased sensitivity to H_2O_2, RND efflux pump expression and antibiotic susceptibility. In ATCC17978:Δ*katG*, ATCC17978:Δ*katE* and ATCC17978:Δ*katG* Δ*katE*, *adeB,* gene that encodes the inner membrane component and *adeR*, the regulator of AdeABC RND efflux pump, was shown to be overexpressed via RT-qPCR at 37°C. This phenotype correlated to decreased susceptibility to aminoglycosides which are known substrates of AdeABC. Catalase deletion mutants exhibited a great loss in fitness when exposed to H_2O_2. RNA-seq studies performed to understand the changes in expression of the genes resulting from deletion of Δ*katG* and Δ*katE* showed that expression of 44 genes were upregulated and 115 genes were downregulated.

In future, to elucidate the relationship between efflux mediated antibiotic susceptibility and stress response, a number of important studies need to be conducted. The impact oxidative stress on the membrane composition of *A. baumannii* is worth considering. Many external stressors have been shown to induce changes in bacterial membrane composition, lipid profiling will aid in determining the impact of oxidative stress on the membrane. Additionally, determining the involvement of biofilm production will also be of interest due to the upregulation seen in biofilm

adhesin genes. This study showed that the relationship between stress response and efflux pumps is vast and understanding the physiological and regulatory mechanisms of efflux pumps is key to developing therapeutics against opportunistic pathogens like *A. baumannii* and will aid in overcoming antibiotic resistance.

2.7 Bibliography

1. Michalopoulos A, Falagas ME (2010) Treatment of *Acinetobacter* infections. *Expert Opinion on Pharmacotherapy* 11: 779–788.

2. Zeidler S, Müller V (2019) Coping with low water activities and osmotic stress in *Acinetobacter baumannii* : significance, current status and perspectives. *Environmental Microbiology* 21: 2212–2230.

3. Calhoun JH, Murray CK, Manring MM (2008) Multidrug-resistant organisms in military wounds from Iraq and Afghanistan, *Clinical Orthopaedics and Related Research*, Springer New York, 1356–1362.

4. Zeidler S, Müller V (2019) Coping with low water activities and osmotic stress in *Acinetobacter baumannii* : significance, current status and perspectives. *Environmental Microbiology* 21: 2212–2230.

5. Coyne S, Courvalin P, Périchon B (2011) Efflux-mediated antibiotic resistance in *Acinetobacter* spp. *Antimicrobial Agents and Chemotherapy* 55: 947–953.

6. Lin L, Ling BD, Li XZ (2009) Distribution of the multidrug efflux pump genes, *adeABC*, *adeDE* and *adeIJK*, and class 1 integron genes in multiple-antimicrobial-resistant clinical isolates of *Acinetobacter baumannii-Acinetobacter calcoaceticus* complex. *International Journal of Antimicrobial Agents* 33: 27–32.

7. Fraud S, Poole K (2011) Oxidative stress induction of the MexXY multidrug efflux genes and promotion of aminoglycoside resistance development in *Pseudomonas aeruginosa*. *Antimicrobial Agents and Chemotherapy* 55: 1068–1074.

8. Sun D, Crowell SA, Harding CM, et al. (2016) KatG and KatE confer *Acinetobacter* resistance to hydrogen peroxide but sensitize bacteria to killing by phagocytic respiratory burst. *Life Sciences* 148: 31–40.

9. Loewen PC, De Silva PM, Donald LJ, et al. (2018) KatG-mediated oxidation leading to reduced susceptibility of bacteria to kanamycin. *ACS Omega* 3: 4213–4219.

10. Magnet S, Courvalin P, Lambert T (2001) Resistance-nodulation-cell division-type efflux pump involved in aminoglycoside resistance in *Acinetobacter baumannii* strain BM4454. *Antimicrobial Agents and Chemotherapy* 45: 3375–3380.

11. Hamad MA, Zajdowicz SL, Holmes RK, et al. (2009) An allelic exchange system for compliant genetic manipulation of the select agents *Burkholderia pseudomallei* and *Burkholderia mallei*. *Gene* 430: 123–131.

12. Choi KH, Gaynor JB, White KG, et al. (2005) A Tn*7*-based broad-range bacterial cloning and expression system. *Nature Methods* 2: 443–448.

13. Choi KH, Schweizer HP (2005) An improved method for rapid generation of unmarked *Pseudomonas aeruginosa* deletion mutants. *BMC Microbiology* 5: 30.

14. Liu J, Chang W, Pan L, et al. (2018) An improved method of preparing high efficiency transformation *Escherichia coli* with both plasmids and larger DNA Fragments. *Indian*

Journal of Microbiology 58: 448–456.

15. Walker JM, Dale JW, Greenaway PJ (2003) Bacterial Transformation (Kushner Method), *Nucleic Acids*, Humana Press, 241–244.

16. Choi KH, Kumar A, Schweizer HP (2006) A 10-min method for preparation of highly electrocompetent *Pseudomonas aeruginosa* cells: Application for DNA fragment transfer between chromosomes and plasmid transformation. *Journal of Microbiological Methods* 64: 391–397.

17. Reyrat J-M, Pelicic V, Gicquel B, et al. (1998) Counterselectable markers: untapped tools for bacterial genetics and pathogenesis. *Infection and Immunity* 66: 4011 LP – 4017.

18. Schweizer HP (1991) The *agmR* Gene, an environmentally responsive gene, complements defective *glpR*, which encodes the putative activator for glycerol metabolism in *Pseudomonas aeruginosa*.

19. Amin IM, Richmond GE, Sen P, et al. (2013) A method for generating marker-less gene deletions in multidrug-resistant *Acinetobacter baumannii*. *BMC Microbiology* 13: 158.

20. Choi KH, Schweizer HP (2006) mini-Tn*7* insertion in bacteria with single attTn*7* sites: Example *Pseudomonas aeruginosa*. *Nature Protocols* 1: 153–161.

21. Pfaffl MW (2001) A new mathematical model for relative quantification in real-time RT-PCR. *Nucleic Acids Research* 29: 45e – 45.

22. Ong KS, Cheow YL, Lee SM (2017) The role of reactive oxygen species in the antimicrobial activity of pyochelin. *Journal of Advanced Research* 8: 393–398.

23. M100-S25 Performance standards for antimicrobial susceptibility testing; twenty-fifth informational supplement an informational supplement for global application developed through the clinical and laboratory standards institute consensus process (2015).

24. Fernando DM, Xu W, Loewen PC, et al. (2014) Triclosan can select for an AdeIJK-overexpressing mutant of *Acinetobacter baumannii* ATCC 17978 that displays reduced susceptibility to multiple antibiotics. *Antimicrobial Agents and Chemotherapy* 58: 6424–6431.

25. Coyne S, Rosenfeld N, Lambert T, et al. (2010) Overexpression of resistance-nodulation-cell division pump AdeFGH confers multidrug resistance in *Acinetobacter baumannii*. *Antimicrobial Agents and Chemotherapy* 54: 4389–4393.

26. EggNOG Database | Orthology predictions and functional annnotaion Available from: http://eggnog5.embl.de/#/app/home.

27. Huerta-Cepas J, Szklarczyk D, Heller D, et al. (2019) EggNOG 5.0: A hierarchical, functionally and phylogenetically annotated orthology resource based on 5090 organisms and 2502 viruses. *Nucleic Acids Research* 47: D309–D314.

28. Fraud S, Poole K (2011) Oxidative stress induction of the MexXY multidrug efflux genes and promotion of aminoglycoside resistance development in *Pseudomonas aeruginosa*. *Antimicrobial Agents and Chemotherapy* 55: 1068–1074.

29. Bogomolnaya LM, Andrews KD, Talamantes M, et al. (2013) The ABC-type efflux pump MacAB protects *Salmonella enterica* serovar Typhimurium from oxidative stress. *mBio* 4: e00630-13.

30. Richter HE, Loewen PC (1981) Induction of catalase in *Escherichia coli* by ascorbic acid involves hydrogen peroxide. *Biochemical and Biophysical Research Communications* 100: 1039–1046.

31. Wang X, Preston JF, Romeo T (2004) The pgaABCD locus of *Escherichia coli* promotes the synthesis of a polysaccharide adhesin required for biofilm formation. *Journal of Bacteriology* 186: 2724–2734.

32. Vatansever F, de Melo WCMA, Avci P, et al. (2013) Antimicrobial strategies centered around reactive oxygen species - bactericidal antibiotics, photodynamic therapy, and beyond. *FEMS Microbiology Reviews* 37: 955–989.

33. Dagley S, Fewster E, Happold FC (1952) The bacterial oxidation of phenylacetic acid. *Journal of bacteriology* 63: 327–336.

34. Teufel R, Mascaraque V, Ismail W, et al. (2010) Bacterial phenylalanine and phenylacetate catabolic pathway revealed. *Proceedings of the National Academy of Sciences* 107: 14390 LP – 14395.

35. Perera IC, Grove A (2010) Molecular mechanisms of ligand-mediated attenuation of DNA binding by MarR family transcriptional regulators. *Journal of Molecular Cell Biology* 2: 243–254.

36. Lan L, Murray TS, Kazmierczak BI, et al. (2010) *Pseudomonas aeruginosa* OspR is an oxidative stress sensing regulator that affects pigment production, antibiotic resistance and dissemination during infection. *Molecular Microbiology* 75: 76–91.

Chapter 3 Characterization of a novel regulator, AdeQ of AdeDE RND efflux pump in *Acinetobacter pittii*

3.1 Introduction

Acinetobacter pittii, previously known as *Acinetobacter* species 3 [1], is an opportunistic pathogen causing nosocomial infection worldwide [2]. In the past few decades, *A. baumannii* has been the focus of most studies, and only a few studies have been conducted on *A. nosocomalis* and *A. pittii,* perhaps due to their low prevalence and rates of resistance. However, *A. pittii* has been increasingly reported in clinical specimens and in blood cultures [3,4] and the emergence of carbapenem-resistant *A. pittii* strains are becoming a big concern. *A. pittii* is very diverse as it can be found in soil, water, food and in both clinically ill and healthy individuals [5]. Moreover, the factor contributing to its propensity in the environment is the ability to withstand desiccation and survive on abiotic objects. Surfaces such as curtains in hospitals, medical devices, bed rails, tables, clothing, towels etc., have been the source of outbreaks from nosocomial pathogens like *A. pittii* [6].

It has been well established that efflux mechanisms play a key role in multidrug resistance in Gram-negative bacteria. The major clinically relevant efflux systems are of the RND superfamily. These are tripartite complexes typically composed of an inner membrane protein (IMP), a membrane fusion protein (MFP), and an outer membrane channel protein (OMP) [7].

In *A. pittii,* AdeDE RND efflux pump was first discovered in a blood culture *Acinetobacter* isolate at Prince of Wales hospital, Hong Kong [2]. In the same study, authors discovered two open reading frames (ORFs) which were named *adeD* and *adeE* and the products were assigned as AdeD and AdeE [2]. To elucidate the function of these ORFs, a deletion mutant lacking *adeE* was constructed. The mutant strain was shown to have reduced antibiotic susceptibility to multiple antibiotics like amikacin, ceftazidime, ciprofloxacin, meropenem, rifampin, chloramphenicol, and erythromycin [2]. The substrate specificity is most similar to both AdeABC and AdeIJK.

Unlike in other efflux systems, AdeDE lacks an outer membrane factor which means that AdeDE recruits an OMF encoded elsewhere in the genome, as seen for some other efflux pumps [8].

Expression of RND efflux pumps is under tight regulation and most efflux pump-encoding operons are associated with a gene encoding a transcriptional regulator [9]. Regulatory mechanism(s) that control the expression of AdeDE pump are not known. In this study, we characterize a TetR-type family transcriptional regulator, AdeQ, that controls the expression of AdeDE pump.

3.2 Materials and Methods

Table 3.1. All bacterial strains and plasmids used in this study.

Strain or Plasmid	Characteristics	Reference or Source
E. coli DH5*α*	F– Φ80lacZΔM15 Δ(lacZYA-argF) U169 *recA1 endA1 hsdR17* (rK–, mK+) *phoA supE44* λ– thi-1 *gyrA96* relA1	Laboratory collection
E. coli SM10	*thi thr leu tonA lacY supE recA*::RP4-2-Tc::Mu Km λpir	Laboratory collection
pMO130	Suicide vector, Km^r	[10]
pUC18T-miniTn*7*-Gm-LAC	Single copy insertion vector, Gm^r, Amp^r	[11]
pFLP2	Plasmid expressing Flp-recombinase, Amp^r	[12]
pTNS2	Plasmid expressing transposon insertion machinery	[13]
pRK2013	Helper plasmid for conjugation, Kan^r	Laboratory collection
pUC18T-miniTn*7*-Gm-*adeQ*	Single copy insertion vector, Gm^r, Amp^r	This study
Agrobacterium tumefaciens	AHL biosensor strain, Gm^r	[14]
A. pittii AP007	Type-Strain	This study
A. pittii AP012	AP007:Δ*adeQ*	This study
A. pittii AP013	AP012::*lacI*^{q} *adeQ*	This study
A. pittii AP016	AP012::Δ*adeQ* Δ*adeDE*	This study

Table 3.2. All primers used in this study.

Primer	Sequence	Purpose	Source or Reference
AdeDE-REG F1	GCCAGAGGTCACTAACCAAC	Amplification of 1kb fragment upstream of *adeQ*	This study
AdeDE-REG R1	AGGAACTTCAAGATCCCCAATTCG GAATTCGAGAGGGACGACC	Amplification of 1kb fragment downstream of *adeQ*	This study
AdeDE-REG F2	TCAGAGCGCTTTTGAAGCTAA TTCGAAGAAGTGTGTCGTACC	Amplification of 1kb fragment upstream of *adeQ*	This study
AdeDE-REG R2	CATGTCTGGCAGAACTCC	Amplification of 1kb fragment downstream of *adeQ*	This study
AdeDE-F1	GAGATCAAACTGACCTATCC	Amplification of 1kb fragment upstream of *adeDE*	This study
AdeDE-R1	AGGAACTTCAAGATCCCCAATTCG GGCTGATCAGAATCACATCC		
AdeDE-F2	TCAGAGCGCTTTTGAAGCTAATTC AGTAGCAGAAGGCAATACGG	Amplification of 1kb fragment downstream of *adeDE*	This study
AdeDE-R2	CTGGATAAGTTGCTCAATGC		
AdeDE_Conf_F	TGCTCAATGAAAGGTGCTTC	*adeDE* knockout screening Primer	This study
AdeDE_Conf_R	GAGTTCATTCAAGCCGATCT		
Gm-Fwd	CGAATTAGCTTCAAAAGCGCTCTGA	Amplification of Gm^r cassette	This study
Gm-Rev	CGAATTGGGGATCTTGAAGTTCCT		
AdeDE-REG_Conf_F	CTACTCCATTGACTTGTGG	*adeQ* screening Primer	This study
AdeDE-REG_Conf_R	AGCCTATATAACCGCAATG		
AdeDE-REG-FL-Fwd-PstI	ATACTGCAGATGTTAAAAAAATCTCCAGG	Amplification of full length *adeQ* with *Pst*I and *Hind*III restriction sites for cloning into pUC18T-miniTn*7*-Gm	This study
AdeDE-REG-FL-Rev-HindIII	AATAAGCTTCTATTCTTTATATTGCCATGCT		
GlmS_Fwd	TTTGCTGATGAAAATAGCGG	Primers for confirmation of miniTn*7* insertion downstream of *glmS2*	This study
Tn*7*R_Rev	CACAGCATAACTGGACTGATTTC		
16S-RT-Fwd	CTTCGGACCTTGCGCTAATA	qRT PCR primer for the 16S rRNA housekeeping gene	This study
16S-RT-Rev	ATCCTCTCAGACCCGCTACA		

AdeDE_Reg qRT_F	TGTCTTGGTCGGGAAGTGAT	qRT PCR primer for the *adeQ* gene	This study
AdeDE_Reg qRT_R	GCCCGTGAACTATTCCTTGA		
AdeE qRT_F	TGCCTGCGTTATTTCTACCC	*adeE*, Gene expression qRT primers	This study
AdeE qRT_R	GAAACAGAGCGGGTTGGTAA		

3.2.1 Media and Growth Conditions

Bacterial strains described here were routinely cultured in LB and LB agar unless otherwise stated. Both LB and LB agar was obtained from Difco Laboratories, Mississauga, ON, Canada. The culture conditions for liquid medium were at 37°C shaking at 250 rpm unless otherwise stated and static incubation at 37°C was used for solid media.

3.2.2 DNA Extraction

Genomic DNA (gDNA) extraction of *A. baumannii* was carried out using 3 mL of overnight liquid culture using a commercially available DNA isolation kit (Norgen Biotek Corp, ON, Canada) using the manufacturer's instructions. Plasmid DNA extractions from overnight liquid cultures were performed using BioBasic Plasmid Miniprep Kit (BioBasic Inc. Markham, ON, Canada) following manufacturer's instructions and provided solutions. gDNA and plasmid DNA were eluted in 50μL of the supplied buffers from each kit.

3.2.3 PCR

Genomic DNA and plasmids extracted using the above-mentioned protocols were used as templates for general PCR reactions. Taq DNA polymerase (Froggabio, ON, Canada) or Q5 DNA polymerase (NEB, Pickering, Canada) were used in all reactions following the manufacturers' recommendations. dNTPs (FroggaBio) were used at a concentration of 100 μM. Primers were ordered from IDT (Integrated DNA Technologies, Toronto, ON, Canada) and diluted to 9 μM for all PCRs.

3.2.4 Splice Overlap Extension PCR (SOEing PCR)

Splice Overlap Extension (SOEing) PCR was the choice of PCR technique [11] used to construct the knockout cassettes for the gene deletions in. SOEing PCR was carried out following a previously described method [11] with modifications using the primers listed in Table 3.2. Briefly,

the forward set of primers amplifying a ~1kb upstream region of the desired gene and the reverse set of primers amplifying a ~1kb downstream region of the desired gene were used in two separate PCR reactions with Taq DNA polymerase. The *aacC1* (Gm^R) gene conferred resistance to gentamicin along with the FRT sites were also amplified using Taq DNA polymerase and each fragment was gel extracted. These fragments were used as templates for the SOEing PCR reaction using Taq DNA polymerase. The reaction mixture consisted of 50 ng of each fragment as template and contents of a Taq DNA polymerase PCR reaction mixture except for primers. This PCR was cycled for 3 times with an annealing temperature of 55°C after which the reaction was paused, and the upstream forward and the downstream reverse primers were added, and the reaction cycled for 30 times with an annealing temperature specific to the primers used to facilitate the amplification of the ~3kb knockout cassette. The knockout cassette was then gel extracted and used to ligate into the suicide vector used.

3.2.5 Preparation of Competent Cells

3.2.5.1 Chemically competent cells

Overnight cultures of *E. coli* cells were subcultured 1:100 (v/v dilution) in 125 mL of fresh LB and grown to A600 of 0.4-0.6. Cultures were pelleted by centrifugation at 5000rpm for 5 minutes at 4°C. While maintaining cells on ice supernatants were decanted before resuspending in 40% of the original culture volume of ice-cold TFB1 buffer (100 mM rubidium chloride, 50 mM manganese chloride, 30 mM potassium acetate, 10 mM calcium chloride, and 15% w/v glycerol; pH 5.8) and incubated for 5 minutes on ice. The cell suspension was centrifuged again at 5000 x g for 5 minutes at 4°C and the supernatant was discarded. The cell pellet was resuspended in 5 mL of sterile ice-cold TFB2 buffer (10mM MOPS, 10 mM rubidium chloride, 75 mM calcium chloride, and 15% w/v glycerol; pH 6.5) and incubated on ice for 30 – 60 minutes. 100 µL aliquots

of the cells were then placed onto pre-chilled 1.5 mL microfuge tubes and frozen immediately in a dry ice/ethanol bath for 30 – 40 seconds. The frozen cells were immediately transferred to the -80°C freezer and stored there until used [15].

3.2.5.2 Electrocompetent cells

Four aliquots of 1.5 mL overnight cultures of *A. pittii* were grown overnight and centrifuged at 10000 xg for 2 minutes [16]. Culture supernatants were removed from the cell pellet and discarded. Cell pellets were then washed three times with sterile ice-cold water with centrifuging at 10000 xg for 2 minutes between washes. Washed cells were then pooled together and made up to a final volume of 100 µL with sterile ice-cold water. Cells prepared by this method were used immediately.

3.2.6 Transformation of Bacterial Cells

3.2.6.1 Electroporation

Freshly made electrocompetent *A. pittii* cells were transferred into 2 mm electroporation cuvettes (Thermo Fisher Scientific) and then mixed with 100-200 ng of the plasmid DNA to be transformed [16]. The mixture was incubated on ice for 15 minutes and then electroporated at 2.5 kV in an Eppendorf Electroporator 2510 (Eppendorf, Mississauga, ON, Canada) and 1mL of prewarmed SOC (Super Optimal Broth) was immediately added following charge. The entire content of the cuvette was transferred into a 1.5 mL microfuge tube. The time constant was observed for each electroporation and any reaction with less than 5 ms time constant was discarded. The microfuge tubes were then incubated for 1 hour at 37°C with shaking to facilitate the outgrowth of transformed cells. The microfuge tubes were then centrifuged at 13000 xg for 2 minutes and the supernatant was discarded. The cell pellet was resuspended in 100 µL of sterile LB and spread plated onto LB agar plates with the appropriate antibiotics.

3.2.6.2 Chemical transformation

Chemical transformation carried out with either *E. coli* DH5α and SM10 were performed with chemically competent cells using the heat shock method [15]. The cells were allowed to thaw on ice for 10 minutes and 50 µL of competent cells were incubated with 50-100 ng of plasmid DNA to be transformed for 15 minutes before heat shock. Transformation mixture was placed in the 42°C dry bath for 45 seconds and were immediately placed on ice for 2 minutes. 900 µL of prewarmed sterile LB was added into the transformation tubes and incubated at 37°C with shaking for 1 hour to facilitate the outgrowth of transformed cells. The tubes were then centrifuged at 13000 xg for 2 minutes and the cell pellet was resuspended in 100 µL of sterile LB and spread plated onto LB agar plates containing the appropriate antibiotic.

3.2.7 Gene Deletions in *A. pittii*

3.2.7.1 Conjugation

The gene deletions were carried out based on a homologous recombination method previously described with minor modifications [17]. Briefly 200 µL of overnight cultures of the SM10 cells carrying the suicide vector and the recipient *A. pittii* AP007 were mixed in a 1.5 mL centrifuge tube. The mixture was then centrifuged at 10000 xg for 2 minutes to pellet the cells and the supernatant was discarded. The cell pellet was washed three times using sterile LB to remove residual antibiotics from the overnight growth medium. After washing, the cell pellet was resuspended in 10 µL of sterile LB and spotted onto a sterile 3cm x 3cm nitrocellulose filter paper placed on a pre-warmed LB agar plate. The spot was allowed to dry and then incubated at 30°C for 16 hours to facilitate conjugation. After the incubation period, the nitrocellulose filter paper was carefully removed from the LB agar plate and placed into a 1.5 mL centrifuge tube containing 400 µL of sterile 0.85% saline. The bacterial cells were carefully mixed with the saline to remove

it from the nitrocellulose paper into the saline. The nitrocellulose paper was then removed and the saline containing the bacterial cells was then plated onto Simmons citrate agar (Sigma-Aldrich, St. Louise, MO, USA) plates supplemented with 50µg/mL kanamycin. These plates were then incubated at 37°C for 48 hours or until colonies appeared. Colonies were patched on LB agar plates supplemented with 50 µg/mL kanamycin and 50µg/mL gentamicin (BioBasic, Markham, ON, Canada), respectively. Patches resistant to both kanamycin and gentamicin, representing merodiploid cells with successful insertion of the suicide plasmid, were selected for the next step of curing of the suicide plasmid.

3.2.7.2 Homologous recombination

To select for the second recombination event required for the curing of the suicide plasmid, the *sacB* gene present on the pMO130 was utilized. *sacB* encodes an enzyme from *B. subtilis* called levansucrase which converts sucrose into levans, lethal for most Gram negative bacterial species [18]. Merodiploid colonies were streaked onto Vogel-Bonner minimal medium (VBMM) agar [19] supplemented with 10% sucrose (BioBasic) and 30µg/mL gentamicin and incubated at 30°C for 48 hours. Colonies from these plates were patched on gentamicin 50µg/mL LB agar and kanamycin 50µg/mL LB agar. Colonies that retained resistance to gentamicin and but displayed susceptibility to kanamycin had undergone the second recombination event resulting in a marked deletion of the target gene. Gene disruptions were further confirmed by PCR using the primers flanking the target gene with a PCR product of ~3kb as compared to the size of the wild type gene.

3.2.7.3 Excision of the Gm^R marker

To achieve the markerless deletion of the target gene, conjugations were set up with *E. coli* SM10 harbouring pFLP2 plasmid and the *A. pittii* strains with the genes disrupted with the knockout cassette containing the Gm^R marker [11]. Conjugations were carried out as described above with

overnight cultures of both strains and conjugation mixtures were incubated for 16 hours at 30°C. After the incubation period, the conjugation mixtures were plated onto Simmons citrate agar supplemented with 200µg/mL carbenicillin to select for the *A. pittii* colonies with the pFLP2 plasmid present. These colonies were cross patched onto LB agar supplemented with 50µg/mL gentamicin and LB agar supplemented with 200µg/mL carbenicillin to screen for the loss of Gm^R marker. Colonies that were only able to grow on carbenicillin were streaked onto LB+10% sucrose to facilitate the curing of the pFLP2 plasmid. The colonies from the LB+10% sucrose was then cross patched onto 50µg/mL gentamicin, 200µg/mL carbenicillin, and LB agar to phenotypically reconfirm the loss of Gm^R marker as well as pFLP2 plasmid.

3.2.8 Genetic Complementation

3.2.8.1 Construction of the plasmid vector

Complementation of the deleted genes were carried out using the previously described pUC18Tmini- Tn*7*T-Gm plasmid vector [13]. The gene to be complemented was amplified was amplified with its native promoter using gDNA from *A. pittii* AP007 as the template with the primers containing suitable restriction sites (Table 3.2). The PCR product was then gel purified and digested with their respective restriction enzymes. The digested product was purified again from agarose gel. The plasmid vector was digested with the same enzymes and gel extracted. Ligation reactions with the vector and the insert were set up using T4 DNA ligase (Thermo Scientific) following the manufacturer's guidelines and ligation mixtures were incubated at 16°C overnight before transforming into chemically competent *E. coli* DH5α cells.

3.2.8.2 Creating chromosomal insertions for gene complementations

Four parental conjugations were set up, as described before [11], to introduce the plasmid vector into the *A. pittii* strain with gene deletions. The positive colonies for the insertion were selected

based on their growth on 50μg/mL gentamicin and then confirmed by PCR using the primers listed in Table 3.2. The positive colonies were electroporated with pFLP2 to excise the Gm^R cassette and selected on 200μg/mL carbenicillin plates. The colonies that grew on carbenicillin were then cross patched onto gentamicin plates to confirm the successful removal of the Gm^R cassette. The colonies that grew on carbenicillin but not on gentamicin were selected for streaking onto LB+10% (w/v) sucrose plates. The colonies from the LB+10% sucrose plate was cross patched onto LB agar + 50μg/mL gentamicin, LB agar + 200μg/mL carbenicillin, and LB agar, respectively to confirm the loss of Gm^R marker and pFLP2 plasmid. The resulting colonies had the full-length gene with its native promoter inserted into the *att*Tn*7* site that is downstream of the *glmS* gene and it was further confirmed using PCR using the primers *glmS* F and Tn7R listed in Table 3.2. The expression of the inserted gene was confirmed using qRT-PCR before using the strain in phenotypic experiments.

3.2.9 Quantitative Reverse Transcriptase PCR

Overnight cultures were diluted in a 1:100 (v/v) ratio into fresh LB broth and grown to an OD_{600} of 0.6-0.8. 1.5 mL of each culture was pelleted using centrifugation and the supernatant was removed. Pelleted cells were stored in -70°C overnight before total RNA extraction. RNA extraction was carried out using a RNeasy Mini Kit (Qiagen Sciences Inc) according to the manufacturer's protocol. Sterile Milli-Q water was used to make 1 μg/μL solutions of RNA before carrying out DNase treatments using a RNase Free DNase Set (Qiagen, Maryland, USA) according to the manufacturer's protocol. Complimentary DNA (cDNA) was synthesized from DNase-treated RNA using a SuperScript VILO cDNA Synthesis Kit (Invitrogen, Burlington, Canada) according to the manufacturer's protocol. For RT-qPCR, SYBR Select Master Mix (Applied Biosystems Inc, Foster City, USA) was used for fluorescent detection of product DNA on a

StepOnePlus Real-Time PCR System (Applied Biosystems Inc). To ensure there was no genomic contamination of cDNA samples, DNase treated RNA was used as a negative control for all primer sets in addition to a No-Template-Control which substituted water for cDNA. Relative expression was calculated using 16S rRNA as the reference gene by Pfaffl method [20]. DNA primers used to target each gene of interest are listed in Table 3.2.

3.2.10 Biofilm Assays

Biofilm assays were performed as previously described [21] with the following modifications. Overnight cultures were subcultured and grown to an OD_{600} of 0.6 before 1:100 (v/v) dilution in Mueller Hinton Broth (Sigma Aldrich, Oakville, ON, Canada). 150 µL of diluted cultures were distributed into at least six wells of a 96-well polystyrene, round-bottom microtiter plate (Sarstedt) before stationary incubation at 37°C for 48 hr. Planktonic cells were removed by washing the plates twice with MilliQ water. Biofilms were stained with 200µL of 0.5% w/v crystal violet (Thermo Fisher Scientific) in ethanol (95%) and incubated with gentle shaking for 30 minutes. Crystal violet was washed out of the wells by gently submerging the plates in MilliQ water 3-4 times. Plates were then air dried overnight, before crystal violet was extracted with 200 µL 30% Acetic acid by incubating at room temperature with gentle shaking for 30 minutes. Following extraction, the solution was transferred to a fresh 96-well plate and absorbance was measured at 550 nm using a SpectraMax M2 plate reader (Molecular Devices).

3.2.11 N-acyl-homoserine lactones (AHLs) detection soft agar assay

Detection of AHL was carried out using a bioassay described previously [14]. *A. tumefaciens* NTL4 (pZLR4) was utilized to detect AHLs with long acyl chains. This strain carries the plasmid pZLR4, which contains a *traG::lacZ* fusion and *traR*. In the presence of AHLs with long acyl chains the TraR protein is activated, transcription of the *traG::lacZ* fusion is turned on,

and LacZ (β-galactosidase) activity can be used as a reporter of *traG* transcription [14]. *A. tumefaciens* biosensor strain was grown overnight at 28 °C, stationary in 3mL of LB containing gentamicin (30 μg/mL). LB agar soft plates were prepared by pouring a mixture of 20 mL of molten agar (7 g agar/L, cooled to 45°C), 80 μL of X-gal (20 μg/mL) and 250 μL of the *A. tumefaciens* culture (OD A_{600} = 0.2) in Petri plates. Plates were dried inverted at 37°C for 30–45 min. Three μL of the desired strains at 0.2 OD were spotted, and plates were incubated at 28°C. Strains of interest that are positive for AHL secretion will produce a blue halo.

3.2.12 Motility

Motility assays were performed in semi-solid agar (0.3% agar) with overnight cultures that had been normalized to an OD600 of 1.0 in LB broth as described previously [22]. Three μL of normalized cultures were stab inoculated into the center of the semi-solid agar plates and allowed to dry for 10 minutes before overnight incubation at 37°C. Motility was then evaluated by measuring the maximum distance travelled from the inoculation point. Assays were performed using 3 biological replicates and at least 5 technical replicates.

3.2.13 Growth curves

Overnight cultures of bacterial cells were standardized to an OD 0.1 in fresh LB medium and 150μL of each standardized culture was then distributed into 3 wells of a round bottom 96 well polystyrene microtitre plate (Sarstedt, Montreal, QC, Canada). Plates were then incubated at 37°C in a SpectraMax M2 plate reader (Molecular Devices) with shaking at 200 rpm before each reading which occurred every thirty minutes. Three biological replicates were used for all strains.

3.2.14 Antibiotic susceptibility testing

Antibiotic susceptibility testing was performed by the broth microdilution method described by the Clinical and Laboratory Standards Institute using at least three biological replicates (Clinical

and Laboratory Standards Institute 2012). Results are shown as the Minimum Inhibitory Concentration (MIC) of the antibiotic that inhibited visible growth of the culture.

3.3 Results and Discussion

Infections with *A. pittii* are becoming more challenging due to its ability to develop antibiotic resistance [6]. With rising reports of antibiotic resistant *A. pittii* isolated from hospital environments, infections are becoming more challenging to treat. Intrinsic drug-resistance mechanisms such as the natural tolerance of bacteria to certain antibiotics and efflux pump genes further exacerbates the drug-resistance problem of *A. pittii*.

Upstream of the open reading frame of *adeD* lies a 555nt long TetR/AcrA type regulator which we believe is the regulator for this efflux pump. To understand the regulatory mechanism of AdeDE efflux pump, we created strains with deletion in *adeQ* and a double deletion of a strain lacking both *adeQ* and *adeDE*. *adeQ* deletion mutant was complemented via a single-copy chromosomal insertion using a mini-Tn*7* system under IPTG inducible synthetic P_{tac} promoter. Next, these set of strains were subjected to a variety of phenotypic assays which are responsible for resistance and survival of *A. pittii* to allow us to elucidate how AdeDE is regulated in *A. pittii*.

3.3.1 AdeQ knock-out results in overexpression of the AdeDE efflux pump

Previous studies in *Acinetobacter* spp. have shown that the linked regulator gene's product commonly acts as the repressor of the pump operon as its deletion leads to overexpression of the pump and changes in the antibiotic susceptibility profile [23]. We observed similar phenotypes where deletion of *adeQ* shows a ~24-fold overexpression of the *adeE* as analyzed via RT-qPCR. (Fig 3.1). Upon complementation of AdeQ using a mini-Tn*7* single copy insertion system, *adeQ* expression was restored to wild-type level. This suggests that AdeQ is acting as a repressor for the AdeDE efflux pump.

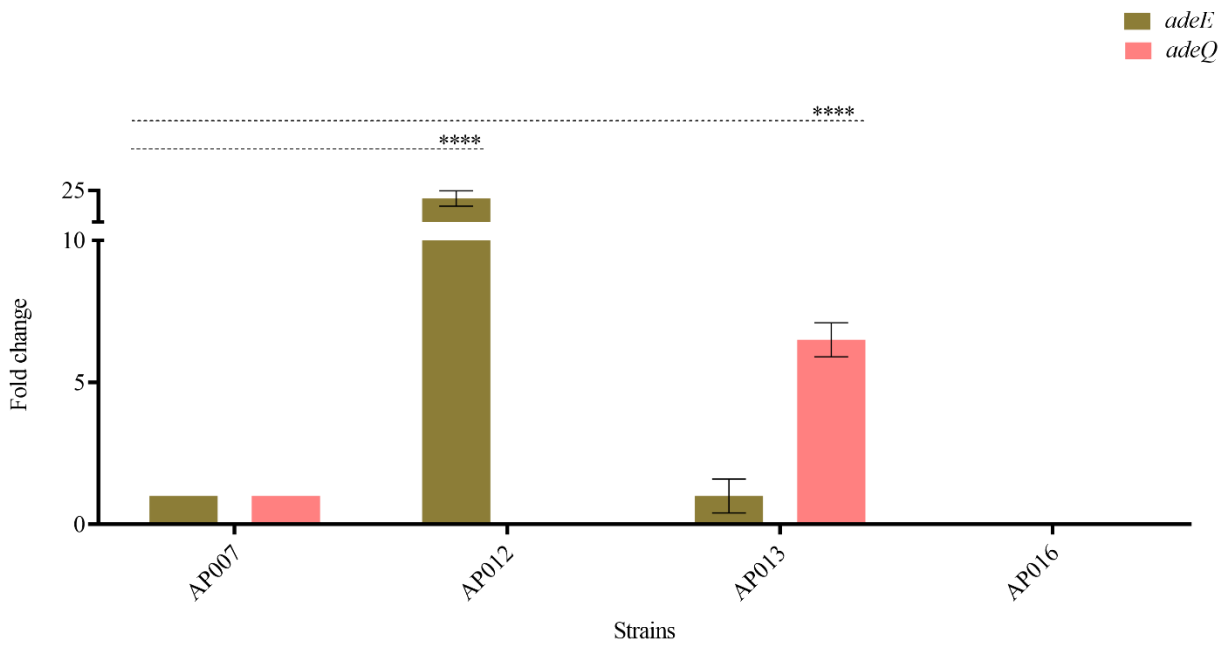

Figure 3.1. Relative expression of *adeE* and *adeQ* in *A. pittii* strains
AP012 (AP007:Δ*adeQ*) shows ~24-fold overexpression of the AdeDE efflux pump compared to the parental strain. Expression of *adeQ* is restored in the AP013 (AP012::*lacI*^{q} *adeQ*). AP016 (AP012::Δ*adeDE*) shows no expression of *adeE* and *adeQ*. 16S rRNA gene was used as the housekeeping control for all four strains. Error bars represent standard deviation. **** indicates $P<0.0001$. Graphs generated in GraphPad Prism 6.0.

3.3.2 Minimum inhibitory concentrations assay

To assess whether gene deletion and complementation of AdeQ displayed phenotypic changes, minimum inhibitory concentration were performed for substrates of the AdeDE efflux pump [2]. Deletion of AdeDE efflux pump has been shown to have increased susceptibility to multiple antibiotics such as ciprofloxacin, imipenem, gentamicin, methicillin, and ceftazidime. *adeQ* mutant shows at least 2-fold decrease in susceptibility to gentamicin, ciprofloxacin, ceftazidime, and moxifloxacin. These changes are analogous to a previous study characterizing the AdeDE efflux pump [2]. Interestingly, upregulation of *adeDE* upon *adeQ* deletion results in minor (2-fold) decrease in the susceptibility (Table 3.3), a phenotype that is restored in the complemented strain, AP013 (AP012::*lacI*^{q} *adeQ*). On the other hand, deletion of *adeDE* (in AP012 background) results in more significant increase in susceptibility ($\geq$ 4-fold) to antibiotics that are a substrate of AdeDE pump. This suggests that mere upregulation of the AdeDE pump is not able to decrease the susceptibility of *A. pittii* to antibiotics, and that the amount of as yet OMF (encoded elsewhere in the genome) controls the antibiotic susceptibility mediated by the AdeDE pump. However, this would need further investigation.

3.3.3 Fitness of *A. pittii* strains in LB medium

Studies have shown that strain fitness is critical and can have an effect on phenotypes such as efflux pump expression and antibiotic susceptibility [8,24]. To rule out the fact the observed differences in antibiotic susceptibility and efflux pump expression is not due to a defect in growth, we assessed the fitness of these strains in rich media (LB). Growth of mutant and complemented strains was tested to see if the deletion of *adeQ* would result in any significant growth defects under non-stress conditions (Fig 3.2). In LB broth, none of the strains exhibited any significant

growth defects compared to the wild type *A. pittii*. Although, we saw that the double deletion mutant was growing slow initially but growth was similar to other strains after 12 hours.

3.3.4 Motility of *A. pittii* strains on semi-solid agar medium

Having established that deletion of *adeQ* results in overexpression of AdeDE and increased susceptibility to multiple antibiotics. We sought to test other phenotypic characteristics associated with virulence. Various studies have shown motility of isolates that belong to the *Acinetobacter calcoaceticus-baumannii* complex [24]. This phenotype has not been extensively studied in *A. pittii*. As such we evaluated twitching motility in the WT, deletion mutant, and complemented strains by growth in semi-solid agar (0.3%) (Fig 3.5). We observed that deletion strain shows a decrease in motility compared to WT *A. pittii* and the phenotype is restored upon complementation of *adeQ*. A similar result was observed in *A. baumannii* where deletion of a regulator of an efflux pump can have a negative impact on twitching motility [25].

3.3.5 Biofilm formation

The ability to form biofilm is one the most significant factors that allow members of the Acb complex to persist in hospital environments and medical devices [4]. *A. pittii* has been shown to form more robust biofilm compared to *A. baumannii* isolates. As this is such an important phenotype contributing to clinical significance of *A. pittii*, biofilm formation was evaluated in the Δ*adeQ*, Δ*adeDE*Δ*adeQ* and complementation strains (Fig 3.3). Mutant strains show an increase in biofilm formation and restoration to WT levels is seen in the complemented strain. The double deletion mutant, however, showed a significant decrease in biofilm production suggesting that it was the overexpression of the AdeDE efflux pump causing increase in biofilm production and not the lack of the regulator.

Table 3.3. Antibiotic susceptibilities of *A. pittii* strains.
Data expressed in μg/mL as determined by Broth dilution method and representative of three independent biological replicates and at least three technical replicates. MIC values that changed by ≥ 4-fold are indicated in bold.

	AP007 (Type-Strain)	AP012 (AP007:Δ*adeQ*)	AP013 (AP012::*lacI*^{q} *adeQ*)	AP016 (AP007::Δ*adeQ* Δ*adeDE*)
GEN	2	4	2	**0.0625**
CIP	0.25	0.5/1	0.5	**0.0625**
CEF	1	2	1	**0.125**
ZEO	1	1	1	1/2
TET	4	4	2	**0.125**
MER	0.25	0.25/0.5	0.25	0.125
RIF	2	2	2	**0.0625/0.125**
MOX	0.25	0.5/1	0.5	0.125
CLI	4	4/8	4	2/4
APR	8	8	8	4
ERT	4	4	4	**0.125**
KAN	4	2/4	2	2
AMI	2	2/4	2	1

GEN – gentamicin, CIP – ciprofloxacin, CEF – ceftazidime, TET- tetracycline, MOX - moxifloxacin, ERT – erythromycin, MER – meropenem, RIF – rifampicin, CLI – clindamycin, APR – apramycin, ZEO – zeocin, AMI – amikacin, KAN - kanamycin

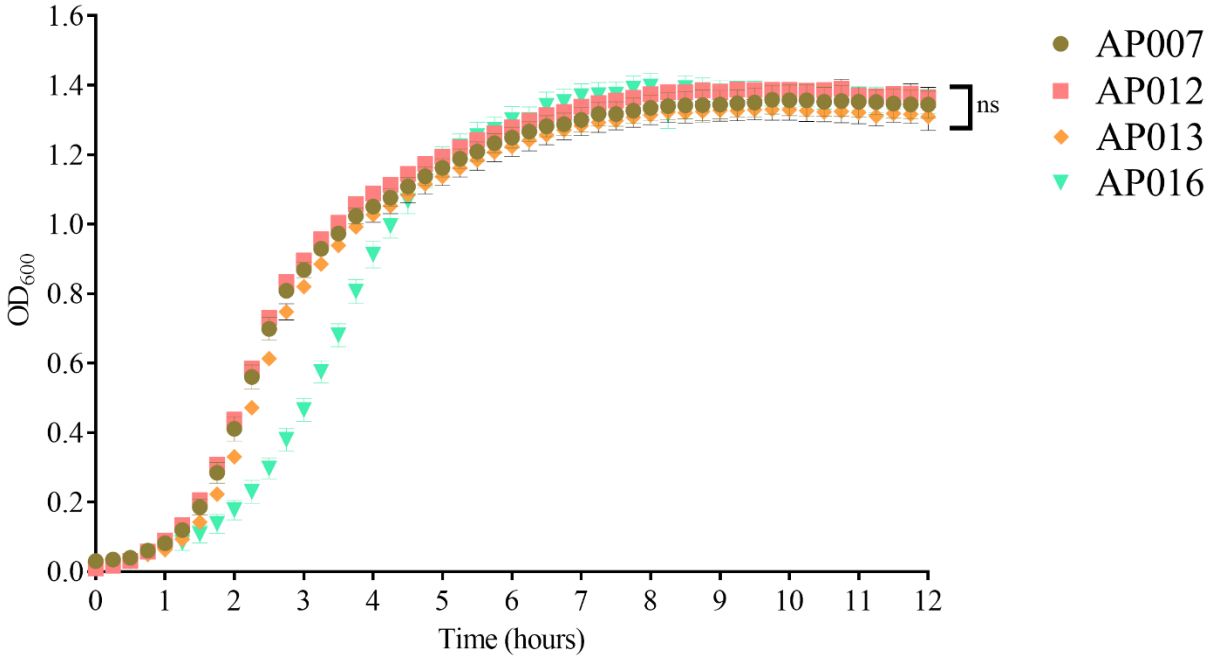

Figure 3.2. Fitness of *A. pittii* strains in LB medium
AP012 (AP007:Δ*adeQ*) and AP013 (AP012::*lacI*^{q} *adeQ*) show no statistical change in fitness when compared to the parent strain AP007. AP016 (AP007::Δ*adeQ* Δ*adeDE*) shows a slow initial growth but levels are comparable to WT after 12 hours. Growth was monitored for 12 hrs at 37°C with continuous shaking. Data shown is representative of three biological replicates. Graphs generated in GraphPad Prism 6.0.

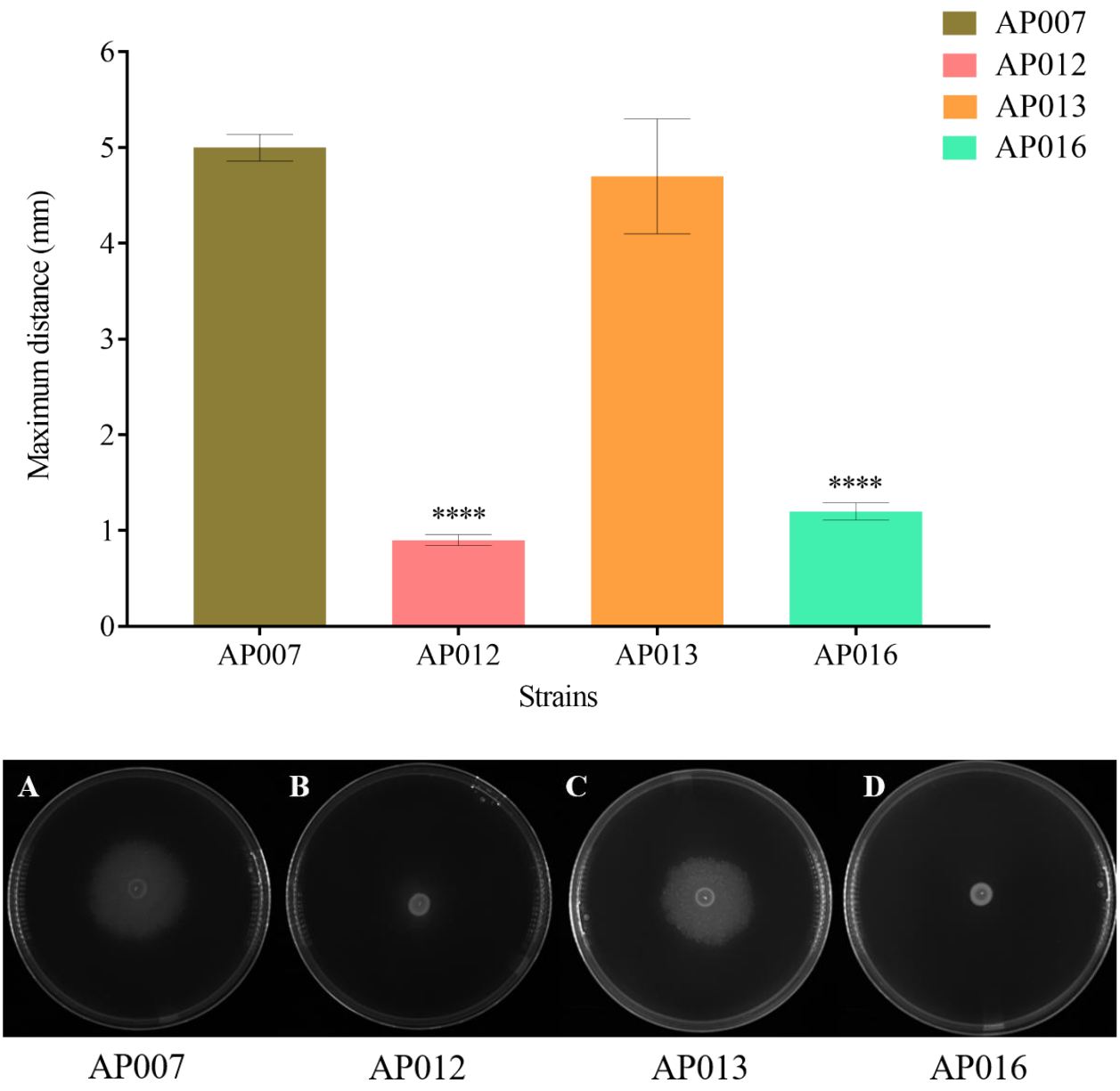

Figure 3.3. Motility of *A. pittii* strains on semi-solid agar medium
AP012 (AP007:Δ*adeQ*) shows decreased motility relative to AP007. The phenotype is restored in AP013 (AP012::*lacI*^{q} *adeQ*) upon complementation of *adeQ*. AP016 (AP007::Δ*adeQ* Δ*adeDE*) shows lack of motility. Experiment was performed in 3 biological replicates with 5 technical replicates. **** indicate ($P < 0.0001$). Graphs generated in GraphPad Prism 6.0.

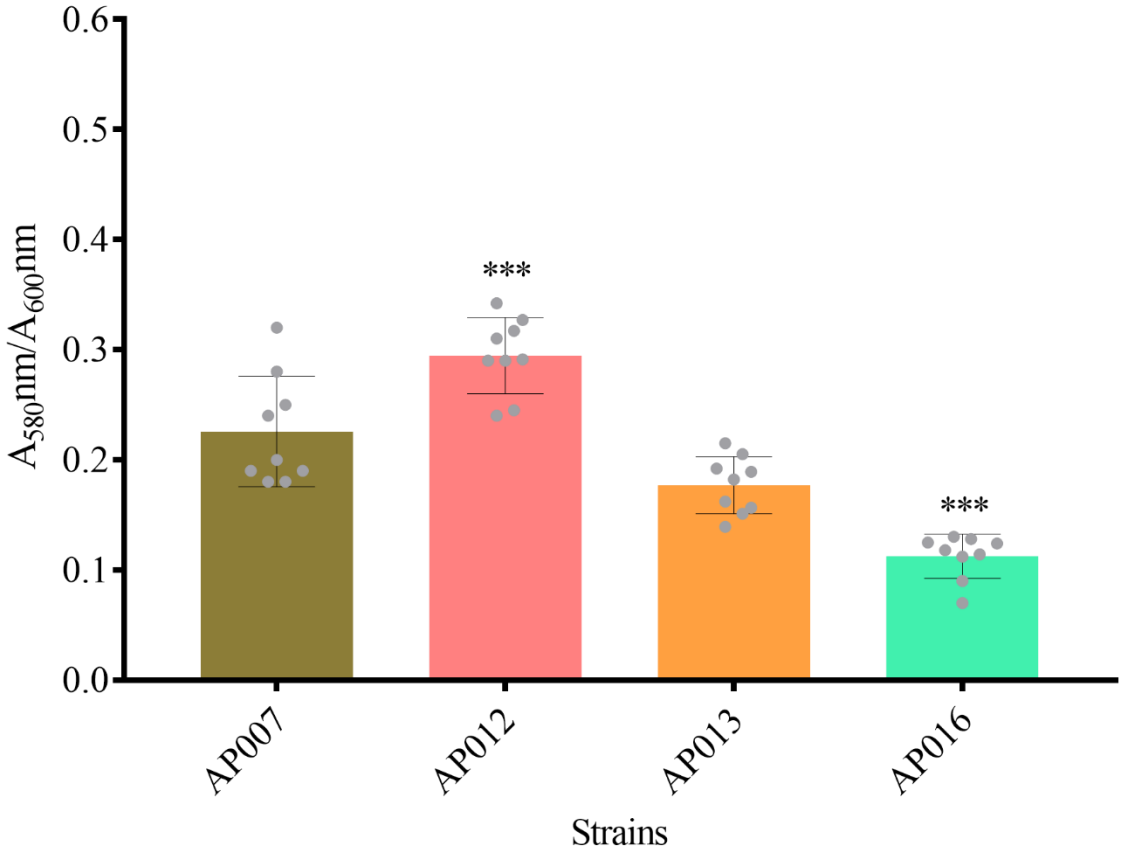

Figure 3.4. Biofilm formation by *A. pittii* strains.
Biofilm formation was monitored after 48 hours and biofilms were quantified by measuring the optical density at 580nm. AP007 was used as control. AP012 (AP007:Δ*adeQ*) shows an increase in biofilm production compared to AP007. Upon complementation in AP013 (AP012::*lacI*^{q} *adeQ*), the phenotype is restored to wild-type levels. AP016 (AP007::Δ*adeQ* Δ*adeDE*) shows decreased levels of biofilm production as it is lacking both AdeDE and *adeQ*. Data shown are representative of three biological replicates. Error bars represent standard deviation. *** indicates $P<0.0001$. Graphs generated in GraphPad Prism 6.0 for Windows.

3.3.6 N-acyl-homoserine lactones (AHLs) detection

One of the major factors contributing to resistance in *Acinetobacter* spp. is biofilm development [14]. In *A. pittii*, not much is known regarding the impact of biofilm formation and quorum sensing is what drove us to examine the link. Quorum sensing is a natural phenomenon that plays a role in biofilm formation. It is controlled by release of *N*-acyl homoserine lactones (AHLs) and helps bacteria communicate. In this assay, we qualitatively measured the production and secretion of AHL by utilizing a bacterial biosensor strains containing a reporter gene that is transcriptionally activated in the presence of AHL signals to form a correlation with biofilm production. *adeQ* mutant (AP012) secretes increased levels of AHLs compared to WT. Upon complementation of *adeQ* in WT, the levels of AHL are comparable to WT at both 12 and 24 hrs. However, in AP016, the levels of AHL are reduced at 12 and 24hrs compared to AP007 which is expected as the strain lacks both AdeDE and AdeQ. This indicates that increased AHL secretion from AdeDE efflux pump may be the reason we observed increased biofilm production in the *adeQ* knockout.

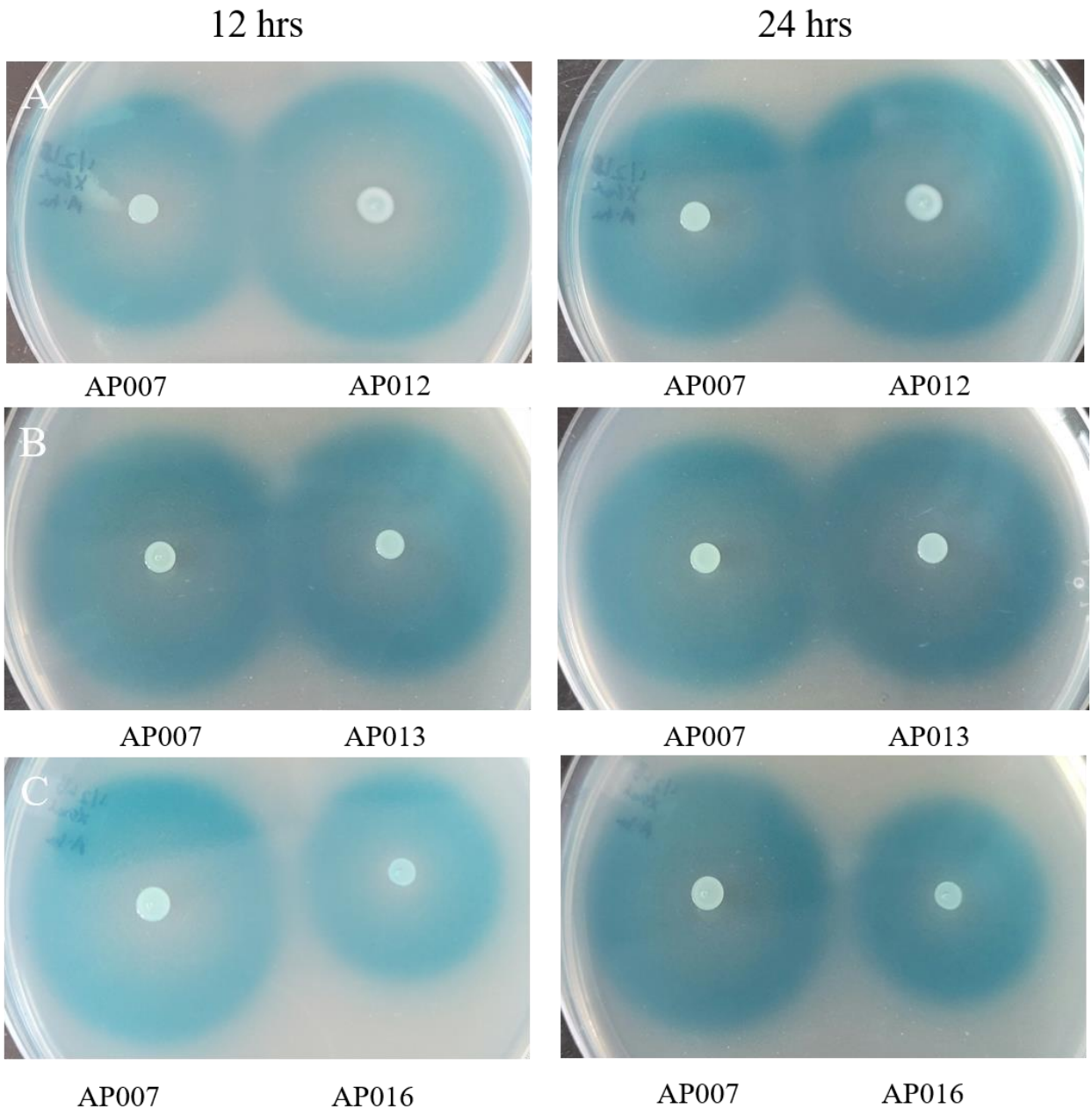

Figure 3.5. Bioassay for AHL secretion by *A. pittii* strains
3μL of 0.2 OD *A. pittii* wild-type AP007 control (left), (A) AP012 (AP007:Δ*adeQ*), (B) AP013 (AP012::*lacI*^{q} *adeQ*), (C) AP016 (AP012::Δ*adeQ* Δ*adeDE*) were patched onto a soft agar lawn of *A. tumefaciens traG-lacZ* biosensor and X-gal. The plate was incubated for 12 hrs and 24 hrs at 28 °C. The blue halo surrounding the wild-type *A. pittii* patch indicates production and diffusion of AHL through the medium, resulting in activation of the *traG-lacZ* fusion in the biosensor strain.

3.4 Conclusion

In this study, we characterize a novel regulator upstream of AdeDE efflux pump, the regulator was deleted from the wild-type *A. pittii* AB007. This study showed that AdeDE, efflux pump has a regulator that controls the expression and antibiotic susceptibility phenotype contributing to resistance of *A. pittii*. Genotypic and phenotypic characterization showed that deletion of AdeQ results in overexpression of AdeDE efflux pump, reduced antibiotic susceptibility to pump substrates and altered surface associated motility. Additionally, biofilm production was also increased due to the overexpression of the AdeDE efflux pump. We also saw increase in AHL secretion in the AdeQ deletion mutant and phenotype was restored upon complementation. In future, RNA seq studies will be required to understand the global transcriptomic change that results from deleting AdeDE and AdeQ.

3.5 Bibliography

1. Nemec A, Krizova L, Maixnerova M, et al. (2011) Genotypic and phenotypic characterization of the *Acinetobacter calcoaceticus-Acinetobacter baumannii* complex with the proposal of *Acinetobacter pittii* sp. nov. (formerly *Acinetobacter* genomic species 3) and *Acinetobacter nosocomialis*. *Research in Microbiology* 162: 393–404.

2. Chau SL, Chu YW, Houang ETS (2004) Novel resistance-nodulation-cell division efflux system AdeDE in *Acinetobacter* genomic DNA group 3. *Antimicrobial Agents and Chemotherapy* 48: 4054–4055.

3. Chusri S, Chongsuvivatwong V, Rivera JI, et al. (2014) Clinical outcomes of hospital-acquired infection with *Acinetobacter nosocomialis* and *Acinetobacter pittii*. *Antimicrobial Agents and Chemotherapy* 58: 4172–4179.

4. Pailhoriès H, Tiry C, Eveillard M, et al. (2018) *Acinetobacter pittii* isolated more frequently than *Acinetobacter baumannii* in blood cultures: the experience of a French hospital. *Journal of Hospital Infection* 99: 360–363.

5. Houang ETS, Chu YW, Leung CM, et al. (2001) Epidemiology and infection control implications of *Acinetobacter* spp. in Hong Kong. *Journal of Clinical Microbiology* 39: 228–234.

6. Pailhoriès H, Tiry C, Eveillard M, et al. (2018) *Acinetobacter pittii* isolated more frequently than *Acinetobacter baumannii* in blood cultures: the experience of a French hospital. *Journal of Hospital Infection* 99: 360–363.

7. Lin L, Ling BD, Li XZ (2009) Distribution of the multidrug efflux pump genes, *adeABC*, *adeDE* and *adeIJK*, and class 1 integron genes in multiple-antimicrobial-resistant clinical isolates of *Acinetobacter baumannii-Acinetobacter calcoaceticus* complex. *International Journal of Antimicrobial Agents* 33: 27–32.

8. Singh MK (2019) Functional analysis of MexXY resistance nodulation division efflux pumps in *Pseudomonas aeruginosa*.

9. Richmond GE, Evans LP, Anderson MJ, et al. (2016) The *Acinetobacter baumannii* two-component system AdeRS regulates genes required for multidrug efflux, biofilm formation, and virulence in a strain-specific manner. *mBio* 7: 1–12.

10. Hamad MA, Zajdowicz SL, Holmes RK, et al. (2009) An allelic exchange system for compliant genetic manipulation of the select agents *Burkholderia pseudomallei* and *Burkholderia mallei*. *Gene* 430: 123–131.

11. Choi KH, Schweizer HP (2005) An improved method for rapid generation of unmarked *Pseudomonas aeruginosa* deletion mutants. *BMC Microbiology* 5: 30.

12. Choi KH, Schweizer HP (2005) An improved method for rapid generation of unmarked *Pseudomonas aeruginosa* deletion mutants. *BMC Microbiology* 5: 30.

13. Choi KH, Schweizer HP (2006) mini-Tn*7* insertion in bacteria with single attTn*7* sites: Example *Pseudomonas aeruginosa*. *Nature Protocols* 1: 153–161.

14. Paulk Tierney AR, Rather PN (2019) Methods for detecting *N*-Acyl homoserine lactone production in *Acinetobacter baumannii*, *Methods in Molecular Biology*, Humana Press Inc., 253–258.

15. Liu J, Chang W, Pan L, et al. (2018) An improved method of preparing high efficiency transformation *Escherichia coli* with both plasmids and larger DNA Fragments. *Indian Journal of Microbiology* 58: 448–456.

16. Choi KH, Kumar A, Schweizer HP (2006) A 10-min method for preparation of highly electrocompetent *Pseudomonas aeruginosa* cells: Application for DNA fragment transfer between chromosomes and plasmid transformation. *Journal of Microbiological Methods* 64: 391–397.

17. Amin IM, Richmond GE, Sen P, et al. (2013) A Method for generating marker-less gene deletions in multidrug-resistant *Acinetobacter baumannii*. *BMC Microbiology* 13: 158.

18. Reyrat J-M, Pelicic V, Gicquel B, et al. (1998) Counterselectable markers: untapped tools for bacterial genetics and pathogenesis. *Infection and Immunity* 66: 4011 LP – 4017.

19. Schweizer HP (1991) The *agmR* Gene, an Environmentally Responsive Gene, Complements Defective *glpR*, Which Encodes the Putative Activator for Glycerol Metabolism in *Pseudomonas aeruginosa*.

20. Pfaffl MW (2001) A new mathematical model for relative quantification in real-time RT-PCR. *Nucleic Acids Research* 29: 45e – 45.

21. Iwashkiw JA, Seper A, Weber BS, et al. (2012) Identification of a general O-linked protein glycosylation system in *Acinetobacter baumannii* and its role in virulence and biofilm formation. *PLoS Pathogens* 8: e1002758.

22. Harding CM, Tracy EN, Carruthers MD, et al. (2013) *Acinetobacter baumannii* strain M2 produces type IV pili which play a role in natural transformation and twitching motility but not surface-associated motility. *mBio* 4.

23. Rosenfeld N, Bouchier C, Courvalin P, et al. (2012) Expression of the resistance-nodulation-cell division pump AdeIJK in *Acinetobacter baumannii* is regulated by AdeN, a TetR-type regulator. *Antimicrobial Agents and Chemotherapy* 56: 2504–2510.

24. Barker J, Maxted H (1975) Observations on the growth and movement of *Acinetobacter* on semi solid media. *Journal of Medical Microbiology*.

25. De Silva PM, Kumar A (2018) Effect of Sodium Chloride on Surface-Associated Motility of Acinetobacter baumannii and the Role of AdeRS Two-Component System. *The journal of membrane biology* 251: 5–13.

Chapter 4 Conclusion and future directions

The overall objective of this study was to examine to regulatory mechanism that control the expression of RND pumps in *Acinetobacter* spp. We analyzed the role of oxidative stress in the expression of AdeAB efflux pump in *A. baumannii.* In addition, we also characterized a TetR-family repressor of the AdeDE pump of *A. pittii.*

A. baumannii has the ability to sense and adapt to host signals and environmental stressors. Bacteria encounter a variety of stressors the moment they contact the host allowing bacteria to survive and initiate infection. A better understanding of the complex regulatory mechanisms of efflux pumps and stress response is essential for finding treatment options to combat antibiotic resistance.

In this study, we have showed that deletion of *katG* and *katE* was responsible for altering antibiotic susceptibility, increased sensitivity to hydrogen peroxide, and upregulation of efflux pumps in *A. baumannii*. Together, our data suggests that the interaction between efflux mediated antimicrobial resistance and oxidative stress response is much more complex than previously thought. Other studies like membrane lipid composition, deletion of AdeAB and testing alternative stressors are needed to further understand the role of catalase in *A. baumannii*. In future, with the RNA-seq data we can target specific genes that could be involved in regulating the stress response and efflux pump mechanism(s) in *A. baumannii*. This will largely be aided by proteomics and metabolomics studies. This study showed that a dynamic relationship between oxidative stress response and RND efflux pump-mediated antibiotic susceptibility exists in *Acinetobacter baumannii*.

In the second part of this thesis, characterization a novel regulator upstream of AdeDE efflux pump revealed that AdeQ controls the expression of the AdeDE RND efflux pump and antibiotic susceptibility phenotype contributing to resistance of *A. pittii*. Genotypic and phenotypic characterization showed that deletion of *adeQ* results in overexpression of AdeDE efflux pump,

increased antibiotic susceptibility to pump substrates and altered surface associated motility. Additionally, biofilm production was also increased due to the overexpression of the AdeDE efflux pump. In future, RNA seq studies will be required to understand the global transcriptomic change that results from deleting AdeDE and the regulator, AdeQ.

Together, our data suggests that the regulatory mechanisms underlying stress response and efflux pumps in *Acinetobacter* spp. will aid in generation and development new therapeutics against *A. baumannii* to help overcome antibiotic resistance and emphasizes the importance of taking into consideration, the possibility of crosstalk between efflux pumps and stress response when assessing the usefulness of an antimicrobial.

Appendix

Appendix 1. List of upregulated genes in AB189 (ATCC17978:Δ*katG*Δ*katE*) compared to ATCC17978

Locus_tag	Name	Differential Expression Log2 Ratio	Differential Expression p-value
AUO97_RS00055	DUF2171 domain-containing protein	1.598000217	8.92E-08
AUO97_RS01060	hypothetical protein	1.538995346	2.18E-03
AUO97_RS01135	alpha-keto acid decarboxylase family protein	2.889308459	6.94E-04
AUO97_RS01145	aldehyde dehydrogenase family protein	1.842134008	6.00E-05
AUO97_RS01430	pyridoxal phosphate-dependent aminotransferase	2.049283962	3.21E-02
AUO97_RS02330	folD	1.678873284	1.12E-02
AUO97_RS02410	greA	1.52014767	2.64E-02
AUO97_RS02520	sdhD	1.540130084	2.99E-02
AUO97_RS02525	sdhC	1.954780175	3.12E-03
AUO97_RS04810	trmD	1.797776396	1.77E-08
AUO97_RS10170	TetR/AcrR family transcriptional regulator	1.964836862	4.20E-04
AUO97_RS13765	DUF2147 domain-containing protein	1.781035271	1.43E-03
AUO97_RS14185	paaJ	1.731856897	1.95E-10
AUO97_RS14195	enoyl-CoA hydratase/isomerase family protein	1.514854307	0.001190687
AUO97_RS14200	2-(1,2-epoxy-1,2-dihydrophenyl)acetyl-CoA isomerase	1.631137823	0.000475805
AUO97_RS14205	3-hydroxyacyl-CoA dehydrogenase	1.862559427	4.79E-05
AUO97_RS14285	NAD(P)H-dependent oxidoreductase	1.632904877	2.23E-05
AUO97_RS15045	hypothetical protein	1.722078375	7.27E-09
AUO97_RS15050	EamA family transporter	2.995408804	2.15E-05

AUO97_RS15180	hypothetical protein	2.369847178	1.21E-08
AUO97_RS15810	rpsT	2.457034965	2.79E-09
AUO97_RS16010	HAD family hydrolase	1.679496064	2.38E-07
AUO97_RS16150	cell envelope integrity protein TolA	1.629998522	1.00E-08
AUO97_RS16395	hypothetical protein	1.668468092	1.45E-08
AUO97_RS16465	GntP family permease	1.793704219	2.19E-02
AUO97_RS16470	3-hydroxybutyrate dehydrogenase	1.585706683	4.47E-10
AUO97_RS16535	adeB	2.102924874	0.000522945
AUO97_RS16545	adeR	1.559308431	0.001018652
AUO97_RS16595	PAAR domain-containing protein	1.555007775	1.86E-09
AUO97_RS16875	hypothetical protein	1.753307969	3.05E-06
AUO97_RS17170	MarR family transcriptional regulator	1.543765386	5.42E-04
AUO97_RS17525	DUF2750 domain-containing protein	1.676481921	1.46E-04
AUO97_RS17705	tetratricopeptide repeat protein	1.686862249	8.75E-07
AUO97_RS18450	mgtA	1.862027041	1.18E-10
AUO97_RS18745	hypothetical protein	2.105147768	8.01E-11
AUO97_RS18775	hypothetical protein	1.88215239	5.34E-10
AUO97_RS18925	pgaD	1.562592416	3.19E-17
AUO97_RS18930	pgaC	1.664442718	8.45E-07
AUO97_RS18935	pgaB	1.664368743	8.33E-06
AUO97_RS18940	pgaA	1.676022526	9.65E-07
AUO97_RS19055	fis	2.304959845	2.52E-11
AUO97_RS19130	GNAT family N-acetyltransferase	1.554953444	2.85E-13

AUO97_RS19555	hypothetical protein	1.816721201	6.17E-18

Appendix 2. List of downregulated genes in AB189 (ATCC17978:Δ*katG*Δ*katE*) compared to ATCC17978

Locus_tag	Name	Differential Expression Log2 Ratio	Differential Expression p-value
AUO97_RS00005	alpha/beta fold hydrolase	-2.191948987	3.35E-02
AUO97_RS00260	RtcB family protein	-2.01811104	5.51E-01
AUO97_RS00825	TonB-dependent siderophore receptor	-1.529898954	1.41E-02
AUO97_RS01330	hypothetical protein	-1.617769644	2.28E-01
AUO97_RS01455	hypothetical protein	-1.949273143	9.84E-02
AUO97_RS02345	alkaline phosphatase D family protein	-1.545603268	4.27E-01
AUO97_RS03185	RtcB family protein	-1.77702376	5.74E-02
AUO97_RS03410	acyl-CoA dehydrogenase C-terminal domain-containing protein	-1.938353718	4.64E-03
AUO97_RS03560	integrase arm-type DNA-binding domain-containingprotein	-1.552057457	1.15E-02
AUO97_RS03820	YfbU family protein	-1.691831778	1.12E-02
AUO97_RS04195	hypothetical protein	-1.805886844	3.31E-02
AUO97_RS04265	acyl-CoA dehydrogenase family protein	-1.508977162	2.09E-02
AUO97_RS04270	NAD(P)/FAD-dependent oxidoreductase	-1.545392067	7.48E-01
AUO97_RS04560	acyl-CoA dehydrogenase C-terminal domain-containing protein	-2.104373702	4.92E-03
AUO97_RS05105	sel1 repeat family protein	-1.600459356	6.96E-02
AUO97_RS05140	bifunctional SulP family inorganic anion transporter/carbonic anhydrase	-1.542623455	4.12E-01
AUO97_RS05635	putative porin	-1.503425807	6.81E-01
AUO97_RS05675	TMEM165/GDT1 family protein	-1.509667671	9.64E-02
AUO97_RS05750	TonB-dependent siderophore receptor	-1.54412291	6.53E-03

AUO97_RS05805	HPF/RaiA family ribosome-associated protein	-2.586932537	1.69E-04
AUO97_RS06695	amino acid permease	-2.323176464	3.47E-05
AUO97_RS06700	RidA family protein	-1.840636137	1.25E-02
AUO97_RS06705	alr	-1.504854126	6.48E-02
AUO97_RS06800	hypothetical protein	-1.547392022	1.31E-03
AUO97_RS06825	acnD	-1.617472084	1.14E-03
AUO97_RS06830	prpC	-1.660335995	1.06E-03
AUO97_RS07160	alpha/beta hydrolase	-1.667521765	5.33E-03
AUO97_RS07645	hppD	-3.114793551	1.16E-03
AUO97_RS07655	VOC family protein	-3.283606378	3.22E-05
AUO97_RS07660	maiA	-3.967940903	5.47E-07
AUO97_RS07665	fahA	-4.373432247	1.40E-07
AUO97_RS07670	amino acid permease	-2.097915746	1.24E-02
AUO97_RS07825	catalase	-1.662398457	9.82E-02
AUO97_RS07850	alpha/beta fold hydrolase	-1.719214207	1.01E-01
AUO97_RS08110	hypothetical protein	-1.865013684	9.87E-03
AUO97_RS08115	hypothetical protein	-1.761066529	5.79E-02
AUO97_RS08410	hypothetical protein	-1.573132193	2.32E-02
AUO97_RS08745	response regulator transcription factor	-1.549739767	4.37E-01
AUO97_RS08915	htpG	-1.556707821	1.68E-03
AUO97_RS09480	katG	-8.914255336	0
AUO97_RS09875	NADP-dependent glyceraldehyde-3-phosphate dehydrogenase	-1.598866581	9.82E-02
AUO97_RS10295	crotonase/enoyl-CoA hydratase family protein	-1.737945859	1.00E-02

AUO97_RS10320	bifunctional (p)ppGpp synthetase/guanosine-3',5'-bis(diphosphate) 3'-pyrophosphohydrolase	-2.925188629	1.80E-08
AUO97_RS10375	acyl-CoA synthetase	-1.672277635	1.84E-02
AUO97_RS10770	zinc-binding dehydrogenase	-1.793267354	6.07E-02
AUO97_RS11505	pirin family protein	-2.127866175	6.33E-02
AUO97_RS11750	gamma-glutamyltransferase family protein	-2.013880221	3.39E-04
AUO97_RS11940	non-heme iron oxygenase ferredoxin subunit	-2.024337415	1.31E-04
AUO97_RS11945	hypothetical protein	-1.616564921	3.34E-03
AUO97_RS12565	NADPH-dependent 2,4-dienoyl-CoA reductase	-2.170506009	6.53E-04
AUO97_RS12575	hypothetical protein	-1.539130429	2.36E-04
AUO97_RS12620	D-amino acid dehydrogenase	-2.048892587	2.53E-06
AUO97_RS12630	hypothetical protein	-2.016325308	6.12E-05
AUO97_RS12700	nuclear transport factor 2 family protein	-1.971738203	3.99E-04
AUO97_RS12705	gamma-aminobutyraldehyde dehydrogenase	-2.925731145	5.29E-03
AUO97_RS12715	aspartate aminotransferase family protein	-1.622013195	3.76E-01
AUO97_RS13470	LysR family transcriptional regulator	-2.05994643	2.27E-03
AUO97_RS13475	heavy-metal-associated domain-containing protein	-1.720757679	1.03E-02
AUO97_RS13480	copper-translocating P-type ATPase	-1.922925085	5.11E-05
AUO97_RS13535	transposase	-2.237344194	5.23E-04
AUO97_RS14350	indolepyruvate ferredoxin oxidoreductase family protein	-2.054776018	5.18E-05
AUO97_RS14400	DcaP-like protein	-1.539110249	5.65E-09
AUO97_RS14450	katE	-3.800087024	5.72E-06
AUO97_RS15945	siderophore biosynthesis protein	-1.638432214	3.47E-07

AUO97_RS15950	SidA/IucD/PvdA family monooxygenase	-1.772821137	2.07E-03
AUO97_RS17355	NADPH-dependent 2,4-dienoyl-CoA reductase	-1.842871556	8.11E-02
AUO97_RS18405	3-oxoacyl-ACP reductase	-1.587839417	2.71E-01
AUO97_RS18410	acetyl-CoA C-acetyltransferase	-2.026796508	3.71E-03
AUO97_RS18615	iron-containing alcohol dehydrogenase	-2.129985359	1.95E-02
AUO97_RS18630	aldehyde dehydrogenase family protein	-2.128010335	1.90E-02
AUO97_RS19320	hypothetical protein	-1.891262452	2.28E-09

Appendix 3. List of downregulated genes in AB370 (ATCC17978:Δ*katG*::*lacI*^{q}-*katG*) compared to ATCC17978

Locus_tag	Name	Differential Expression Log2 Ratio	Differential Expression p-value
AUO97_RS00405	YfhL family 4Fe-4S dicluster ferredoxin	-1.659427021	2.48E-02
AUO97_RS00825	TonB-dependent siderophore receptor	-2.095591126	1.63E-07
AUO97_RS00830	bauB	-1.676208835	2.73E-09
AUO97_RS00850	basB	-1.747011903	3.16E-07
AUO97_RS01035	ATP-binding protein	-1.859281617	7.63E-04
AUO97_RS01455	hypothetical protein	-1.978602097	1.33E-06
AUO97_RS01700	hypothetical protein	-1.647078514	9.25E-09
AUO97_RS01705	cupin-like domain-containing protein	-1.514026159	1.46E-02
AUO97_RS02420	RidA family protein	-1.511026348	1.27E-03
AUO97_RS02750	porin	-2.340291772	2.00E-03
AUO97_RS02830	fatty acid desaturase family protein	-1.584155263	5.36E-04
AUO97_RS02840	NAD(P)H-dependent oxidoreductase	-1.613360679	2.13E-02
AUO97_RS02845	outer membrane protein transport protein	-2.329113072	1.71E-04
AUO97_RS03050	methyl-accepting chemotaxis protein	-2.081972733	1.26E-03
AUO97_RS03060	response regulator	-1.758642662	3.79E-06
AUO97_RS03065	pilG	-1.944961819	1.09E-02
AUO97_RS03160	mscL	-1.983792062	9.39E-04
AUO97_RS03250	acetyl-CoA C-acetyltransferase	-1.578885849	1.12E-06
AUO97_RS03255	enoyl-CoA hydratase/isomerase family protein	-1.525402225	1.91E-01
AUO97_RS03410	acyl-CoA dehydrogenase C-terminal domain-containing protein	-1.926242656	2.04E-02

AUO97_RS03580	LemA family protein	-2.431842953	2.52E-03
AUO97_RS03615	bestrophin	-1.792504138	1.04E-02
AUO97_RS03670	restriction endonuclease	-1.748031266	9.31E-05
AUO97_RS03775	hypothetical protein	-1.640239848	2.16E-01
AUO97_RS04270	NAD(P)/FAD-dependent oxidoreductase	-2.139240543	3.53E-02
AUO97_RS04545	hemF	-3.312972852	5.03E-04
AUO97_RS04555	hypothetical protein	-1.748138248	5.87E-03
AUO97_RS04560	acyl-CoA dehydrogenase C-terminal domain-containing protein	-2.504162313	2.15E-04
AUO97_RS04605	hypothetical protein	-1.804464848	3.13E-02
AUO97_RS04930	gltB	-1.73377616	1.40E-02
AUO97_RS04955	pilus assembly protein PilP	-1.634054454	2.94E-01
AUO97_RS04970	pilus assembly protein PilM	-1.741637116	3.42E-02
AUO97_RS05025	hypothetical protein	-2.063690084	1.03E-04
AUO97_RS05105	sel1 repeat family protein	-2.299982804	1.06E-03
AUO97_RS05195	DUF805 domain-containing protein	-1.787595878	2.66E-07
AUO97_RS05215	DMT family transporter	-1.523690132	1.21E-08
AUO97_RS05440	hydrolase	-1.512757949	1.64E-02
AUO97_RS05475	AzlC family ABC transporter permease	-1.631784934	1.24E-03
AUO97_RS05665	MBL fold metallo-hydrolase	-1.55930296	2.82E-03
AUO97_RS05805	HPF/RaiA family ribosome-associated protein	-3.51414071	9.93E-01
AUO97_RS06110	hypothetical protein	-1.776292473	9.12E-05
AUO97_RS06415	DUF2846 domain-containing protein	-2.640219807	1.96E-06
AUO97_RS06750	SDR family NAD(P)-dependent oxidoreductase	-2.912203979	4.46E-06

AUO97_RS06820	hypothetical protein	-2.049552357	5.03E-03
AUO97_RS06850	dld	-2.586892848	5.26E-03
AUO97_RS06855	lldD	-2.901003315	4.29E-03
AUO97_RS06860	lldR	-2.663270452	9.50E-03
AUO97_RS06865	lldP	-4.552520102	5.27E-08
AUO97_RS07040	YciK family oxidoreductase	-1.678803757	2.71E-01
AUO97_RS07160	alpha/beta hydrolase	-1.585754523	5.45E-02
AUO97_RS07240	low temperature requirement protein A	-1.766258178	6.01E-03
AUO97_RS07475	ppc	-1.68306313	1.05E-02
AUO97_RS07535	hypothetical protein	-1.90813717	3.88E-01
AUO97_RS07665	fahA	-1.671760541	1.18E-01
AUO97_RS07825	catalase	-1.755560156	6.31E-04
AUO97_RS07850	alpha/beta fold hydrolase	-2.979787435	5.05E-06
AUO97_RS07870	SDR family NAD(P)-dependent oxidoreductase	-1.646388673	6.23E-01
AUO97_RS08530	hypothetical protein	-1.8030865	2.31E-02
AUO97_RS08745	response regulator transcription factor	-1.707915368	2.77E-02
AUO97_RS09145	Na+/H+ antiporter subunit C	-1.799423231	2.13E-02
AUO97_RS09150	monovalent cation/H+ antiporter subunit A	-1.69476729	4.42E-02
AUO97_RS09430	long-chain-acyl-CoA synthetase	-1.513208526	2.57E-02
AUO97_RS09530	hypothetical protein	-2.149121609	1.72E-02
AUO97_RS09560	hypothetical protein	-1.630635538	3.06E-02
AUO97_RS09595	LysE family translocator	-1.652558092	1.25E-02

AUO97_RS09875	NADP-dependent glyceraldehyde-3-phosphate dehydrogenase	-2.569765399	1.59E-03
AUO97_RS10320	bifunctional (p)ppGpp synthetase/guanosine-3',5'-bis(diphosphate) 3'-pyrophosphohydrolase	-2.678858521	1.02E-06
AUO97_RS10325	SDR family oxidoreductase	-1.55317731	4.32E-02
AUO97_RS10590	raiA	-1.89461793	4.33E-03
AUO97_RS10770	zinc-binding dehydrogenase	-1.80018439	2.75E-02
AUO97_RS10835	amidohydrolase	-1.768081904	2.13E-02
AUO97_RS10885	ImmA/IrrE family metallo-endopeptidase	-1.699326137	3.32E-01
AUO97_RS10900	type I secretion C-terminal target domain-containing protein	-3.33212424	4.73E-09
AUO97_RS10945	hypothetical protein	-1.687796304	1.73E-02
AUO97_RS11270	threonylcarbamoyl-AMP synthase	-1.634322689	2.72E-01
AUO97_RS11325	DUF2157 domain-containing protein	-1.75583352	3.66E-02
AUO97_RS11505	pirin family protein	-1.700845699	1.98E-01
AUO97_RS11560	arginyltransferase	-1.97173587	1.65E-02
AUO97_RS11580	rhtC	-1.543517761	3.85E-01
AUO97_RS11750	gamma-glutamyltransferase family protein	-1.828343452	1.35E-02
AUO97_RS12490	hypothetical protein	-1.687438236	5.67E-01
AUO97_RS12565	NADPH-dependent 2,4-dienoyl-CoA reductase	-2.200775368	2.86E-02
AUO97_RS12620	D-amino acid dehydrogenase	-2.003554196	4.25E-01
AUO97_RS12630	hypothetical protein	-1.852019965	6.15E-01
AUO97_RS12865	GMC family oxidoreductase	-1.586719974	3.06E-01
AUO97_RS13390	glutathione S-transferase N-terminal domain-containing protein	-1.706643943	1.72E-02
AUO97_RS13480	copper-translocating P-type ATPase	-1.612379108	3.18E-06

AUO97_RS13825	divalent metal cation transporter	-1.802670455	4.23E-02
AUO97_RS13830	LamB/YcsF family protein	-1.600215728	9.30E-01
AUO97_RS14530	cysteine ABC transporter substrate-binding protein	-1.662914907	3.02E-01
AUO97_RS14965	glutathione S-transferase	-1.502758528	2.02E-01
AUO97_RS17350	nuclear transport factor 2 family protein	-1.504504159	8.81E-01
AUO97_RS17355	NADPH-dependent 2,4-dienoyl-CoA reductase	-2.119499544	4.21E-02
AUO97_RS17465	cytochrome ubiquinol oxidase subunit I	-2.579319548	1.59E-05
AUO97_RS17470	cydB	-3.25992461	8.62E-01
AUO97_RS17475	cydX	-3.416047269	4.07E-01
AUO97_RS17480	cyd operon YbgE family protein	-3.394066257	2.37E-01
AUO97_RS17515	hypothetical protein	-1.508667541	6.97E-01
AUO97_RS18410	acetyl-CoA C-acetyltransferase	-1.634555629	9.55E-02
AUO97_RS19320	hypothetical protein	-1.956789351	3.90E-01
AUO97_RS19665	hypothetical protein	-1.651733398	8.48E-01

Appendix 4. List of upregulated genes in AB370 (ATCC17978:Δ*katG*::*lacI*^{q}-*katG*) compared to ATCC17978

Locus_tag	Name	Differential Expression Log2 Ratio	Differential Expression p-value
AUO97_RS00030	NirD/YgiW/YdeI family stress tolerance protein	3.284309256	1.87E-06
AUO97_RS00040	class I SAM-dependent methyltransferase	1.865817396	5.75E-02
AUO97_RS00045	PIG-L family deacetylase	2.273038905	8.41E-03
AUO97_RS00050	hypothetical protein	1.94191019	1.58E-02
AUO97_RS00055	DUF2171 domain-containing protein	8.133402527	0
AUO97_RS00065	CoA-acylating methylmalonate-semialdehyde dehydrogenase	2.0540957	2.99E-03
AUO97_RS00070	aspartate aminotransferase family protein	2.249228789	1.46E-04
AUO97_RS00160	CvpA family protein	1.598628436	1.46E-02
AUO97_RS00720	Smr/MutS family protein	1.714821782	1.97E-02
AUO97_RS01060	hypothetical protein	1.990651798	2.61E-02
AUO97_RS01130	amino acid permease	4.434091763	1.59E-01
AUO97_RS01135	alpha-keto acid decarboxylase family protein	6.330844157	1.31E-02
AUO97_RS01145	aldehyde dehydrogenase family protein	4.303374922	1.44E-07
AUO97_RS01410	uvrB	1.575022805	2.78E-01
AUO97_RS01425	hypothetical protein	1.888631069	2.43E-02
AUO97_RS01430	Pyridoxal phosphate-dependent aminotransferase	1.694337843	6.26E-02
AUO97_RS01605	hypothetical protein	1.579576964	3.22E-02
AUO97_RS02235	ttcA	1.706970248	1.65E-02
AUO97_RS02330	folD	1.766475002	1.68E-02
AUO97_RS02520	sdhD	1.920700646	2.86E-02

AUO97_RS02525	sdhC	1.991194509	1.50E-02
AUO97_RS02850	thrH	2.638011687	1.34E-06
AUO97_RS03030	icidin A/B family lipoprotein	1.757613378	3.01E-02
AUO97_RS03300	peroxiredoxin	2.087884733	1.02E-02
AUO97_RS04780	hemerythrin domain-containing protein	2.006950154	6.67E-02
AUO97_RS05275	hypothetical protein	1.73925133	5.65E-02
AUO97_RS05455	gabT	1.811362079	4.85E-01
AUO97_RS06670	AMP-binding protein	2.744491884	2.05E-03
AUO97_RS06675	mmsB	3.125894217	2.88E-04
AUO97_RS06680	CoA-acylating methylmalonate-semialdehyde dehydrogenase	2.938932156	2.55E-05
AUO97_RS07170	hypothetical protein	2.644864899	5.05E-03
AUO97_RS07185	grpE	1.669719381	1.42E-02
AUO97_RS07220	purE	1.598322313	3.43E-02
AUO97_RS07470	pyrimidine permease	1.795147472	3.62E-02
AUO97_RS07500	dnaJ	1.769342434	1.39E-01
AUO97_RS07580	DUF1328 domain-containing protein	2.795946144	1.43E-04
AUO97_RS08110	hypothetical protein	1.769263116	1.10E-02
AUO97_RS08115	hypothetical protein	1.7217727	1.57E-03
AUO97_RS08120	hypothetical protein	1.803127941	1.28E-03
AUO97_RS08125	DotG/IcmE/VirB10 family protein	2.137289468	5.32E-04
AUO97_RS08130	hypothetical protein	2.302587992	3.12E-03
AUO97_RS08135	DotI/IcmL/TraM family protein	1.888163498	2.23E-01
AUO97_RS08175	DotD/TraH family lipoprotein	1.997727178	1.34E-02

AUO97_RS08180	type IV secretory system conjugative DNA transfer family protein	1.737127015	2.42E-02
AUO97_RS08335	hypothetical protein	1.561469393	8.09E-02
AUO97_RS08340	hypothetical protein	1.521637468	1.70E-02
AUO97_RS08345	hypothetical protein	1.518281967	3.87E-02
AUO97_RS08910	DUF1311 domain-containing protein	1.559241304	4.38E-01
AUO97_RS08945	serine hydrolase family protein	1.790149136	2.04E-01
AUO97_RS08980	peptidoglycan hydrolase	1.522641318	4.20E-09
AUO97_RS09255	Hsp33 family molecular chaperone HslO	1.798632729	6.26E-02
AUO97_RS09540	infA	1.645060185	5.20E-07
AUO97_RS09700	MotA/TolQ/ExbB proton channel family protein	1.527827179	2.74E-03
AUO97_RS09810	TonB-dependent siderophore receptor	1.810278401	6.81E-09
AUO97_RS09840	fumarate hydratase	1.575501496	5.38E-07
AUO97_RS09920	ndk	1.840557314	7.42E-06
AUO97_RS10405	nreB	1.500314982	4.41E-02
AUO97_RS10915	hypothetical protein	2.116579943	4.50E-04
AUO97_RS11085	LysE family translocator	1.652804625	4.02E-02
AUO97_RS11220	trehalose-6-phosphate synthase	2.988393893	3.26E-06
AUO97_RS11225	otsB	2.261614771	1.94E-02
AUO97_RS11335	aspartate 1-decarboxylase	1.830655371	3.29E-02
AUO97_RS11350	ribose-phosphate pyrophosphokinase	1.628375514	3.24E-01
AUO97_RS11880	hypothetical protein	3.283955525	6.52E-04
AUO97_RS11895	YaeQ family protein	1.579598627	3.69E-01

AUO97_RS11900	FKBP-type peptidyl-prolyl cis-trans isomerase	1.897167362	2.29E-03
AUO97_RS12135	carbonic anhydrase	1.661885197	1.54E-02
AUO97_RS12955	hypothetical protein	2.108302528	7.80E-03
AUO97_RS13355	aspartate carbamoyltransferase catalytic subunit	1.840447601	3.14E-03
AUO97_RS13450	1,6-dihydroxycyclohexa-2,4-diene-1-carboxylate dehydrogenase	1.681230592	5.08E-02
AUO97_RS13455	ring-hydroxylating dioxygenase ferredoxin reductase family protein	2.420221536	9.21E-04
AUO97_RS13460	benB	2.684248434	1.04E-04
AUO97_RS13465	benA	2.187038625	1.18E-03
AUO97_RS13495	four-helix bundle copper-binding protein	3.938379459	1.44E-06
AUO97_RS13500	hypothetical protein	2.657520107	1.15E-05
AUO97_RS13515	hypothetical protein	1.987105591	3.17E-06
AUO97_RS13585	hypothetical protein	2.922348325	9.68E-06
AUO97_RS13590	hypothetical protein	3.742244429	1.46E-08
AUO97_RS13595	minor capsid protein	3.166840477	2.05E-07
AUO97_RS13600	MFS transporter	1.722341291	1.26E-09
AUO97_RS13620	DUF4142 domain-containing protein	3.22324786	1.16E-06
AUO97_RS13625	hypothetical protein	2.244367584	7.43E-08
AUO97_RS13790	hypothetical protein	2.668548861	5.06E-02
AUO97_RS13880	glutathione-dependent formaldehyde dehydrogenase	4.618156059	4.95E-06
AUO97_RS13955	SUMF1/EgtB/PvdO family nonheme iron enzyme	1.618750848	1.66E-03
AUO97_RS14080	epoxyqueuosine reductase QueH	2.145871646	2.62E-07
AUO97_RS14165	paaZ	3.840436214	5.22E-04

AUO97_RS14170	paaA	3.562088239	3.33E-01
AUO97_RS14175	paaB	3.810724482	3.10E-07
AUO97_RS14180	paaC	4.807704447	7.11E-09
AUO97_RS14185	paaJ	4.825971771	3.96E-07
AUO97_RS14190	paaK	4.646068097	1.80E-07
AUO97_RS14195	enoyl-CoA hydratase/isomerase family protein	5.037076488	2.74E-06
AUO97_RS14200	2-(1,2-epoxy-1,2-dihydrophenyl)acetyl-CoA isomerase	5.097920454	1.43E-05
AUO97_RS14205	3-hydroxyacyl-CoA dehydrogenase	5.453393036	3.24E-01
AUO97_RS14210	pcaF	4.699888235	4.85E-01
AUO97_RS14215	paaF	3.912948033	2.00E-08
AUO97_RS14220	paaX	2.394871342	1.41E-04
AUO97_RS14225	carbonic anhydrase	2.655328384	9.59E-06
AUO97_RS14230	PaaI family thioesterase	2.081269712	2.89E-01
AUO97_RS14420	hypothetical protein	5.563827236	7.77E-08
AUO97_RS14425	hypothetical protein	4.559148993	4.85E-05
AUO97_RS14430	hypothetical protein	6.952689508	0
AUO97_RS14435	hypothetical protein	8.823193776	0
AUO97_RS14440	CinA family protein	2.783699592	2.93E-03
AUO97_RS14445	iron-containing redox enzyme family protein	4.035503167	5.75E-08
AUO97_RS14450	katE	4.335475258	9.24E-04
AUO97_RS14455	glucose 1-dehydrogenase	6.701388742	1.28E-05
AUO97_RS14460	hypothetical protein	3.295597137	8.67E-03

AUO97_RS14465	stress-induced protein	6.809897776	0
AUO97_RS14845	dicarboxylate/amino acid:cation symporter	2.864979384	3.79E-02
AUO97_RS15045	hypothetical protein	3.031027689	1.56E-06
AUO97_RS15050	EamA family transporter	4.780592836	1.01E-01
AUO97_RS15180	hypothetical protein	2.885535976	3.86E-06
AUO97_RS15275	phosphoglycerate kinase	1.844674509	3.09E-02
AUO97_RS15410	SRPBCC family protein	1.714246064	1.30E-02
AUO97_RS15435	pyrF	1.828485343	6.86E-03
AUO97_RS15555	hypothetical protein	1.51569725	3.37E-01
AUO97_RS15565	hypothetical protein	1.831171944	5.13E-03
AUO97_RS15570	hypothetical protein	4.291025175	2.88E-09
AUO97_RS15575	hypothetical protein	3.668288031	7.60E-07
AUO97_RS15580	hypothetical protein	3.437862808	5.22E-03
AUO97_RS15585	hypothetical protein	3.13705029	1.54E-03
AUO97_RS15590	hypothetical protein	3.348089258	6.39E-04
AUO97_RS15595	HNH endonuclease	3.322835027	1.31E-04
AUO97_RS15600	terminase small subunit	2.349323899	6.93E-03
AUO97_RS15605	hypothetical protein	2.250220118	2.97E-01
AUO97_RS15610	terminase large subunit	2.566587093	3.11E-02
AUO97_RS15615	phage portal protein	2.591326802	3.69E-04
AUO97_RS15620	HK97 family phage prohead protease	3.553768736	2.30E-07
AUO97_RS15625	phage major capsid protein	4.057994943	9.39E-01
AUO97_RS15630	phage head-tail connector protein	3.402083887	4.05E-04

AUO97_RS15635	phage head closure protein	3.727346558	2.05E-05
AUO97_RS15640	HK97 gp10 family phage protein	3.392596021	5.82E-04
AUO97_RS15645	DUF3168 domain-containing protein	3.627548417	1.04E-07
AUO97_RS15650	hypothetical protein	3.274878577	7.78E-07
AUO97_RS15655	hypothetical protein	3.649798086	1.31E-08
AUO97_RS15670	hypothetical protein	1.573321446	2.27E-02
AUO97_RS15680	hypothetical protein	1.535359941	6.15E-01
AUO97_RS15690	hypothetical protein	1.653404343	3.57E-02
AUO97_RS15695	hypothetical protein	2.441666262	8.77E-05
AUO97_RS15700	hypothetical protein	2.080452712	4.56E-03
AUO97_RS15705	hypothetical protein	2.60081844	1.38E-02
AUO97_RS15710	glycoside hydrolase family protein	2.796608953	4.07E-05
AUO97_RS15715	hypothetical protein	2.715709999	1.01E-04
AUO97_RS15810	rpsT	2.140290568	2.07E-03
AUO97_RS15935	hypothetical protein	2.302267388	1.27E-03
AUO97_RS16050	sulfite exporter TauE/SafE family protein	1.876519116	2.33E-02
AUO97_RS16105	DUF2797 domain-containing protein	1.787016773	4.03E-02
AUO97_RS16130	YARHG domain-containing protein	1.806371365	2.08E-03
AUO97_RS16140	hypothetical protein	1.519147394	1.72E-01
AUO97_RS16170	hypothetical protein	2.474562117	2.53E-04
AUO97_RS16255	thiamine pyrophosphate-dependent dehydrogenase E1 component subunit alpha	5.019139056	1.33E-03
AUO97_RS16260	alpha-ketoacid dehydrogenase subunit beta	5.108227565	3.25E-02

AUO97_RS16265	2-oxo acid dehydrogenase subunit E2	4.989374962	1.49E-02
AUO97_RS16270	lpdA	4.299511093	1.06E-01
AUO97_RS16275	acetoin reductase	2.342165955	2.29E-03
AUO97_RS16415	thiolase family protein	1.826990528	2.34E-01
AUO97_RS16470	3-hydroxybutyrate dehydrogenase	1.732365908	8.15E-01
AUO97_RS16595	PAAR domain-containing protein	1.809624941	7.03E-03
AUO97_RS16990	type 1 glutamine amidotransferase domain-containing protein	1.604752876	2.64E-01
AUO97_RS17065	muconate cycloisomerase	4.032473673	1.42E-09
AUO97_RS17070	catC	4.102886293	1.74E-08
AUO97_RS17075	catA	3.72952163	4.26E-07
AUO97_RS17080	3-oxoacid CoA-transferase subunit A	3.327065277	1.07E-08
AUO97_RS17085	CoA transferase subunit B	3.291620747	2.93E-06
AUO97_RS17090	pcaF	2.180469562	2.11E-03
AUO97_RS17095	pcaD	2.531072894	1.93E-04
AUO97_RS17100	penicillin acylase family protein	2.413066805	5.04E-03
AUO97_RS17125	flavin reductase family protein	4.294434477	1.22E-03
AUO97_RS17130	oxidoreductase	4.934862171	8.36E-05
AUO97_RS17135	SDR family oxidoreductase	5.175246059	2.57E-06
AUO97_RS17140	aromatic-ring-hydroxylating dioxygenase subunit beta	5.07685043	6.08E-01
AUO97_RS17145	aromatic ring-hydroxylating dioxygenase subunit alpha CDS	5.062121891	2.69E-01
AUO97_RS17150	nuclear transport factor 2 family protein	5.140566827	9.21E-01
AUO97_RS17155	hypothetical protein	4.997938865	5.79E-01
AUO97_RS17160	acyl-CoA dehydrogenase	4.625728912	1.69E-05

AUO97_RS17165	amidase	4.746782368	6.20E-10
AUO97_RS17170	MarR family transcriptional regulator	1.612074613	7.85E-02
AUO97_RS17175	MFS transporter	2.915955597	4.00E-02
AUO97_RS17180	OprD family outer membrane porin	2.451048017	8.83E-02
AUO97_RS17315	eno	1.683394879	3.44E-02
AUO97_RS17330	hypothetical protein	1.669794526	7.46E-02
AUO97_RS17440	TonB-dependent siderophore receptor	2.623861735	3.64E-04
AUO97_RS17445	adenosine kinase	1.529278183	1.18E-01
AUO97_RS17450	Rieske (2Fe-2S) protein	1.530783377	4.87E-02
AUO97_RS17525	DUF2750 domain-containing protein	2.291595753	1.04E-03
AUO97_RS17540	grxD	1.845933587	1.63E-02
AUO97_RS17545	hypothetical protein	1.792936064	1.06E-02
AUO97_RS17625	SOS response-associated peptidase family protein	3.482270664	2.63E-07
AUO97_RS17635	S8 family peptidase	1.718071131	1.09E-02
AUO97_RS17665	hypothetical protein	2.621691875	2.75E-04
AUO97_RS17750	uppS	1.710349258	2.56E-02
AUO97_RS17755	frr	1.700988701	1.13E-02
AUO97_RS17760	pyrH	2.318971342	8.84E-04
AUO97_RS17765	rimO	1.827173944	8.17E-02
AUO97_RS17825	hypothetical protein	1.79169501	2.37E-02
AUO97_RS17835	galE	1.565557844	1.86E-02
AUO97_RS18230	DNA cytosine methyltransferase	1.7665551	1.13E-02
AUO97_RS18235	hypothetical protein	1.96977619	1.19E-02

AUO97_RS18240	hypothetical protein	1.719538272	3.19E-01
AUO97_RS18245	hypothetical protein	1.683513824	3.34E-01
AUO97_RS18250	hypothetical protein	1.734089386	1.50E-01
AUO97_RS18270	hypothetical protein	1.737385203	7.95E-02
AUO97_RS18275	hypothetical protein	1.507734567	1.28E-01
AUO97_RS18325	TetR/AcrR family transcriptional regulator	1.601008471	1.30E-01
AUO97_RS18450	mgtA	2.379769953	4.70E-03
AUO97_RS18475	hypothetical protein	3.986045189	3.62E-06
AUO97_RS18505	hypothetical protein	5.44381765	5.03E-02
AUO97_RS18520	TonB-dependent receptor	2.508722735	4.68E-03
AUO97_RS18570	fimbrial biogenesis outer membrane usher protein	1.578012645	2.26E-02
AUO97_RS18575	molecular chaperone	2.660571637	1.32E-04
AUO97_RS18580	spore coat protein U domain-containing protein	3.678488616	5.31E-08
AUO97_RS18865	acyl-CoA dehydrogenase family protein	1.848924763	1.79E-01
AUO97_RS19040	hypothetical protein	3.144352795	8.27E-05
AUO97_RS19055	fis	1.88762691	7.29E-03
AUO97_RS19460	hypothetical protein	1.593234521	3.62E-02
AUO97_RS19530	hypothetical protein	2.906810477	6.59E-04
AUO97_RS19580	hypothetical protein	4.801775478	2.75E-04
AUO97_RS19595	hypothetical protein	1.773809979	8.18E-09
AUO97_RS19600	hypothetical protein	3.665191479	1.04E-06

Appendix 5. List of downregulated genes in AB376+IPTG (ATCC17978:Δ*katE*::*lacI*^{q}-*katE*) compared to ATCC17978

locus_tag	Name	Differential Expression Log2 Ratio	Differential Expression p-value
AUO97_RS00005	alpha/beta fold hydrolase	-1.6	6.00E-22
AUO97_RS00260	RtcB family protein	-1.95	0
AUO97_RS00400	tRNA 5-hydroxyuridine modification protein YegQ	-2.53	0
AUO97_RS00405	YfhL family 4Fe-4S dicluster ferredoxin	-3.09	0
AUO97_RS00680	glnA	-1.57	0
AUO97_RS00690	aminopeptidase P family protein	-1.58	0
AUO97_RS00825	TonB-dependent siderophore receptor	-1.52	0
AUO97_RS00830	bauB	-1.53	1.90E-24
AUO97_RS00985	YbdD/YjiX family protein	-3.47	0
AUO97_RS00990	carbon starvation protein A	-3.21	0
AUO97_RS01035	ATP-binding protein	-1.83	0
AUO97_RS01275	icd	-1.71	0
AUO97_RS01355	nitronate monooxygenase	-1.59	0
AUO97_RS01455	hypothetical protein	-1.64	0
AUO97_RS01525	Do family serine endopeptidase	-1.51	0
AUO97_RS01630	enoyl-CoA hydratase/isomerase family protein	-1.98	0
AUO97_RS01650	DDE-type integrase/transposase/recombinase	-1.54	0
AUO97_RS01655	AAA family ATPase	-1.84	0
AUO97_RS01660	TniQ family protein	-1.75	0
AUO97_RS01700	hypothetical protein	-1.98	0

AUO97_RS02045	FAD-binding protein	-2.16	0
AUO97_RS02050	electron transfer flavoprotein subunit beta/FixAfamily protein	-2.1	0
AUO97_RS02080	amino acid permease	-2.11	0
AUO97_RS02135	nitroreductase family protein	-1.65	0
AUO97_RS02280	groL	-2.72	0
AUO97_RS02285	co-chaperone GroES	-2.42	0
AUO97_RS02315	MFS transporter	-1.91	0
AUO97_RS02355	hypothetical protein	-1.59	0
AUO97_RS02480	sucD	-1.8	0
AUO97_RS02485	sucC	-1.81	0
AUO97_RS02490	lpdA	-1.85	0
AUO97_RS02750	porin	-3.35	0
AUO97_RS02790	prpF	-2.03	0
AUO97_RS02830	fatty acid desaturase family protein	-1.57	0
AUO97_RS02845	outer membrane protein transport protein	-2.23	0
AUO97_RS02905	DJ-1/PfpI family protein	-2.42	0
AUO97_RS02935	threonine ammonia-lyase	-1.67	0
AUO97_RS03050	methyl-accepting chemotaxis protein	-1.74	0
AUO97_RS03060	response regulator	-1.67	0
AUO97_RS03065	pilG	-1.78	0
AUO97_RS03160	mscL	-1.64	0
AUO97_RS03250	acetyl-CoA C-acetyltransferase	-2.25	0
AUO97_RS03255	enoyl-CoA hydratase/isomerase family protein	-2.42	0

AUO97_RS03410	acyl-CoA dehydrogenase C-terminal domain-containing protein	-1.86	0
AUO97_RS03415	acyl-CoA dehydrogenase C-terminal domain-containing protein	-1.93	0
AUO97_RS03420	phosphate-starvation-inducible PsiE family protein	-1.64	0
AUO97_RS03450	aspS	-1.59	0
AUO97_RS03505	branched-chain amino acid transaminase	-1.73	0
AUO97_RS03580	LemA family protein	-2.36	0
AUO97_RS03615	bestrophin	-1.87	0
AUO97_RS03700	copper-binding protein	-2.7	0
AUO97_RS03725	copper resistance protein B	-1.86	0
AUO97_RS03730	multicopper oxidase domain-containing protein	-1.66	0
AUO97_RS03750	heavy metal translocating P-type ATPase	-1.55	0
AUO97_RS03775	hypothetical protein	-2.17	0
AUO97_RS03780	hypothetical protein	-2.03	0
AUO97_RS03820	YfbU family protein	-1.95	0
AUO97_RS03860	trxC	-1.57	0
AUO97_RS04160	YihY family inner membrane protein	-1.78	0
AUO97_RS04225	M3 family metallopeptidase	-1.61	0
AUO97_RS04265	acyl-CoA dehydrogenase family protein	-1.72	0
AUO97_RS04545	hemF	-2.92	0
AUO97_RS04555	hypothetical protein	-1.6	0
AUO97_RS04560	acyl-CoA dehydrogenase C-terminal domain-containing protein	-2	0
AUO97_RS04605	hypothetical protein	-1.8	0
AUO97_RS04725	superoxide dismutase family protein	-1.63	0

AUO97_RS04890	bfr	-1.59	0
AUO97_RS05020	sulfate ABC transporter substrate-binding protein	-1.6	0
AUO97_RS05025	hypothetical protein	-1.54	0
AUO97_RS05075	cation transporter	-1.78	0
AUO97_RS05105	sel1 repeat family protein	-2.44	0
AUO97_RS05160	acetyl-CoA hydrolase/transferase family protein	-1.95	0
AUO97_RS05270	DNA/RNA non-specific endonuclease	-1.66	0
AUO97_RS05595	acs	-1.67	0
AUO97_RS05770	arsenate reductase	-1.86	0
AUO97_RS05805	HPF/RaiA family ribosome-associated protein	-3.57	0
AUO97_RS06405	glutathione peroxidase	-2.16	0
AUO97_RS06415	DUF2846 domain-containing protein	-2.48	0
AUO97_RS06695	amino acid permease	-2.02	0
AUO97_RS06700	RidA family protein	-2.27	0
AUO97_RS06705	alr	-2.47	0
AUO97_RS06710	D-amino acid dehydrogenase	-2.42	0
AUO97_RS06850	dld	-3.24	0
AUO97_RS06855	lldD	-3.75	0
AUO97_RS06860	lldR	-3.27	0
AUO97_RS06865	lldP	-4.54	0
AUO97_RS07190	dnaK	-1.52	0
AUO97_RS07420	glutathione S-transferase family protein	-1.57	0
AUO97_RS07475	ppc	-4	0

AUO97_RS07570	HIT family protein	-1.53	0
AUO97_RS07700	hutU	-1.69	0
AUO97_RS07715	imidazolonepropionase	-1.69	0
AUO97_RS07830	ankyrin repeat domain-containing protein	-1.64	0
AUO97_RS07850	alpha/beta fold hydrolase	-1.77	0
AUO97_RS08425	hypothetical protein	-1.82	0
AUO97_RS08625	response regulator	-1.85	0
AUO97_RS08690	cpdA	-1.78	0
AUO97_RS08915	htpG	-2.91	0
AUO97_RS08925	hypothetical protein	-1.76	0
AUO97_RS09430	long-chain-acyl-CoA synthetase	-1.87	0
AUO97_RS09875	NADP-dependent glyceraldehyde-3-phosphate dehydrogenase	-1.73	0
AUO97_RS10055	hypothetical protein	-2.14	0
AUO97_RS10140	acetolactate synthase 3 large subunit	-1.58	0
AUO97_RS10145	ilvN	-2.24	0
AUO97_RS10150	ilvC	-1.99	0
AUO97_RS10250	RidA family protein	-1.64	0
AUO97_RS10510	mechanosensitive ion channel family protein	-1.52	0
AUO97_RS10650	hypothetical protein	-1.58	0
AUO97_RS10835	amidohydrolase	-1.92	0
AUO97_RS11070	HlyD family secretion protein	-1.69	0
AUO97_RS11210	bfr	-1.61	0
AUO97_RS11270	threonylcarbamoyl-AMP synthase	-1.67	0

AUO97_RS11470	Rieske 2Fe-2S domain-containing protein	-1.97	0
AUO97_RS11510	hemJ	-1.55	0
AUO97_RS11560	arginyltransferase	-1.79	0
AUO97_RS11580	rhtC	-1.95	0
AUO97_RS11650	bacteriohemerythrin	-1.92	0
AUO97_RS11750	gamma-glutamyltransferase family protein	-1.84	0
AUO97_RS12235	CitMHS family transporter	-2.16	0
AUO97_RS12295	ureE	-1.87	0
AUO97_RS12300	urease accessory protein	-1.61	0
AUO97_RS12305	ureG	-1.87	0
AUO97_RS12310	HupE/UreJ family protein	-1.75	0
AUO97_RS12350	gdhA	-1.65	0
AUO97_RS12435	hypothetical protein	-2.2	0
AUO97_RS12565	NADPH-dependent 2,4-dienoyl-CoA reductase	-2.12	0
AUO97_RS12680	FAD-binding oxidoreductase	-2.2	0
AUO97_RS12700	nuclear transport factor 2 family protein	-2.12	0
AUO97_RS12705	gamma-aminobutyraldehyde dehydrogenase	-2.76	0
AUO97_RS12715	aspartate aminotransferase family protein	-1.54	0
AUO97_RS12990	hypothetical protein	-3.3	6.20E-12
AUO97_RS13045	YdaU family protein	-3.62	4.10E-16
AUO97_RS13090	hypothetical protein	-2	0.0015
AUO97_RS13305	NADP(H)-dependent aldo-keto reductase	-2.02	0
AUO97_RS13390	glutathione S-transferase N-terminal domain-containing protein	-3.1	0

AUO97_RS13400	ahpF	-2.6	0
AUO97_RS13470	LysR family transcriptional regulator	-1.86	0
AUO97_RS13475	heavy-metal-associated domain-containing protein	-1.79	0
AUO97_RS13480	copper-translocating P-type ATPase	-1.85	0
AUO97_RS13790	hypothetical protein	-1.68	0
AUO97_RS14095	DUF333 domain-containing protein	-1.61	0
AUO97_RS14360	hydroxymethylglutaryl-CoA lyase	-1.84	0
AUO97_RS14365	acetyl/propionyl/methylcrotonyl-CoA carboxylase subunit alpha	-2.07	0
AUO97_RS14370	enoyl-CoA hydratase/isomerase family protein	-1.85	0
AUO97_RS14375	methylcrotonoyl-CoA carboxylase subunit beta	-1.69	0
AUO97_RS14480	LysE family translocator	-2.09	0
AUO97_RS14530	cysteine ABC transporter substrate-binding protein	-1.69	0
AUO97_RS14810	ahpF	-2.23	0
AUO97_RS14815	alpha/beta fold hydrolase	-1.66	0
AUO97_RS14855	msrB	-1.52	0
AUO97_RS14980	amino acid ABC transporter permease	-1.54	0
AUO97_RS14985	amino acid ABC transporter ATP-protein	-1.92	0
AUO97_RS15195	putA	-1.73	0
AUO97_RS15725	synthase G	-1.79	0
AUO97_RS15980	TonB-dependent receptor	-2.22	0
AUO97_RS16330	NAD(P)H-dependent oxidoreductase	-2.31	0
AUO97_RS17230	hypothetical protein	-1.68	0
AUO97_RS17355	NADPH-dependent 2,4-dienoyl-CoA reductase	-2.43	0

AUO97_RS17465	cytochrome ubiquinol oxidase subunit I	-1.75	0
AUO97_RS17470	cydB	-1.8	0
AUO97_RS17475	cydX	-1.87	0
AUO97_RS17480	cyd operon YbgE family protein	-1.6	0
AUO97_RS17530	CBS domain-containing protein	-1.6	0
AUO97_RS17950	accB	-1.6	0
AUO97_RS17955	accC	-1.66	0
AUO97_RS18360	lactonase family protein	-1.66	0
AUO97_RS18585	pepN	-1.72	0
AUO97_RS18765	bifunctional aconitate hydratase 2/2-methylisocitrate dehydratase	-1.64	0
AUO97_RS18945	kinase/pyrophosphorylase	-1.56	0
AUO97_RS18960	cyoA	-1.69	0
AUO97_RS18965	cyoB	-1.76	0
AUO97_RS18970	cyoC	-1.63	0
AUO97_RS19240	gltS	-2.78	0

Appendix 6. List of upregulated genes in AB376+IPTG (ATCC17978:Δ*katE*::*lacI*^{q}-*katE*) compared to ATCC17978

locus_tag	Name	Differential Expression Log2 Ratio	Differential Expression p-value
AUO97_RS00015	LysE family translocator	2.14	6.10E-17
AUO97_RS00020	hypothetical protein	4.45	0
AUO97_RS00025	BLUF domain-containing protein	2.8	0
AUO97_RS00045	PIG-L family deacetylase	1.91	9.60E-17
AUO97_RS00050	hypothetical protein	1.82	3.30E-16
AUO97_RS00055	DUF2171 domain-containing protein	4.23	0
AUO97_RS00060	amino acid permease	1.59	7.70E-15
AUO97_RS00065	CoA-acylating methylmalonate-semialdehyde dehydrogenase	1.87	1.50E-73
AUO97_RS00070	aspartate aminotransferase family protein	2.19	2.90E-48
AUO97_RS00205	cold-shock protein	1.83	0
AUO97_RS00365	NirD/YgiW/YdeI family stress tolerance protein	1.59	0
AUO97_RS01115	pstA	1.83	3.30E-52
AUO97_RS01120	pstC	1.89	2.00E-36
AUO97_RS01125	substrate-binding domain-containing protein	2.27	0
AUO97_RS01130	amino acid permease	2.93	0
AUO97_RS01135	alpha-keto acid decarboxylase family protein	4.29	0
AUO97_RS01145	aldehyde dehydrogenase family protein CDS	4.05	0
AUO97_RS01385	hypothetical protein	1.68	4.40E-29
AUO97_RS01390	hypothetical protein	1.61	2.70E-37
AUO97_RS01435	hypothetical protein	1.95	0

AUO97_RS02295	NAD(+)/NADH kinase	1.53	2.10E-47
AUO97_RS02655	adeI	2.28	0
AUO97_RS02660	adeJ	1.97	0
AUO97_RS02665	adeK	1.64	0
AUO97_RS03090	YegP family protein	1.69	0
AUO97_RS03105	SRPBCC family protein	2.89	0
AUO97_RS04195	hypothetical protein	2.28	0
AUO97_RS04525	DEAD/DEAH box helicase	2.74	0
AUO97_RS04810	trmD	1.64	0
AUO97_RS04885	(2Fe-2S)-binding protein	2.89	0
AUO97_RS05870	haloacid dehalogenase-like hydrolase	1.89	4.00E-31
AUO97_RS05880	SH3 domain-containing protein	1.59	4.10E-11
AUO97_RS06595	4'-phosphopantetheinyl transferase superfamily protein	2.06	9.40E-62
AUO97_RS06600	alpha/beta fold hydrolase	3.35	0
AUO97_RS06605	hypothetical protein	3.94	0
AUO97_RS06610	outer membrane lipoprotein-sorting protein	6.03	0
AUO97_RS06615	non-ribosomal peptide synthetase	6.61	0
AUO97_RS06620	acyl carrier protein	6.37	0
AUO97_RS06625	acyl-CoA dehydrogenase	7.48	0
AUO97_RS06630	fatty acyl-AMP ligase	7.16	0
AUO97_RS06645	abaI	3.27	0
AUO97_RS06670	AMP-binding protein	3.12	0
AUO97_RS06675	mmsB	3.62	0

AUO97_RS06680	CoA-acylating methylmalonate-semialdehyde dehydrogenase	3.75	0
AUO97_RS06780	type VI secretion system tip protein VgrG	2.81	0
AUO97_RS06800	hypothetical protein	2.56	1.20E-72
AUO97_RS07170	hypothetical protein	2.78	0
AUO97_RS07580	DUF1328 domain-containing protein	1.94	0
AUO97_RS07745	hypothetical protein	1.91	0
AUO97_RS07750	hypothetical protein	1.56	9.80E-30
AUO97_RS08005	hypothetical protein	1.61	3.80E-23
AUO97_RS08110	hypothetical protein	1.59	0
AUO97_RS08125	DotG/IcmE/VirB10 family protein	2.28	4.20E-60
AUO97_RS08130	hypothetical protein	2.48	2.20E-72
AUO97_RS08135	DotI/IcmL/TraM family protein	2.84	2.50E-65
AUO97_RS08140	hypothetical protein	2.35	3.00E-42
AUO97_RS08155	hypothetical protein	1.64	0
AUO97_RS08165	hypothetical protein	1.83	0
AUO97_RS08170	hypothetical protein	2.04	0
AUO97_RS08175	DotD/TraH family lipoprotein	3.17	0
AUO97_RS08180	type IV secretory system conjugative DNA transfer family protein	2.46	0
AUO97_RS08185	tadA	1.74	5.40E-38
AUO97_RS08190	hypothetical protein	1.68	4.50E-39
AUO97_RS08335	hypothetical protein	2.01	4.30E-65
AUO97_RS08340	hypothetical protein	1.79	0
AUO97_RS08345	hypothetical protein	1.7	6.30E-73

AUO97_RS08355	hypothetical protein	1.67	8.70E-50
AUO97_RS09460	glutathione S-transferase family protein	2.16	0
AUO97_RS09760	tatC	1.85	3.20E-15
AUO97_RS09765	tatB	1.58	3.10E-18
AUO97_RS09770	Sec-independent protein translocase subunit TatA	1.62	3.30E-23
AUO97_RS10170	TetR/AcrR family transcriptional regulator	2.83	0
AUO97_RS10175	hypothetical protein	3.93	0
AUO97_RS10260	Re/Si-specific NAD(P)(+) transhydrogenase subunit alpha	1.62	0
AUO97_RS10265	NAD(P) transhydrogenase subunit alpha	1.5	0
AUO97_RS10780	acyl-CoA dehydrogenase	1.66	0
AUO97_RS10785	MFS transporter	1.77	3.10E-16
AUO97_RS10895	hypothetical protein	2.1	2.30E-21
AUO97_RS10915	hypothetical protein	5.24	0
AUO97_RS11100	hypothetical protein	1.88	0
AUO97_RS11155	hypothetical protein	1.6	4.30E-22
AUO97_RS11215	MFS transporter	2.4	0
AUO97_RS11220	trehalose-6-phosphate synthase	3.72	0
AUO97_RS11225	otsB	4.75	0
AUO97_RS12195	SRPBCC domain-containing protein	1.66	6.20E-28
AUO97_RS12630	hypothetical protein	1.98	0
AUO97_RS12635	alpha/beta hydrolase	1.78	6.00E-18
AUO97_RS12650	hypothetical protein	1.59	2.90E-16
AUO97_RS12730	hypothetical protein	3.23	8.80E-72

AUO97_RS12735	DUF4265 domain-containing protein	2.91	5.10E-65
AUO97_RS12740	hypothetical protein	2.76	4.60E-57
AUO97_RS12935	hypothetical protein	1.8	3.80E-63
AUO97_RS13435	OprD family outer membrane	2.4	1.30E-24
AUO97_RS13440	aromatic acid/H+ symport family MFS transporter	3.02	2.90E-51
AUO97_RS13445	benE	1.85	4.40E-18
AUO97_RS13450	1,6-dihydroxycyclohexa-2,4-diene-1-carboxylate dehydrogenase	2.62	2.60E-64
AUO97_RS13455	ring-hydroxylating dioxygenase ferredoxin reductase family protein	3.81	0
AUO97_RS13460	benB	4.49	0
AUO97_RS13465	benA	4.57	0
AUO97_RS13500	hypothetical protein	2.78	0
AUO97_RS13510	LysE family transporter	1.51	7.30E-16
AUO97_RS13535	transposase	1.64	0
AUO97_RS13560	LysE family translocator	1.72	2.80E-24
AUO97_RS13565	cold-shock protein	3.69	0
AUO97_RS13570	hypothetical protein	2.81	0
AUO97_RS13575	NAD(P)-binding domain-containing protein	1.96	0
AUO97_RS13585	hypothetical protein	1.97	0
AUO97_RS13590	hypothetical protein	2.21	2.70E-32
AUO97_RS13620	DUF4142 domain-containing protein	2.01	3.20E-57
AUO97_RS13625	hypothetical protein	3.77	0
AUO97_RS13745	hypothetical protein	1.58	1.40E-10
AUO97_RS13890	DUF1989 domain-containing protein	1.53	0.000037

AUO97_RS13955	SUMF1/EgtB/PvdO family nonheme iron enzyme	2.29	0
AUO97_RS13960	hypothetical protein	6.28	0
AUO97_RS13965	tssB	4.76	0
AUO97_RS13970	tssC	2.83	0
AUO97_RS13975	type VI secretion system tube protein Hcp	1.71	0
AUO97_RS13980	tssE	1.67	5.70E-23
AUO97_RS14080	epoxyqueuosine reductase QueH	2.32	0
AUO97_RS14085	hypothetical protein	3.14	5.80E-51
AUO97_RS14090	soxR	1.52	6.30E-25
AUO97_RS14165	paaZ	2.66	0
AUO97_RS14170	paaA	3	0
AUO97_RS14175	paaB	3.29	0
AUO97_RS14180	paaC	3.67	0
AUO97_RS14185	paaJ	3.72	0
AUO97_RS14190	paaK	3.92	0
AUO97_RS14195	enoyl-CoA hydratase/isomerase family protein	4.13	0
AUO97_RS14200	2-(1,2-epoxy-1,2-dihydrophenyl)acetyl-CoA isomerase	4.31	0
AUO97_RS14205	3-hydroxyacyl-CoA dehydrogenase	4.67	0
AUO97_RS14210	pcaF	3.92	0
AUO97_RS14215	paaF	3.05	0
AUO97_RS14230	PaaI family thioesterase	1.78	4.30E-16
AUO97_RS14245	hypothetical protein	1.6	4.10E-17
AUO97_RS14285	NAD(P)H-dependent oxidoreductase	1.96	1.90E-64

AUO97_RS14300	alr	2.42	0
AUO97_RS14340	LysE family translocator	3.12	0
AUO97_RS14430	hypothetical protein	5.52	0
AUO97_RS14435	hypothetical protein	5.47	0
AUO97_RS14440	CinA family protein	3.53	9.00E-56
AUO97_RS14445	iron-containing redox enzyme family protein	4.83	0
AUO97_RS14450	katE	3.93	0
AUO97_RS14455	glucose 1-dehydrogenase	2.82	2.40E-44
AUO97_RS14460	hypothetical protein	3.05	1.90E-34
AUO97_RS14465	stress-induced protein	2.35	6.50E-52
AUO97_RS14505	N-acetyltransferase	2.54	0
AUO97_RS14555	serine acetyltransferase	2.09	1.00E-14
AUO97_RS14630	mdcA	5.13	0
AUO97_RS14635	triphosphoribosyl-dephospho-CoA synthase	5.71	0
AUO97_RS14640	malonate decarboxylase subunit delta	4.15	0
AUO97_RS14645	biotin-independent malonate decarboxylase subunit beta	3.89	0
AUO97_RS14650	mdcE	4.16	0
AUO97_RS14655	malonate decarboxylase holo-ACP synthase	4.34	0
AUO97_RS14660	mdcH	4.45	0
AUO97_RS14665	madL	3.48	0
AUO97_RS14670	madM	2.76	0
AUO97_RS14710	LLM class flavin-dependent oxidoreductase	3.01	2.20E-74
AUO97_RS15005	1-acyl-sn-glycerol-3-phosphate acyltransferase	2.63	0

AUO97_RS15010	TetR/AcrR family transcriptional regulator	2.86	0
AUO97_RS15015	hypothetical protein	1.97	0
AUO97_RS15045	hypothetical protein	3.14	0
AUO97_RS15050	EamA family transporter	4.42	0
AUO97_RS15075	fimbrial biogenesis outer membrane usher protein	2.24	2.90E-35
AUO97_RS15080	fimbria/pilus periplasmic chaperone	3.97	0
AUO97_RS15085	type 1 fimbrial protein	2.2	0
AUO97_RS15180	hypothetical protein	2.64	0
AUO97_RS15280	hypothetical protein	1.94	0
AUO97_RS15500	hypothetical protein	1.59	2.40E-12
AUO97_RS15505	hypothetical protein	1.59	8.90E-15
AUO97_RS15520	hypothetical protein	1.83	2.80E-09
AUO97_RS15525	YdaU family protein	1.53	0.0000012
AUO97_RS15530	AAA family ATPase	1.54	0.000056
AUO97_RS15570	hypothetical protein	2.2	6.70E-18
AUO97_RS15575	hypothetical protein	1.81	1.10E-14
AUO97_RS15580	hypothetical protein	2.3	8.30E-14
AUO97_RS15585	hypothetical protein	1.96	3.20E-10
AUO97_RS15590	hypothetical protein	1.96	6.70E-12
AUO97_RS15595	HNH endonuclease	2.25	5.30E-23
AUO97_RS15610	terminase large subunit	2.15	9.90E-12
AUO97_RS15620	HK97 family phage prohead protease	2.06	9.00E-11
AUO97_RS15625	phage major capsid protein	1.83	1.20E-18

AUO97_RS15630	phage head-tail connector protein	1.93	3.70E-12
AUO97_RS15635	phage head closure protein	2.25	4.90E-20
AUO97_RS15640	HK97 gp10 family phage protein	2.18	4.40E-14
AUO97_RS15645	DUF3168 domain-containing protein	1.52	1.40E-13
AUO97_RS15655	hypothetical protein	1.7	3.40E-15
AUO97_RS15810	rpsT	2	0
AUO97_RS16000	acetyltransferase	2.12	0
AUO97_RS16010	HAD family hydrolase	2.2	1.50E-40
AUO97_RS16135	GFA family protein	1.63	7.70E-19
AUO97_RS16140	hypothetical protein	1.91	0
AUO97_RS16145	hypothetical protein	1.5	8.60E-20
AUO97_RS16190	hypothetical protein	1.52	0
AUO97_RS16245	transcriptional regulator	1.84	1.10E-39
AUO97_RS16250	lipA	2.77	2.70E-53
AUO97_RS16255	thiamine pyrophosphate-dependent dehydrogenase E1 component subunit alpha	3.18	0
AUO97_RS16260	alpha-ketoacid dehydrogenase subunit beta	3	1.10E-77
AUO97_RS16265	2-oxo acid dehydrogenase subunit E2	2.92	1.40E-70
AUO97_RS16270	lpdA	2.9	7.60E-54
AUO97_RS16275	acetoin reductase	2.14	6.10E-23
AUO97_RS16445	DUF3298 domain-containing protein	1.88	4.70E-43
AUO97_RS16465	GntP family permease	1.77	2.70E-64
AUO97_RS16595	PAAR domain-containing protein	1.95	1.60E-76

AUO97_RS16600	hypothetical protein	1.93	1.20E-59
AUO97_RS16605	GNAT family N-acetyltransferase	1.56	2.00E-29
AUO97_RS16610	hypothetical protein	1.96	2.70E-13
AUO97_RS16660	hypothetical protein	2.34	4.00E-24
AUO97_RS16665	TolC family protein	2.74	8.40E-28
AUO97_RS16670	GH3 auxin-responsive promoter family protein	2.06	3.80E-25
AUO97_RS16675	hypothetical protein	1.84	1.20E-23
AUO97_RS16680	DHA2 family efflux MFS transporter permease subunit	2.35	3.00E-22
AUO97_RS16685	HlyD family secretion protein	2.72	0
AUO97_RS16705	hypothetical protein	1.76	1.10E-25
AUO97_RS16710	hypothetical protein	2.05	5.50E-33
AUO97_RS17065	muconate cycloisomerase	4.76	0
AUO97_RS17070	catC	3.91	0
AUO97_RS17075	catA	2.59	0
AUO97_RS17080	3-oxoacid CoA-transferase subunit A	3.32	0
AUO97_RS17085	CoA transferase subunit B	2.93	5.40E-64
AUO97_RS17100	penicillin acylase family protein	2.2	2.70E-14
AUO97_RS17120	feaR	1.88	2.30E-14
AUO97_RS17125	flavin reductase family protein	4.14	0
AUO97_RS17130	oxidoreductase	5.09	0
AUO97_RS17135	SDR family oxidoreductase	4.83	0
AUO97_RS17140	aromatic-ring-hydroxylating dioxygenase subunit beta	4.47	0
AUO97_RS17145	aromatic ring-hydroxylating dioxygenase subunit alpha	4.87	0

AUO97_RS17150	nuclear transport factor 2 family protein	5.63	0
AUO97_RS17155	hypothetical protein	5.46	0
AUO97_RS17160	acyl-CoA dehydrogenase	5.89	0
AUO97_RS17165	amidase	6.79	0
AUO97_RS17175	MFS transporter	3.98	7.10E-89
AUO97_RS17180	OprD family outer membrane porin	3.09	2.80E-33
AUO97_RS17525	DUF2750 domain-containing protein	1.73	0
AUO97_RS17565	heme-binding protein	2.31	0
AUO97_RS17615	universal stress protein	1.7	0
AUO97_RS17635	S8 family peptidase	2.43	5.20E-75
AUO97_RS17665	hypothetical protein	1.86	0
AUO97_RS17995	lysozyme	1.51	5.00E-10
AUO97_RS18100	hypothetical protein	1.56	1.70E-12
AUO97_RS18145	minor capsid protein	1.5	2.00E-11
AUO97_RS18150	DUF4055 domain-containing protein	1.83	3.70E-14
AUO97_RS18155	terL	2.13	7.20E-14
AUO97_RS18160	DUF2280 domain-containing protein	1.88	1.90E-13
AUO97_RS18165	hypothetical protein	2.1	1.70E-14
AUO97_RS18320	iron-containing redox enzyme family protein	1.97	0
AUO97_RS18325	TetR/AcrR family transcriptional regulator	3.2	0
AUO97_RS18475	hypothetical protein	2.96	1.70E-29
AUO97_RS18505	hypothetical protein	1.52	1.10E-11
AUO97_RS18690	miaA	1.81	0

AUO97_RS18755	ion transporter	1.8	1.90E-25
AUO97_RS18760	hypothetical protein	2.15	0
AUO97_RS19055	fis	2.14	0
AUO97_RS19175	NUDIX hydrolase	1.85	1.70E-22
AUO97_RS19190	csuE	3.55	0
AUO97_RS19195	csuD	4.2	0
AUO97_RS19200	csuC	3.95	0
AUO97_RS19205	csuB	3.99	1.10E-68
AUO97_RS19210	csuA	4.63	0
AUO97_RS19215	csuAB	7.46	0
AUO97_RS19220	TetR/AcrR family transcriptional regulator	2.69	2.30E-29
AUO97_RS19350	hypothetical protein	1.51	0
AUO97_RS19390	hypothetical protein	1.55	7.10E-24
AUO97_RS19450	hypothetical protein	2.74	0
AUO97_RS19490	hypothetical protein	1.76	1.20E-11
AUO97_RS19580	hypothetical protein	1.56	6.00E-14
AUO97_RS19600	hypothetical protein	1.82	9.10E-15
AUO97_RS19625	hypothetical protein	2.14	1.60E-08
AUO97_RS19645	BapA prefix-like domain-containing protein	1.61	0
AUO97_RS19680	hypothetical protein	2.75	0

Appendix 7.

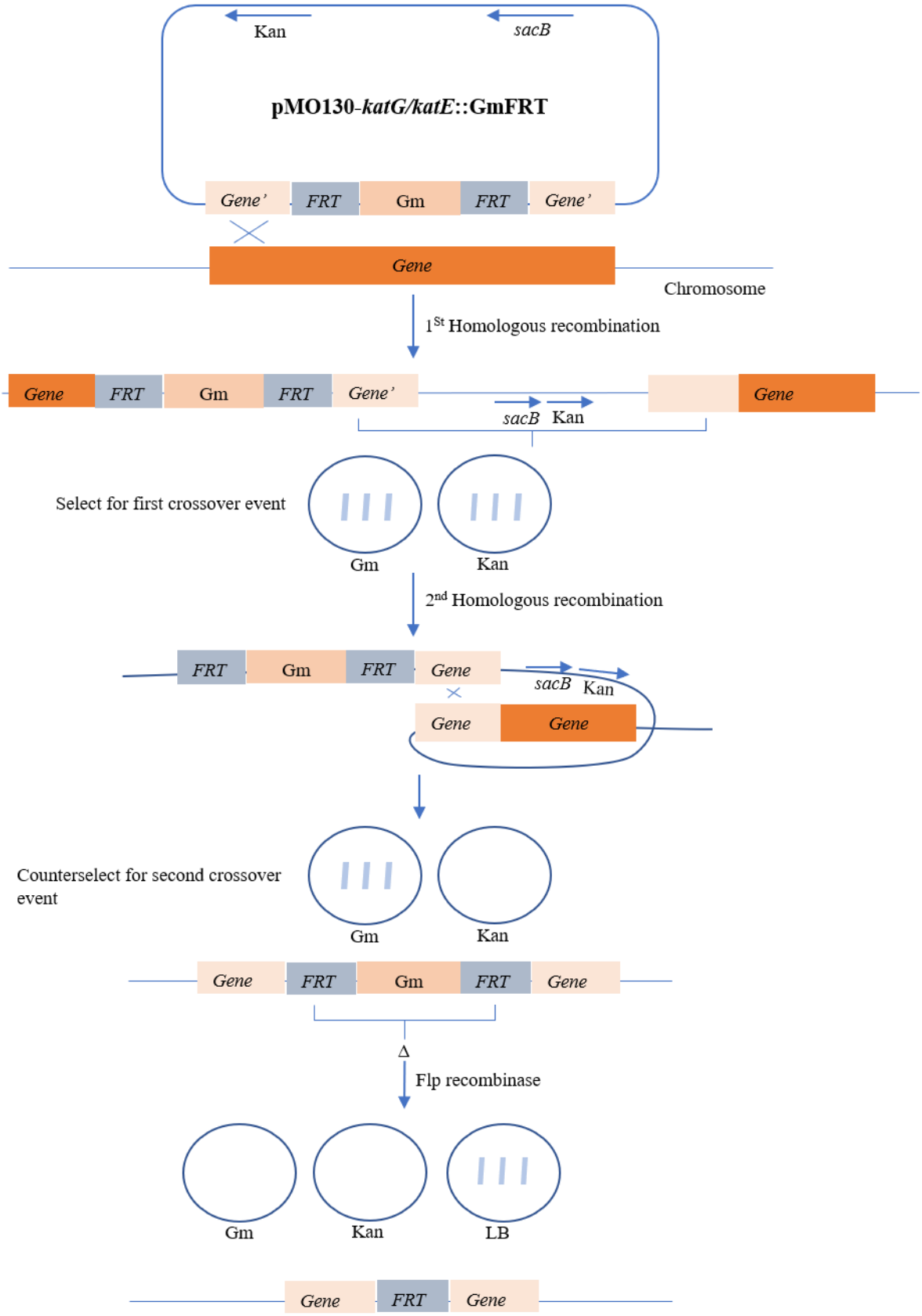
Kan
sacB
pMO130-katG/katE::GmFRT
Gene'
FRT
Gm
FRT
Gene'
Gene
Chromosome
1St Homologous recombination
Gene
FRT
Gm
FRT
Gene'
Gene
sacB
Kan
Select for first crossover event
Gm
Kan
2nd Homologous recombination
FRT
Gm
FRT
Gene
sacB
Kan
Gene
Gene
Counterselect for second crossover event
Gm
Kan
Gene
FRT
Gm
FRT
Gene
Δ
Flp recombinase
Gm
Kan
LB
Gene
FRT
Gene

Schematic representation of markerless gene deletion using homologous recombination strategy

Upstream portion and a downstream portion of the target gene (*katG/katE*) is amplified which contain added FRT regions flanking 3′ and 5′ ends and a gentamicin resistance (Gm^R) marker containing complementary FRT regions cloned between the upstream and the downstream portions of the target gene using sequence overlap extension polymerase chain reaction to generate the gene knockout cassette. The blunt-end fragments are directly cloned into pMO130. The plasmid is introduced into the chromosome via electroporation and homologous recombination. The first recombination event is selected by plating cells on LB + 50 μg/mL gentamicin (Gm) and LB + 50 μg/mL kanamycin (Kan). Patches that are resistant to both Gm and Kan are considered merodiploids and undergo second recombination event. The excision of the plasmid region with Gm^R in the chromosome via a second single-crossover homologous recombination event is done via 10% (w/v) sucrose counterselection utilizing the *sacB* gene. Patches that show growth on LB and not on Gm and Kan indicate a successful markerless deletion mutant.